National Library of Canada
Bibliothèque nationale du Canada

Canadian Theses Service
Service des thèses canadiennes

Ottawa, Canada
K1A 0N4

NOTICE

The quality of this microform is heavily dependent upon the quality of the original thesis submitted for microfilming. Every effort has been made to ensure the highest quality of reproduction possible.

If pages are missing, contact the university which granted the degree.

Some pages may have indistinct print especially if the original pages were typed with a poor typewriter ribbon or if the university sent us an inferior photocopy.

Reproduction in full or in part of this microform is governed by the Canadian Copyright Act, R.S.C. 1970, c. C-30, and subsequent amendments.

AVIS

La qualité de cette microforme dépend grandement de la qualité de la thèse soumise au microfilmage. Nous avons tout fait pour assurer une qualité supérieure de reproduction.

S'il manque des pages, veuillez communiquer avec l'université qui a conféré le grade.

La qualité d'impression de certaines pages peut laisser à désirer, surtout si les pages originales ont été dactylographiées à l'aide d'un ruban usé ou si l'université nous a fait parvenir une photocopie de qualité inférieure.

La reproduction, même partielle, de cette microforme est soumise à la Loi canadienne sur le droit d'auteur, SRC 1970, c. C-30, et ses amendements subséquents.

NL-339 (r. 88/04) c

Canada

THE UNIVERSITY OF ALBERTA

SOME SUSY RELATED ORTHOTOPONIUM PHENOMENOLOGY

by

© MICHAEL MACFIELD BOYCE

A THESIS

SUBMITTED TO THE FACULTY OF GRADUATE STUDIES AND RESEARCH

IN PARTIAL FULFILMENT OF THE REQUIREMENTS FOR THE DEGREE

OF MASTER OF SCIENCE

IN

THEORETICAL PHYSICS

DEPARTMENT OF PHYSICS

EDMONTON, ALBERTA

SPRING 1989 A.D.

Permission has been granted to the National Library of Canada to microfilm this thesis and to lend or sell copies of the film.

The author (copyright owner) has reserved other publication rights, and neither the thesis nor extensive extracts from it may be printed or otherwise reproduced without his/her written permission.

L'autorisation a été accordée à la Bibliothèque nationale du Canada de microfilmer cette thèse et de prêter ou de vendre des exemplaires du film.

L'auteur (titulaire du droit d'auteur) se réserve les autres droits de publication; ni la thèse ni de longs extraits de celle-ci ne doivent être imprimés ou autrement reproduits sans son autorisation écrite.

ISBN 0-315-52774-9

THE UNIVERSITY OF ALBERTA

RELEASE FORM

NAME OF AUTHOR MICHAEL MACFIELD BOYCE

TITLE OF THESIS SOME SUSY RELATED ORTHOTOPONIUM PHENOMENOLOGY

DEGREE FOR WHICH THESIS WAS PRESENTED MASTER OF SCIENCE

YEAR THIS DEGREE GRANTED SPRING 1989 A.D.

Permission is hereby granted to THE UNIVERSITY OF ALBERTA LIBRARY to reproduce single copies of this thesis and to lend or sell such copies for private, scholarly or scientific research purposes only.

The author reserves other publication rights, and neither the thesis nor extensive extracts from it may be printed or otherwise reproduced without the author's written permission.

(SIGNED) .....

PERMANENT ADDRESS:

..11 Yanofsky Way.....

..Winn. Manitoba.....

R2P-1X8.....

DATED November 30th.....1988

THE UNIVERSITY OF ALBERTA

FACULTY OF GRADUATE STUDIES AND RESEARCH

The undersigned certify that they have read, and recommend to the Faculty of Graduate Studies and Research, for acceptance, a thesis entitled SOME SUSY RELATED ORTHOTOPONIUM PHENOMENOLOGY submitted by MICHAEL MACFIELD BOYCE in partial fulfilment of the requirements for the degree of MASTER OF SCIENCE in THEORETICAL PHYSICS.

...B.A. Campbell...

Supervisor

...A. Antaramian...

...T.G. Steele...

...H.P. Kunz-Co...

Date.....4/10/88.....

TO MY PARENTS

Abstract

SUSY models predict the possibility of observing neutralino, $\tilde{\chi}^0$, production from bound state toponium systems. In this thesis we examine neutralino production for the two lightest neutralino states ($\tilde{\chi}^0$ and $\tilde{\chi}^{0'}$) from a low lying $^3S_1$ orthotoponium, θ, state, for extended N=1 SU(2)⊗U(1) and SU(2)⊗U(1)⊗U(1) soft SUSY models.

Acknowledgements

I would like to thank my supervisor, Dr. B. A. Campbell, whose uncanny physical insight helped me out of many conceptually difficult spots. I would also like to thank the rest of my committee, Dr. G. Greeniaus, Dr. A. N. Kamal, and Dr. H. P. Kunzle, without whom this would not have been possible.

I would like to thank my associate K. A. Peterson, whose help ranged from computational problems to finishing a pitcher of beer at the Power Plant. Speaking of which, I would like to thank the rest of the Power Plant crew, including theoretical consultants J. Hebron, J. Johansson, D. McManus, and G. Tsoupros; phenomenological consultants Dr. P. Asthana, I. Hardman, Dr. N. Mobed, and Dr. O. Wong; editorial consultant D. Kokaram; moral support group and just plain drinking buddies R. Beach, Dr. S. C. Cheng, R. Crilley, Dr. P. Crozier, T. Fitzgerald, G. Hayward, T. Kolb, J. Pradko, E. Poisson, Dr. P. Rice, and D. Tembo.

Also, for stimulating theoretical and phenomenological consultations, I would like to thank, Dr. A. N. Kamal, Dr. F. C. Khanna, and Dr. R. Sinha.

I would like to thank R. Teshima (FORTRAN consultant), P. I. Buttuls (graphics consultant), the textform group, and computing services, for all of whom without, I would have been lost.

I would like to thank, Dr. A. Z. Capri, Dr. H. P. Kunzle, Dr. W. Rozmus, Dr. H. Schiff, and Dr. J. Stephenson, whose insatiable appetite for their work has provided further inspiration for mine.

I would like to thank the office staff for providing colour (so to speak) to the sometimes drab and dreary physics department.

Unfortunately, we are all human; so lastly, I would like to thank all those who I have forgotten.

"MAY YOU ALL LIVE LONG AND PROSPER!"

Table of Contents

Chapter — Page

I. Introduction to SUSY 1
A. Introduction 1
B. Some Historical Notes 1
C. SU(5) Grand Unification 5
D. The Gauge Hierarchy Problem 8
E. SUSY 12
F. SUSY Lagrangian 15
G. Remarks 23
II. Broken SUSY 25
A. Introduction 25
B. Squark and Slepton Mass Matrices 25
C. Gaugino and Higgsino Mass Matrices 29
D. An Extra U(1) 42
E. Remarks 50
III. Toponium Decay 51
A. Introduction 51
B. Toponium Decay Calculation 53
Stop squark exchange amplitude 55
Z-exchange amplitude 65
Total amplitude 69
Decay width 75
C. Results 76
D. Toponium Decay Revisited 94
Stop squark exchange amplitude 95
Z-exchange amplitude 96

Total amplitude 96
E. Results 97
F. Observations 107
G. Varying the Top Mass 109
H. Experimental Consequences 117
IV. Summary and Conclusions 122
REFERENCES 123
APPENDIX A--Notation 127
Minkowski Space 127
Dirac Matrices 128
Trace Theorems 132
APPENDIX B--Spinorology 133
Dirac Spinors 133
N.R. Approx. 135
APPENDIX C--Fierz Identities 137

List of Tables

Table		Page
I.1	SUSY Particle Spectrum	14
III.1	Stop Squark exchange Feynman Rules	58
III.2	A list of some typical θ BR's	118
III.3	Some typical Neutralino Events at LEP	119
B.I	N.R. Approx. Expectation Values	136

List of Figures

Figure		Page
II.1	Neutralino mass plots	33
II.2	Neutralino mass plots	34
II.3	Neutralino mass plots	35
II.4	Neutralino mass plots	36
II.5	Neutralino mass plots	37
II.6	Neutralino mass plots	38
II.7	Neutralino mass plots	39
II.8	Neutralino mass plots	40
II.9	Neutralino mass plots with an extra U(1)	44
II.10	Neutralino mass plots with an extra U(1)	45
II.11	Neutralino mass plots with an extra U(1)	46
II.12	Neutralino mass plots with an extra U(1)	47
II.13	Neutralino mass plots with an extra U(1)	48
II.14	Neutralino mass plots with an extra U(1)	49
III.1	Quarkonia to photon, Higgs	51
III.2	Quarkonia to photino, Higgsino	51
III.3	Quarkonia to neutralino, neutralino'	52
III.4	Toponium via Z to neutralino pairs	53
III.5	Z exchange Feynman diagram	65
III.6	Toponium decay in C of M system	74
III.7	Toponium to stop pairs	77
III.8	Toponium to fermion-antifermion pairs	77

Figure		Page
III.9	Toponium beta decay	78
III.10	Toponium width	79
III.11	Toponium BR plots	82
III.12	Toponium BR plots	83
III.13	Toponium BR plots	84
III.14	Toponium BR plots	85
III.15	Toponium BR plots	86
III.16	Toponium BR plots	87
III.17	Toponium BR plots	88
III.18	Toponium BR plots	89
III.19	Toponium BR plots	90
III.20	Toponium BR plots	91
III.21	Toponium BR plots	92
III.22	Toponium BR plots	93
III.23	Toponium BR plots with an extra U(1)	98
III.24	Toponium BR plots with an extra U(1)	99
III.25	Toponium BR plots with an extra U(1)	100
III.26	Toponium BR plots with an extra U(1)	101
III.27	Toponium BR plots with an extra U(1)	102
III.28	Toponium BR plots with an extra U(1)	103
III.29	Toponium BR plots with an extra U(1)	104
III.30	Toponium BR plots with an extra U(1)	105
III.31	Toponium BR plots with an extra U(1)	106
III.32	Toponium BR plots	110
III.33	Toponium BR plots	111
III.34	Toponium BR plots	112

Figure Page

III.35 Toponium BR plots 113

III.36 Toponium BR plots with an extra U(1) 114

III.37 Toponium BR plots with an extra U(1) 115

III.38 Toponium BR plots with an extra U(1) 116

I. Introduction to SUSY

A. Introduction

To a large extent the development of the theory of fundamental forces in nature rested in man's understanding of its underlying symmetries. This, along with the development of quantum field theories, led to remarkably successful field theories of the strong, weak, and electromagnetic interactions. These developments eventually propagated toward Grand Unified Theories (GUTS), in which the strong, weak, and electromagnetic interactions were imbedded. For theorists, GUTS posed a serious problem, or sickness, referred to as the 'Gauge Hierarchy Problem (GHP)'. Cures were developed such as Technicolour (TECC) and Supersymmetry (SUSY). The latest experimental evidence seems to favour the SUSY cure – if any.

To get a bit more of a flavour, for these developments, the rest of this chapter shall be devoted to a brief review of historical developments, leading toward SUSY theories, followed by an introduction to SUSY.

B. Some Historical Notes

Einstein's identification of the invariance group of space time, in 1905 (EIN.05), led to his formulation of the theory of gravity. As time passed, new symmetries (such as isospin, which governs strong interactions (HEI.32,

PER.82)), which have nothing to do with space and time were discovered. Thus, it seemed that different interactions were governed by different internal symmetries. Alas, there seemed to be no hope for a grand unifying scheme.

Initially it was thought that internal symmetries should be global symmetries. However, it was long known that electromagnetism possessed a local U(1) charge symmetry. In fact, in 1954, this motivated Yang, Mills and Shaw to extend the Abelian U(1) theory to a non-Abelian SU(N) theory. Such a generalization led to the prediction that there should exist new vector bosons, like the photon, which should be massless. However, this was very much in contradiction with experiment. Further investigations led to considering approximate symmetries, with massive vector bosons. The idea was that by 'spontaneous' symmetry breaking, one could keep the symmetry of the Lagrangian while destroying the symmetry of the vacuum. So, the symmetry of the physical state need not manifestly exhibit the underlying symmetry of the Lagrangian.

Nambu and Goldstone showed that, for global symmetries, spontaneously broken symmetry gives rise to massless spin zero Nambu-Goldstone Bosons. They found that if one breaks the $SU(2)\otimes SU(2)$ chiral isospin group, one obtains Nambu-Goldstone bosons that could be identified with the pions. Many successful predictions arose from this theory; for example the Adler-Weisberger result relating the ratio

g_A/g_V (the axial vector couplings in β decay (COM.83)) to the pion-nucleon cross section. This suggested that there existed some kind of underlying chiral symmetry between the strong and weak interactions. However, it was not until the development of gauge theories for the strong and weak interactions that the nature of these symmetries was fully understood.

In the 1960's, Anderson, Higgs, Brout and Englert, Guralnick, Hagen and Kibble, worked out the role of spontaneous symmetry breaking in local gauge theories. They showed that, via the so-called 'Higgs mechanism', the massless gauge bosons of the Yang-Mills theory and the massless Nambu-Goldstone bosons could simultaneously be avoided. In this scenario, the vector bosons gain mass by 'eating up' the 'would-be-Nambu-Goldstone bosons'. That is to say, the massless Nambu-Goldstone bosons give an extra degree of freedom to the massless gauge bosons in such a way that they manifest themselves as massive vector bosons. A very desirable, and suspected, property for this theory is that it be renormalizable. Only in a renormalizable theory can one make predictions for physical processes in terms of a finite set of parameters. It was not until 1971 that it was shown by G.'t Hooft that theories of this kind were indeed renormalizable.

In the late 1960's Glashow, Weinberg, and Salam and Ward discovered a unified gauge theory of the

electromagnetic and weak interactions. This discovery was made by employing the 'Higgs mechanism' to break the $SU_L(2)\otimes U_Y(1)$ group down to a $U_{em}(1)$ group, thus giving rise to three massive, $W^{\pm}$(81GeV) and Z^0(94GeV), intermediate vector bosons, and one massless photon, γ. Here the massive $W^{\pm}$ bosons come from a symmetry break down of the $SU_L(2)$ part, whereas the massive Z^0 is the price paid for unifying $SU_L(2)$ with the $U_Y(1)$ part. The Higgs mechanism also gives mass to the charged leptons and automatically produces a massive scalar Higgs H^0 field in order to counteract divergences caused by the charged fermions acquiring a mass. One cannot help but be impressed by this. Recent tests at CERN's UA1 (UA1.83) and UA2 (UA2.83) experiments verified the validility of the $SU_L(2)\otimes U_Y(1)$ model by the discovery of the $W^{\pm}$ and Z^0 intermediate vector bosons. The H^0 has yet to be found. It can be shown through perturbative unitarity constraints that (ELL.85, QUI.83)

$$m_H = O(\sqrt{\alpha}^{0\pm 1})\, m_W. \qquad (1.1)$$

The connection between strong and electroweak interactions was naturally followed by the inclusion of $SU_C(3)$ to the $SU_L(2)\otimes U_Y(1)$ group. This new model was dubbed the 'Standard Model', or, the $SU_C(3)\otimes SU_L(2)\otimes U_Y(1)$ model. Where the $SU_C(3)$ were the non-Abelian gauge group of QCD (Quantum ChromoDynamics). Here the Higgs mechanism is used

to break $SU_C(3)\otimes SU_L(2)\otimes U_Y(1)$ down to $SU_c(3)\otimes U_{em}(1)$. This leaves the gauge and the massive Higgs sectors unchanged from that of the previous $SU_L(2)\otimes U_Y(1)$ model. It also gives the quarks mass while leaving the massless gluon field of the $SU_c(3)$ sector unchanged. As of this day, this theory seems to give a fairly good description of all physical phenomena down to the smallest distance scales yet probed.

C. SU(5) Grand Unification

Although the standard model combines the strong, weak and electromagnetic interactions, it also carries with it three apparently unrelated gauge coupling constants from each of its constituent group parts. Therefore, the $SU_C(3)\otimes SU_L(2)\otimes U_Y(1)$ group in essence is not quite a fully unified group, since it has no predictive power of the relative strengths between the various coupling constants. This problem could be overcome if the underlying gauge group were simple, for then there is only one coupling constant. Thus, to achieve a more complete unification of the $SU_C(3)\otimes SU_L(2)\otimes U_Y(1)$ gauge group we must embed it in a larger group, the so-called grand unified group.

This idea was originally suggested by Pati and Salam. Georgi and Glashow proposed a simpler version based on the minimal group SU(5). This group has 24 vector bosons. Upon employment of the Higgs mechanism 9 of these remain massless. These are identified with the 8 gluons of the

$SU_c(3)$ and the one photon of the $U_{em}(1)$ group. Three of the massive ($O(10^2)$GeV) vector bosons are identified with the $W^{\pm}$ and Z^0 vector bosons of the electro-weak theory. The remaining 12 vector bosons are often referred to as lepto-quarks, since they mediate transitions between quarks and leptons.

One of the most worrying of these transitions is the decay of the proton into leptons. Recent tests on proton decay (LOS.86) show to quite a high degree of accuracy that the proton does not decay and therefore one concludes that these new interactions must be very weak. In fact, in SU(5) the bosons mediating proton decay must have a mass greater than 10^{15} times that of the proton mass.

Another way of getting an estimate of the scale of grand unification comes from the fact that since SU(5) has only one coupling constant, at the scale at which SU(5) is exact, both the electromagnetic and strong couplings (suitably normalized) are the same. That is, the coupling constants actually depend on the scale of momentum. The equality of the strong and electromagnetic couplings occurs at a superheavy scale M_X. By using the logarithmic variation of the coupling constants predicted by the theory and the experimently determined ratio of the couplings in the laboratory, one can find the value of M_X at which the ratio is 1. This yields $M_X \approx 10^{15}$GeV, which is quite close to the value obtained from proton decay. Once M_X is determined, the

ratio of the weak to electromagnetic coupling is predicted. Remarkably the prediction is in reasonably good agreement with what is measured in the laboratory.

Aside from the fact that the SU(5) scheme correctly predicts the free parameter of the Glashow-Weinberg-Salam (or $SU_L(2)\otimes U_Y(1)$) model, it admittedly has very little evidence in support of its other predictions associated with the lepto-quarks, although a great deal of experimental effort has gone into looking for proton decay. However, because of the theoretical simplification achieved by grand unification, theorists feel that its ideas will be relevant to any extension of the standard model (For example, the left-handed and right-handed quarks and leptons fit neatly into the $5^*\oplus 10$ representation of SU(5), thus giving an explanation for their electric and weak charges (ROS.85,87).) On the other hand, it appears that grand unification is not the whole story. In the first place there doesn't exist a symmetry between the bosons and fermions (SUSY), not to mention a connection with gravity. However, there is a more immediate problem with grand unification which suggests something new must happen long before the grand unification mass scale.

D. The Gauge Hierarchy Problem

A theory is regarded as technically 'natural' if corrections to the bare values of physical parameters are no larger than the physical values they take (ELL.85). In the standard model, for example, it can be shown that one-loop radiative corrections for fermions take the form:

$$\delta m_f = O(\frac{\alpha}{\pi}) m_f \ln(\Lambda/m_f), \tag{1.2}$$

which are always $\lesssim m_f$, even if the cut off $\Lambda = M_p$ (Plank mass). Whereas for the scalar Higgs

$$\delta m_H{}^2 = g^2 \int^{\Lambda} \frac{d^4k}{(2\pi)^4} \frac{1}{k^2} = O(\frac{\alpha}{\pi})\Lambda^2, \tag{1.3}$$

which is quadratically divergent. As we can see for fermions, naturalness is inherent in the theory, but for the Higgs boson one must impose naturalness by unitary arguments (1.1) in order to obtain an appropriate cut off:

$$\Lambda \lesssim O(1)\text{TeV}. \tag{1.4}$$

One might say that divergences of this type are perfectly renormalizable in the usual way, and so why bother with naturalness. However, when one attempts a more grand scheme of unification such divergences become symptoms of a more

serious disease. For instance, in the SU(5) GUT theory, breaking is actually done in two stages: i.e. SU(5) breaks down to $SU_C(3)\otimes SU_L(2)\otimes U_Y(1)$ via large-scale Higgses, ϕ, somewhere above $O(10^{15})$GeV, followed by a break down to $SU_c(3)\otimes U_{em}(1)$ via small-scale Higgses, H, at $O(10^2)$Gev. Renormalizability of the theory requires the existence of the coupling $\lambda H^2\phi^2$. Thus, when the ϕ's acquire a VEV (vacuum expectation value) of $O(M_X)$, one finds a Higgs mass shift of

$$\delta m_H^2=\lambda<\phi>^2=O(M_x^2)\geq O(10^{15}\text{GeV})^2. \qquad (1.5)$$

One could attempt to recover the Higgs mass m_H by choosing an appropriate bare mass of $-O(M_X^2)$ with the appropriate coefficient to give a cancellation of O(26) decimal places. However, one still has to deal with radiative corrections to λ which give a further mass shift of

$$\delta m_H^2=O(\frac{\alpha}{\pi})m_X^2\geq O(10^{14}\text{GeV})^2, \qquad (1.6)$$

which again leads to further unnatural cancellations. For those of you that do not like GUTS, Hawking and collaboration assure us that for elementary scalars skipping around in non-trivial non-perturbative topologies of foamy quantum vacuums

$$\delta m_H^2=O(M_p^2)=O(10^{19}\text{GeV})^2. \qquad (1.7)$$

Although not conclusive one can see that these arguments do suggest that small values for the elementary scalar masses are sick and unstable. This is known as the GHP.

Two cures have been proposed for stabilizing m_H. One is to use a TECC scheme in which the Higgs is made out of two tightly bound massless fermions. These fermions, or techniquarks, undergo QCD like interactions which become strong at the scale

$$\Lambda_T \sim O(1)\text{TeV}. \tag{1.8}$$

It is at this scale that they bind tightly together to form Higgses of composite size

$$R_T \sim \frac{1}{\Lambda_T}. \tag{1.9}$$

This provides a natural cut-off $\Lambda \sim \Lambda_T$ for the quadratically divergent loops given by equation (1.3) and gets rid of $\lambda H^2\phi^2$ couplings. The masslessness of the constituent techniquarks ensures us that we will have massless Goldstone bosons available to give mass to the $W^{\pm}$ and Z^0 bosons in the Higgs mechanism:

$$m_W = O(g\Lambda_T). \tag{1.10}$$

In order to give the fermions mass, one must postulate the existence of massive E vector bosons which couple ordinary fermions to technifermions. Unfortunately the E's lead to flavour changing neutral currents that are too large. Several different scenerios have been devised to overcome this problem. However, it is not clear which, if any, of these approaches is relevant.

The other scheme is to notice that the fermionic and bosonic loop contributions to m_H have opposite signs:

$$\delta m_H^2 = O(\tfrac{\alpha}{\pi})\Lambda^2 \Big|_{\text{bosons}} - O(\tfrac{\alpha}{\pi})\Lambda^2 \Big|_{\text{fermions}} \qquad (1.11)$$

If we now postulate a theory in which bosons, B, and fermions, F, have the same quantum numbers and the same couplings within some spin factors and similar masses, we get

$$\delta m_H^2 = O(\tfrac{\alpha}{\pi}) |m_B^2 - m_F^2| \qquad (1.12)$$

Such a symmetry between fermions and bosons is known as approximate SUSY (This theory is also unplagued by large GUT radiative corrections (ROS.85).) By imposing the naturalness condition we obtain the constraint

$$\Lambda^2 = |m_B^2 - m_F^2| \lesssim O(1\text{TeV})^2 \qquad (1.13)$$

which tells us that the supersymmetric partners (spartners) of conventional particles must weigh less than O(1)Tev. This gives us good reason to hope that sparticles may be found in the near future[1].

E. SUSY

SUSY is a new type of symmetry which relates fermions and bosons. That is, a spin $\frac{1}{2}$ Majorana operator, Q, is used to transform fermions into bosons and visa versa:

i.e. $$Q|F\rangle=|B\rangle \ , \ Q|B\rangle=|F\rangle \qquad (1.14)$$

These SUSY operators along with the familiar Lie algebra elements P_μ and $M_{\mu\nu}$, of the Poincaré group, form a graded Lie algebra (JOG.84):

$$[P_\mu,P_\nu]=0 \qquad (1.15.a)$$

$$[M_{\mu\nu},P_\rho]=ig_{\rho[\mu}P_{\nu]} \qquad (1.15.b)$$

$$[M_{\mu\nu},M_{\rho\sigma}]=-\delta^{\alpha\beta}_{\mu\nu}M_{\alpha[\rho}g_{\sigma]\beta} \qquad (1.15.c)$$

$$[Q_\alpha,P_\nu]=0 \qquad (1.15.d)$$

$$[Q_\alpha,M_{\mu\nu}]=\frac{1}{2}(\sigma_{\mu\nu})_{\alpha\beta}Q_\beta \qquad (1.15.e)$$

$$\{Q_\alpha,Q_\beta\}=-(\gamma^\mu C)_{\alpha\beta}P_\mu \qquad (1.15.f)$$

Equations (1.15.a) through (1.15.c) are of the familiar Lie algebra associated with the generators of translations, P_μ,

---

[1] For references see ELL.83A,85.

and rotations, $M_{\mu\nu}$, of the Poincaré group. Equation (1.15.d) tells us that the Q's, or supertranslations, are unaffected by uniform translations in space and time. Equation (1.15.e) tells us that the Q's transform as spinors under the action of the Lorentz group. Finally, equation (1.15.f) tells us that finite SUSY transformations induce a translation in space and time on the state on which they act.

A theory that obeys such an algebra is referred to as N=1 (i.e. number of SUSY charges), or simple SUSY. If the number of SUSY charges is greater than 1 (N>1), then one can admit an internal symmetry group (SOH.85). Such theories are known as extended SUSY (ELL.83A). N≤4 is the realm of possible gauge theories, since helicities between ±1 are tolerable:

$$\lambda = +1 \xrightarrow[Q_1]{} +1/2 \xrightarrow[Q_2]{} 0 \xrightarrow[Q_3]{} -1/2 \xrightarrow[Q_4]{} -1 \qquad (1.16)$$

For N≤8 one can have supersymmetric theories which include gravity (i.e. supergravity or SUGRA theories), since helicities between ±2 are tolerable:

$$\lambda = +2 \xrightarrow[Q_1]{} +3/2 \xrightarrow[Q_2]{} +1 \xrightarrow[Q_3]{} +1/2 \xrightarrow[Q_4]{} 0 \xrightarrow[Q_5]{} -1/2 \xrightarrow[Q_6]{} -1 \xrightarrow[Q_7]{} -3/2 \xrightarrow[Q_8]{} -2 \qquad (1.17)$$

In what follows we shall only be concerned with N=1 SUSY, for which the relavant supermultiplets are:

$$(1,\tfrac{1}{2})\ \text{Gauge} \qquad (1.18.a)$$

$$(\tfrac{1}{2},0)\ \text{Chiral} \qquad (1.18.b)$$

For N=1 SUSY the charges Q_α carry no internal quantum numbers. This means that no known particle can be the spartner of any other, resulting in the rich sparticle sspectroscopy shown in table (1.1) below.

TABLE 1.1. SUSY Particle Spectrum. Multiplet structure for minimal SU(3)⊗SU(2)⊗U(1) SUSY theory.

Gauge(1,½)	Chiral(½,0)
(Gluon g, Gluino $\tilde{g}$)	(Quark q, Squark $\tilde{q}$)
($W^{\pm}$, Wino $\tilde{W}^{\pm}$)	(Lepton l, Slepton $\tilde{l}$)
(Z^0, Zino $\tilde{Z}^0$)	(Higgsino $\tilde{H}^{\pm}$, Higgs $H^{\pm}$)
(photon γ, photino $\tilde{\gamma}$)	(Higgsino $\tilde{H}^0$, Higgs H^0)

Here one introduces two Higgs doublets, $H_{1,2}$, of opposite hypercharge, in order to cancel triangle anomalies and to give mass to the leptons and the, charge $\frac{2}{3}$ and charge $-\frac{1}{3}$, quarks. Unsuccessful searches for charge sparticle pairs in e^+e^- machines have put lower mass limits of O(15)GeV, on the $\tilde{W}^{\pm}$, $\tilde{H}^{\pm}$ and $\tilde{l}^{\pm}$ sparticles, and O(50)GeV on the $\tilde{g}$ gluino. These limits are somewhat model-dependent, since they are obtained by making assumptions about the sparticle decay processes. As for the uncharged colourless sparticles, there are no direct experimental limits.

F. SUSY Lagrangian

In this section we wish to construct a full gauge invariant SUSY (N=1) Lagrangian. Here, we shall assume the gauge group to vary locally and SUSY to be global.

As equation (1.14) suggests, if SUSY were an exact symmetry we would expect

$$m_B = m_F \tag{1.19}$$

just as the proton and neutron would have identical masses if isospin were an exact symmetry. To see this more formally, we consider the following chiral smultiplet (supermultiplet)

$$\Phi^i = (\psi_L^i, \phi^i, F^i), \tag{1.20}$$

where ψ_L^i is a dim $\frac{3}{2}$ chiral (Weyl) fermion field and ϕ^i and F^i are complex scalar fields of dim 1 and 2 respectively. Here we shall adopt the left-handed convention, where the ψ_R species are expressed in terms of their conjugate antiparticle fields $C(\bar{\psi}_R)^T (= (\psi^c)_L \equiv \psi_L^c)$ which are left-handed. Therefore

$$\bar{\Phi}_i = (\psi_{iR}^c, \phi_i^*, F_i^*) \tag{1.21}$$

represents our conjugate smultiplet. The F's are commonly

refered to as auxiliary fields, whose meaning shall soon become obvious.

In order to illustrate relation (1.19), we must first examine the properties of Φ^i under infinitesmal SUSY transformations:

$$\Lambda(Q)=e^{\bar{\epsilon}Q}, \tag{1.22}$$

where ϵ is a infinitesimal anticommuting Majorana spinor parameter. Using the super Poincaré group algebra relation (1.15.f), we easily obtain the relation

$$[\Lambda_1(Q),\Lambda_2(Q)]\cong[\bar{\epsilon}_1 Q,\bar{\epsilon}_2 Q]=\bar{\epsilon}_1\gamma^\mu\epsilon_2 P_\mu. \tag{1.23}$$

Or more explicitly

$$[\delta_1,\delta_2]\Phi^i=-i\bar{\epsilon}_1\gamma^\mu\epsilon_2\partial_\mu\Phi^i. \tag{1.24}$$

It can be shown (PET.87), that in order for the component fields to obey relation (1.24), they must transform as

$$\delta\phi^i=\bar{\epsilon}\psi^i_L \tag{1.24.a}$$

$$\delta\psi^i_L=(F^i-i\not{\partial}\phi^i)_L\epsilon \tag{1.24.b}$$

$$\delta F^i=-i\bar{\epsilon}\not{\partial}\psi^i_L. \tag{1.24.c}$$

A renormalizable Lagrangian which manifests this symmetry was constructed by Wess and Zumino in 1974 (WES.74):

i.e. $$L_{SUSY}=L_{KE}+L_{PE}+L_{YUK}, \tag{1.25}$$

where[2]

$$L_{KE}=i\bar{\psi}_{iL}\partial\!\!\!/\psi^{i}_{L}+|\partial_{\mu}\phi_{i}|^{2}+|F^{i}|^{2} \tag{1.25.a}$$

$$L_{PE}=W(\phi)_{,i}F^{i}+H.C. \tag{1.25.b}$$

$$L_{YUK}=W(\phi)_{,i,j}(\psi^{i}_{L})^{T}C^{-1}\psi^{j}_{L}+H.C. \tag{1.25.c}$$

where we have introduced the superpotential

$$W(\Phi)=C_{i}\Phi^{i}+m_{ij}\Phi^{i}\Phi^{j}+g_{ijk}\Phi^{i}\Phi^{j}\Phi^{k} \tag{1.26}$$

to obtain a more esthetic-looking Lagrangian[3]. The Lagrangian (1.25) can be further simplified to

$$L_{KE}=i\bar{\psi}_{iL}\partial\!\!\!/\psi^{i}_{L}+|\partial_{\mu}\phi_{i}|^{2} \tag{1.27.a}$$

$$L_{PE}=-|W(\phi)_{,i}|^{2} \tag{1.27.b}$$

$$L_{YUK}=W(\phi)_{,i,j}(\psi^{i}_{L})^{T}C^{-1}\psi^{j}_{L}+H.C. \tag{1.27.c}$$

---

[2] Note: $W(\phi)_{,i}\equiv\partial W(\Phi)/\partial\Phi^{i}|_{\Phi=\phi}$ and similarily for $W(\phi)_{,i,j}$.
[3] Notice that, $W(\Phi)$ is an analytic function of Φ^{i} (not $\bar{\Phi}_{i}$) only.

by eliminating the auxiliary fields F^i through their equations of motion:

$$F^i+W(\phi)^{,i^*}=0 \qquad (1.28.a)$$

$$F_i^*+W(\phi)_{,i}=0 \qquad (1.28.b)$$

thus eliminating the F^i dependence in our smultiplet Φ^i:

i.e.[4] $$\Phi^i\equiv(\psi_L^i,\phi^i). \qquad (1.29)$$

One can now make the observation that the algebra (1.24) necessarily implies that the component fields of (1.29) manifestly transform into one another under successive SUSY transformations. In fact, upon examination of (1.27.b) and (1.27.c), one can see that the m_{ij} in the super potential necessarily represents the smultiplet mass matrix as a whole, thus shedding light on relation (1.19).

Now that we have the N=1 SUSY Lagrangian for scalars and spinors, we are ready to introduce the gauge group, G. Therefore, consider an infinitesimal gauge transformation given by

$$\Lambda(L)=e^{i\bar{\theta}\cdot\bar{L}} \qquad (1.30)$$

where the θ^a are parameters of the Hermitian generators

---

[4] cf 1.18.b

$L^{ai}{}_{j}$, of the Lie group, G,

i.e. $$[L_a,L_b]=if^{c}{}_{ab}L_c \tag{1.31}$$

where $f^{c}{}_{ab}$ are the group structure constants. Taking the action (1.30) on the smultiplet (1.20) we obtain[5]

$$\delta\Phi=i\bar{\theta}\cdot\bar{L}\Phi. \tag{1.32}$$

As expected, since the component fields necessarily transform as

$$\delta\phi=i\bar{\theta}\cdot\bar{L}\phi \tag{1.33.a}$$

$$\delta\psi_L=i\bar{\theta}\cdot\bar{L}\psi_L \tag{1.33.b}$$

$$\delta F=i\bar{\theta}\cdot\bar{L}F. \tag{1.33.c}$$

Also a similar relation holds for smultiplet (1.21)

$$\delta\bar{\Phi}=-i\bar{\theta}\cdot\bar{L}^{T}\bar{\Phi}. \tag{1.34}$$

At this point we mention, without proof (CAM.82), that in order for L_{PE} and L_{YUK} to be invariant under G, we require that the coefficients C_i, m_{ij} and g_{ijk} in $W(\Phi)$ should transform as symmetric covariant tensors ($\Rightarrow C_i=0$ except for

---

[5] Where we have suppressed the smultiplet index.

gauge singlets.) To see what becomes of L_{KE}, we must first introduce vector smultiplets

$$V^a=(\chi^a,B^a_\mu,D^a) \tag{1.35}$$

where χ^a is a dim $\frac{3}{2}$ Majorana spinor, B^a_μ a dim 1 vector and D^a a dim 2 scalar field. The component fields of V^a transform under the adjoint representation of G as

$$\delta B^a_\mu=g^{-1}(D_\mu\theta)^a \tag{1.36.a}$$

$$\delta\chi^a=f^a{}_{bc}\chi^b\theta^c \tag{1.36.b}$$

$$\delta D^a=f^a{}_{bc}D^b\theta^c \tag{1.36.d}$$

where

$$(D_\mu\theta)^a=\partial_\mu\theta^a+gf^a{}_{bc}B^b_\mu\theta^c. \tag{1.37}$$

Since we are imposing local gauge invariance for the smultiplets, one might wonder what becomes of the algebra (1.15), or in particular, algebra (1.24). It turns out that the naive assumption

$$[\delta_1,\delta_2]=i\bar{\epsilon}_1\gamma^\mu\epsilon_2D_\mu \tag{1.38}$$

does the job. Equation (1.38) acts on both of the components

of Φ and V. The action of D_μ, on these components is given by (DEW.75)

$$(D_\mu \chi)^a = \partial_\mu \chi^a + g f^a{}_{bc} B^b_\mu \chi^c \tag{1.39.a}$$

$$(D_\mu B_\nu)^a \not= -F^a_{\mu\nu} \tag{1.39.b}$$

$$(D_\mu D)^a = \partial_\mu D^a + g f^a{}_{bc} B^b_\mu D^c \tag{1.39.c}$$

$$D_\mu \Phi = (\partial_\mu - ig\vec{L}\cdot\vec{B}_\mu)\Phi \tag{1.39.d}$$

$$D_\mu \bar{\Phi} = (\partial_\mu + ig\vec{L}^T\cdot\vec{B}_\mu)\bar{\Phi}. \tag{1.39.e}$$

where

$$F^a_{\mu\nu} = \partial_{[\mu} B^a_{\nu]} + g f^a{}_{bc} B^b_\mu \, B^c_\nu. \tag{1.40}$$

In order for the component fields to satisfy algebra (1.38), we must have

$$\delta\vec{B}_\mu = -\frac{1}{\sqrt{2}}\bar{\epsilon}\gamma_\mu\gamma_5\vec{\chi} \tag{1.41.a}$$

$$\delta\vec{\chi} = -\frac{i}{\sqrt{2}}(\frac{1}{2}\vec{F}_{\mu\nu}\gamma^\mu\gamma^\nu\gamma_5 + i\vec{D})\epsilon \tag{1.41.b}$$

$$\delta\vec{D} = -\frac{i}{\sqrt{2}}\bar{\epsilon}\not{\partial}\vec{\chi} \tag{1.41.c}$$

$$\delta\phi = \bar{\epsilon}\psi_L \tag{1.41.d}$$

$$\delta\psi_L = (F - i\not{\partial}\phi)_L\epsilon \tag{1.41.e}$$

$$\delta F = -i\bar{\epsilon}\not{\partial}\psi_L + \sqrt{2}g\bar{\epsilon}_L\vec{L}\cdot\vec{\chi}\phi. \tag{1.41.f}$$

The Lagrangian which obeys this symmetry requires some

modifications to (1.25). It suffices to say that we must replace L_{KE} by L_G, L_M and L_p, where

$$L_G=-\frac{1}{4}\vec{F}_{\mu\nu}\cdot\vec{F}^{\mu\nu}+\frac{1}{2}i\bar{\vec{\chi}}\cdot\not{D}\vec{\chi}+\frac{1}{2}\vec{D}\cdot\vec{D} \tag{1.42.a}$$

$$L_M=|(D_\mu\phi)_i|^2+i\bar{\psi}_{iL}(\not{D}\psi_L)^i+|F_i|^2-\sqrt{2}g\bar{\vec{\chi}}\cdot\phi_i^\dagger(\vec{L}\psi_L)^i$$

$$-\sqrt{2}g\bar{\psi}_{iL}(\vec{L}\phi)^i\cdot\bar{\vec{\chi}}+g(\phi^\dagger\vec{L})_i\cdot\phi^i\vec{D} \tag{1.42.b}$$

$$L_p=\vec{\zeta}\cdot\vec{D}. \tag{1.42.c}$$

The last term L_p is only permitted when the constants ζ^a satisfy the condition

$$f^a{}_{bc}\zeta^a=0 \tag{1.43}$$

for all b and c. This ensures that L_p is invariant under G⊗(N=1 SUSY) by selecting components D^a in invariant Abelian subgroups of the internal symmetry group.

Just as the F's satisfy equations (1.28) the D's satisfy

$$\vec{D}=-g\phi^\dagger\vec{L}\phi-\vec{\zeta}. \tag{1.44}$$

Thus eliminating the D and F fields through their equations of motion we finally obtain the full on shell (RAM.81) G⊗(N=1 SUSY) Lagrangian:

$$L_{SUSY}=L_{GAUGE}+L_{MATTER}+L_{YUKAWA}+L_{SCALAR} \tag{1.45}$$

where

$$L_G=-\frac{1}{4}\vec{F}_{\mu\nu}\cdot\vec{F}^{\mu\nu}+\frac{1}{2}i\vec{\bar{\chi}}\cdot\not{D}\vec{\chi} \tag{1.45.a}$$

$$L_M=|(D_\mu\phi)_i|^2+i\bar{\psi}_{iL}\not{D}^i_j\psi^j_L-\sqrt{2}g\vec{\bar{\chi}}\cdot\phi^\dagger_i\vec{\bar{L}}^i_j\psi^j_L-\sqrt{2}g\bar{\psi}_{iL}\vec{\bar{L}}^i_j\cdot\phi^j\vec{\chi} \tag{1.45.b}$$

$$L_Y=W(\phi)_{,i,j}(\psi^i_L)^TC^{-1}\psi^j_L-W(\phi)_{,i,j}{}^\dagger\bar{\psi}^j_LC(\bar{\psi}^i_L)^T \tag{1.45.c}$$

$$L_S=-|W(\phi)_{,i}|^2-\frac{1}{2}(g\phi^\dagger_i\vec{\bar{L}}^i_j\phi^j-\vec{\zeta})^2. \tag{1.45.d}$$

One can also impose a local SUSY structure, which further modifies the algebra (1.15) (MOH.86). Such modifications lead to the inclusion of a spin 2 graviton and its spartner the spin $\frac{3}{2}$ gravitino. We shall not go into the explicit construction here, nor state the full local SUSY Lagrangian (BAG.85), since it shall not be of any useful value to us in what lies ahead.

G. Remarks

The particle-sparticle spectrum predicted by equation (1.45), as suggested by relation (1.19), gives particles degenerate in mass with their spartners. However, as suggested in section (E), SUSY must be broken. From relation (1.13), we see that, naturalness constraints tell us sparticle masses can be no larger that O(1)TeV.

While searches for supersymmetry are underway (ELL.83B), theorists are busy calculating experimental consequences of the large phenomenological spectrum of reactions predicted by SUSY (HAB.85). One such place that is of interest, is toponium decay. Although some work has been done on toponium decay (DOB.88, ELL.83C, SCO.85,···), there still remain other possibilities to explore. Before delving into the various facets of toponium decay (chap. 3), it shall be necessary to take a brief look at broken SUSY phenomenology.

II. Broken SUSY

A. Introduction

As previously mentioned SUSY must be broken. The breaking should be at least enough to put the sparticles above experimental limits. Breaking can occur spontaneously, dynamically or by the inclusion of explicit 'soft' breaking terms. The various scenarios associated with these types of breaking represents a study in themselves, and therefore we refer you to various paraphernalia on the subject: ELL.85, ROS.85, MOH.86, ZUM.84, $\cdots$.

In what follows we shall be interested in low energy phenomenology ($O(10^2 GeV)$). Here, phenomenologically acceptable models have SUSY Lagrangians that contain spontaneously broken supergravity remnants (so to speak) which manifest themselves as explicit soft SUSY breaking terms.

B. Squark and Slepton Mass Matrices

In addition to mass terms m_{ij}, of the superpotential, one can obtain further contributions from its Yukawa terms. For example

$$W(\Phi) \sim g_{H\bar{q}q} \Phi_{q_L} \Phi_{q_L^c} \Phi_H, \qquad (2.1)$$

where

$$g_{H\bar{q}q}=\frac{1}{\sqrt{2}}gm_q/m_W. \tag{2.2}$$

In particular,

$$L_S \supseteq |g_{H\bar{q}q}|^2(|\tilde{q}_L H|^2+|\tilde{q}_L^c H|^2+|q_L q_L^c|^2) \tag{2.3}$$

leads to the following contribution to the $(\tilde{q}_L,\tilde{q}_R)$ mass matrix elements, for each flavour:

$$(\bar{\tilde{q}}_L \ \bar{\tilde{q}}_R)\begin{bmatrix} m_q^2 & 0 \\ 0 & m_q^2 \end{bmatrix}\begin{bmatrix} \tilde{q}_L \\ \tilde{q}_R \end{bmatrix}, \tag{2.4}$$

where

$$m_q=g_{H\bar{q}q}v \tag{2.5}$$

and

$$v=\langle H\rangle\equiv\langle 0|H|0\rangle. \tag{2.6}$$

Clearly matrix (2.4) can be simultaneously diagonalized in flavour space, and we find, as expected from (1.19), that

$$m_q=m_{\tilde{q}_{L,R}}. \tag{2.7}$$

A similar result also holds for the leptons. In general there are also extra contributions from the gauge

interaction terms

$$L_S \supseteq -\frac{1}{2}g^2(\phi^\dagger \bar{L}\phi - \bar{\xi})^2. \qquad (2.8)$$

However, these terms do not affect the problem at hand (E11.83A).

Since such degeneracies, as (2.7), are unacceptable experimentally, we must break SUSY. To do this, we add explicit soft SUSY breaking terms of the general form:

$$m_{\tilde{q}}^2|\tilde{q}|^2 + m_{\tilde{l}}^2|\tilde{l}|^2 + m_{\tilde{\nu}}^2|\tilde{\nu}|^2. \qquad (2.9)$$

Phenomenological considerations (E11.83A) severely constrain the form of the mass matrices (2.9). Ellis (E11.83A) assures us that such constraint problems can be avoided if we adopt the following ansatz:

$$m_{\tilde{q}}^2 = \tilde{m}^2 1 + C_2 m_q^2 + C_1 m_q \qquad (2.10)$$

where 1 is the unit matrix in flavour space, while $\tilde{m}^2$ and C_2 may differ between $\tilde{q}_L$ and $\tilde{q}_R$ and the C_1 term mixes L and R 'helicities'. If we now assume that we can write the squark matrix in flavour-diagonalized form, we obtain

$$(\bar{\tilde{q}}_L \; \bar{\tilde{q}}_R)\begin{bmatrix} \tilde{m}_L^2+C_{2_L}m_q^2 & C_1 m_q \\ C_1 m_q & \tilde{m}_R^2+C_{2_R}m_q^2 \end{bmatrix}\begin{bmatrix} \tilde{q}_L \\ \tilde{q}_R \end{bmatrix}. \qquad (2.11)$$

Terms such as (2.10) arise naturally from spontaneously broken supergravity models. In many of these models

$$\tilde{m}_L^2=L^2\tilde{m}^2,\ \tilde{m}_R^2=R^2\tilde{m}^2,\ C_1=A\tilde{m},\ C_{2_{L,R}}\approx 1 \qquad (2.12)$$

where $\tilde{m}=O(20\text{-}10^3)$GeV, $L^2\neq R^2$ in general and $A=O(1)$. Upon substitution of this into equation (2.11) we obtain

$$(\bar{\tilde{q}}_L \; \bar{\tilde{q}}_R)\begin{bmatrix} L^2\tilde{m}^2+m_q^2 & A\tilde{m}m_q \\ A\tilde{m}m_q & R^2\tilde{m}^2+m_q^2 \end{bmatrix}\begin{bmatrix} \tilde{q}_L \\ \tilde{q}_R \end{bmatrix}. \qquad (2.13)$$

This is the most general form of the squark mass matrix, since contributions such as (2.8) can be subsumed into a redefinition of the parmeters L, R and A.

The squark mass eigenstates

$$m_{\tilde{q}_{L,R}}^2=m_q^2+\left\{\frac{(L^2+R^2)\tilde{m}^2\pm\sqrt{(L^2-R^2)^2\tilde{m}^4+4A^2m_q^2\tilde{m}^2}}{2}\right\} \qquad (2.14)$$

are simply obtained by a 'helicity' diagonalization of mass matrix (2.13) through a $(\tilde{q}_L,\tilde{q}_R)$ rotation angle θ_{LR}:

$$\mathrm{Tan}2\theta_{LR}=\frac{-2Am_q}{(L^2-R^2)\tilde{m}} \qquad (2.15)$$

The SUSY breaking mass scale $\tilde{m} \geq 20$GeV is so large the L-R mixing (2.15) may be negligable with the exception being that of the heavy t quark.

C. Gaugino and Higgsino Mass Matrices

As mentioned before (§1.E), in order to give masses to all the quarks and leptons and to cancel out triangle anomalies, we need two Higgs chiral smultiplets which are weak isodoublets of equal and opposite hypercharge:

$$\begin{bmatrix} \Phi_{H_1^+} \\ \Phi_{H_1^0} \end{bmatrix}, \quad \begin{bmatrix} \Phi_{H_2^0} \\ \Phi_{H_2^-} \end{bmatrix}. \tag{2.16}$$

This can be seen as a direct consequence of the fact that $W(\Phi)$ is an analytic function of Φ only, and not $\bar{\Phi}$.

The Gaugino and Higgsino mass mixing matrices are determined by the Lagrangian terms

$$\epsilon(\tilde{H}_1^0\tilde{H}_2^0 - \tilde{H}_1^+\tilde{H}_2^-) + M_3(\tilde{g}^a\tilde{g}^a) + M_2\tilde{W}^a\tilde{W}^a + M_1\tilde{B}^0\tilde{B}^0, \tag{2.17}$$

where $\tilde{g}^a$, $\tilde{W}^a$ and $\tilde{B}^0$ (denote $SU_c(3)$, $SU_L(2)$ and $U_Y(1)$ gaugino fields respectively. If the standard $SU_c(3)\otimes SU_L(2)\otimes U_Y(1)$ model is to eventually be embedded in a grand unifying group, one would expect (ELL.83A):

$$M_3:M_2:M_1=\alpha_3:\alpha_2:\frac{5}{3}\alpha_1 \tag{2.18}$$

where α_i are the gauge coupling constants: $g_i^2/4\pi$ for i=1,2,3. In most models ϵ and M_2 are expected to be of $O(M_W)$. Using (2.17) along with the appropriate gaugino-Higgsino couplings,

$$-\sqrt{2}\, g\bar{\chi}^a\phi_i L^{ai}_{\ j}\psi^j_L+\text{H.C.}\subseteq L_M \tag{2.19}$$

obtained from (1.45), one can construct general gaugino-Higgsino mass mixing matrices.

For the charged fields we have (NAN.84)

$$(\tilde{W}^+,\ \tilde{H}_1^+)\begin{bmatrix} M_2 & g_2\nu_2 \\ g_2\nu_1 & -\epsilon \end{bmatrix}\begin{bmatrix} \tilde{W}^- \\ \tilde{H}_2^- \end{bmatrix} \tag{2.20}$$

where

$$<H^0_{1,2}>=\nu_{1,2} \tag{2.21}$$

such that $\nu_{1,2}$ satisfies

$$m_W^2=\frac{1}{2}g_2^2(\nu_1^2+\nu_2^2). \tag{2.22}$$

Matrix (2.20) can be diagonalized by rotations through angles $\theta_\pm$ among positively and negatively charged fields respectively, where

$$\text{Tan}\theta_{\pm}=\frac{b_{\pm}+\sqrt{b_{\pm}^2+4a_{\pm}^2}}{2a_{\pm}} \qquad (2.23)$$

with

$$a_{(\pm)}=M_2 g_2 \nu_{(\frac{1}{2})} - \epsilon g_2 \nu_{(\frac{2}{1})} \qquad (2.23.a)$$

$$b_{(\pm)}=M_2^2-\epsilon^2 \pm g_2^2(\nu_2^2-\nu_1^2). \qquad (2.23.b)$$

The mass eigenstates of the newly formed $\tilde{\chi}^{\pm}_{1,2}$ states are

$$m_1=M_2 C_+ C_- - g_2\nu_2 C_+ S_- - g_2\nu_1 S_+ C_- - \epsilon S_+ S_- \qquad (2.24.a)$$

and

$$m_2=M_2 S_+ S_- + g_2\nu_2 S_+ C_- + g_2\nu_1 C_+ S_- - \epsilon C_+ C_-, \qquad (2.24.b)$$

where $C_{\pm}$ and $S_{\pm}$ represent $\cos\theta_{\pm}$ and $\sin\theta_{\pm}$ respectively.

In the neutral sector we obtain the following $(\tilde{W}^3,\tilde{B}^0,\tilde{H}_1^0,\tilde{H}_2^0)$ mass mixing matrix (ELL.84):

$$(\tilde{W}^3,\tilde{B}^0,\tilde{H}_1^0,\tilde{H}_2^0)\begin{bmatrix} M_2 & 0 & -\frac{g_2\nu_1}{\sqrt{2}} & \frac{g_2\nu_2}{\sqrt{2}} \\ 0 & \frac{5a_1}{3a_2}M_2 & \frac{g_1\nu_1}{\sqrt{2}} & -\frac{g_1\nu_2}{\sqrt{2}} \\ -\frac{g_2\nu_1}{\sqrt{2}} & \frac{g_1\nu_1}{\sqrt{2}} & 0 & \epsilon \\ \frac{g_2\nu_2}{\sqrt{2}} & -\frac{g_1\nu_2}{\sqrt{2}} & \epsilon & 0 \end{bmatrix}\begin{bmatrix} \tilde{W}^3 \\ \tilde{B}^0 \\ \tilde{H}_1^0 \\ \tilde{H}_2^0 \end{bmatrix}. \qquad (2.25)$$

To diagonalize (2.25) we must use numerical methods. Since

H_1 gives mass to the charge $\frac{2}{3}$ and $m_c >> m_s$, $m_t >> m_b$, it seems reasonable to assume $v_1 \geq v_2$. This allows us to explore a more plausable region of the ϵ, M_2, v_1, v_2, parameter space. In figures (2.1) through (2.8), we examine this parameter space, for values of ϵ and M_2 near m_w and ratios of $v_1/v_2=1$, 4, for the two lightest neutralino eigenstates, $\tilde{\chi}^0_{1,2}$ (such that $m_1 \leq m_2$, $\tilde{\chi}^0_1 \equiv \tilde{\chi}^0$ and $\tilde{\chi}^0_2 \equiv \tilde{\chi}^{0'}$.)

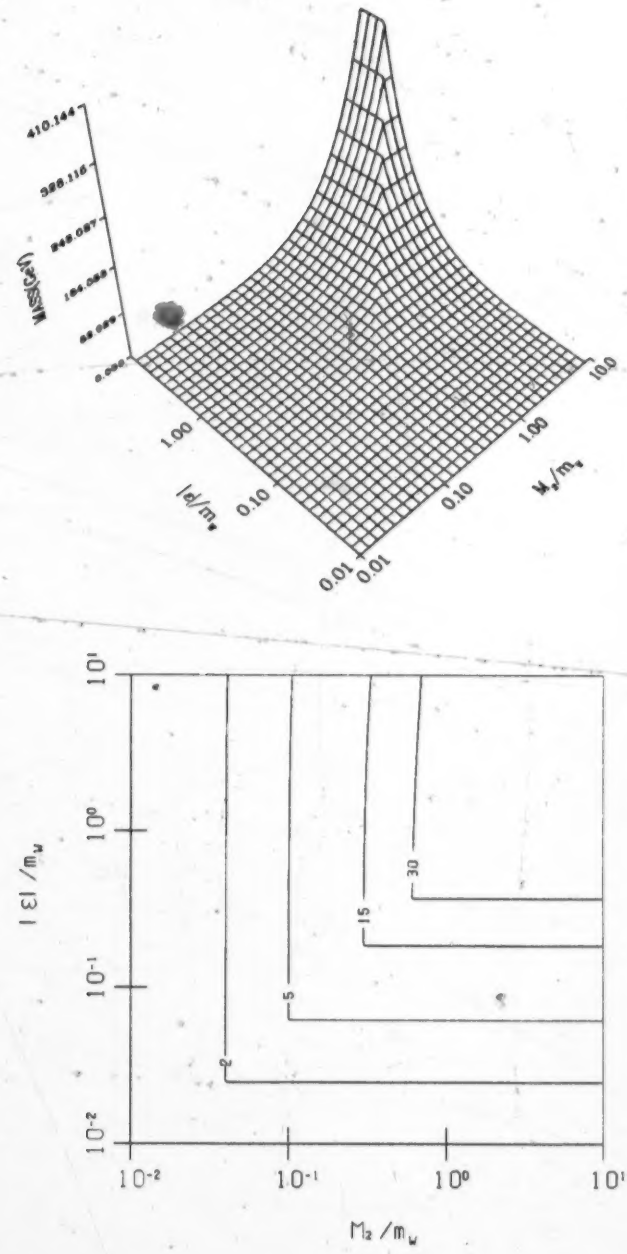

Fig. 2.1: Neutralino mass plots. 3D plot (top) and mass (GeV) contour plot (bottom) for the lightest $\tilde{\chi}^0$ state as a function of $|\epsilon|$ and M_2, for $v_1/v_2=1$ and $\epsilon>0$.

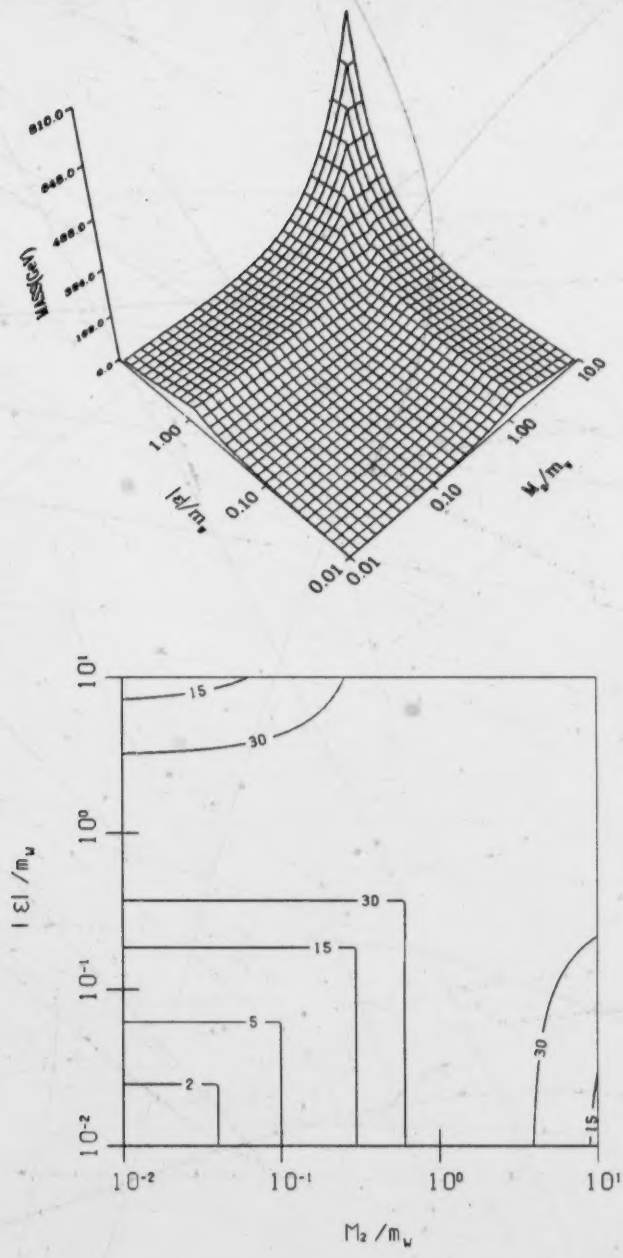

Fig. 2.2: Neutralino mass plots. 3D plot (top) and mass (GeV) contour plot (bottom) for the second lightest $\tilde{\chi}^0$ state as a function of $|\epsilon|$ and M_2, for $v_1/v_2=1$ and $\epsilon>0$.

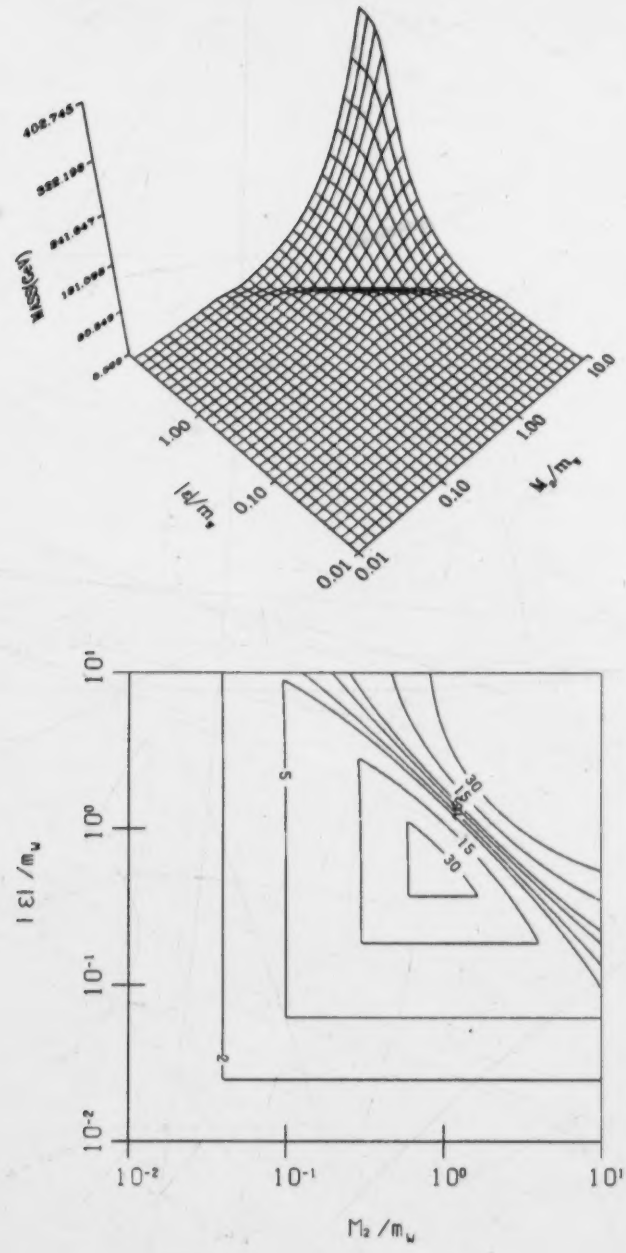

Fig. 2.3: Neutralino mass plots. 3D plot (top) and mass (GeV) contour plot (bottom) for the lightest $\tilde{\chi}^0$ state as a function of $|\epsilon|$ and M_2, for $v_1/v_2=1$ and $\epsilon<0$.

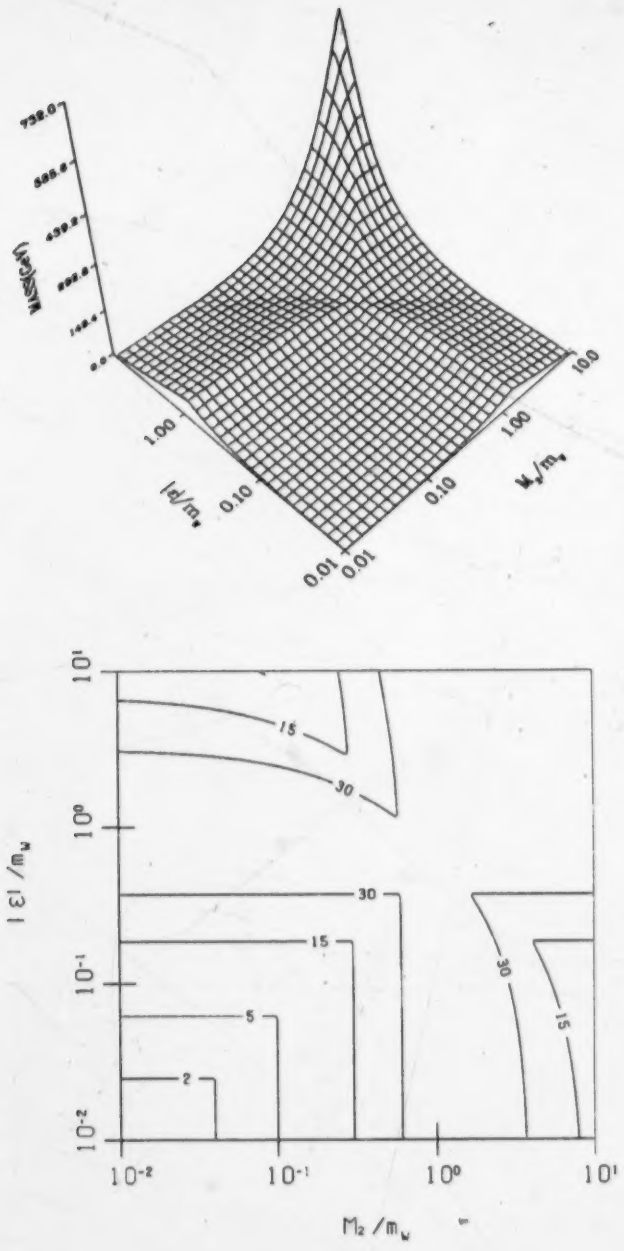

Fig. 2.4: Neutralino mass plots. 3D plot (top) and mass (GeV) contour plot (bottom) for the second lightest $\tilde{\chi}^0$ state as a function of $|\epsilon|$ and M_2, for $v_1/v_2=1$ and $\epsilon<0$.

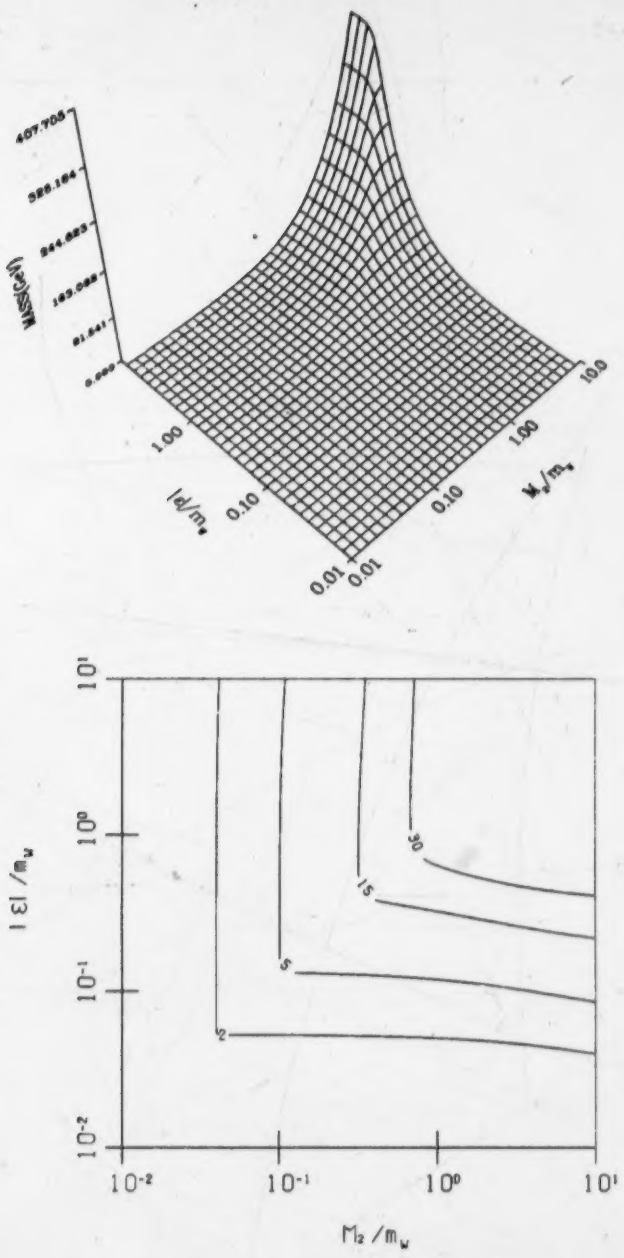

Fig. 2.5: Neutralino mass plots. 3D plot (top) and mass (GeV) contour plot (bottom) for the lightest $\tilde{\chi}^0$ state as a function of $|\epsilon|$ and M_2, for $v_1/v_2=4$ and $\epsilon>0$.

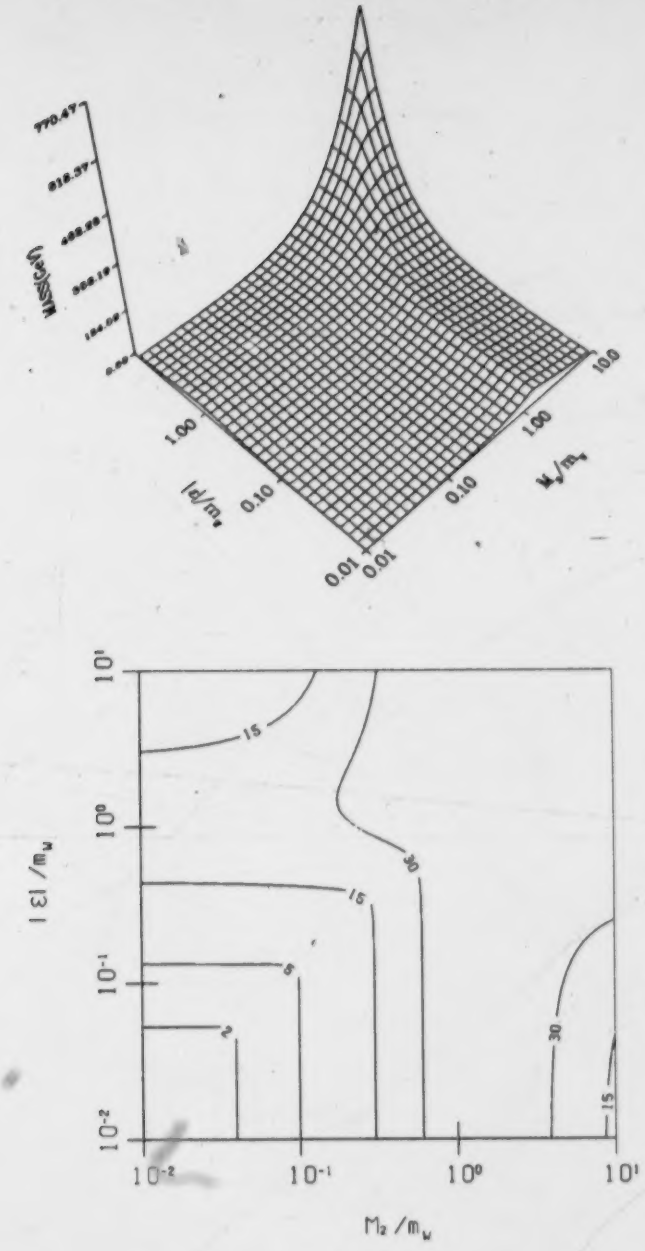

Fig. 2.6: Neutralino mass plots. 3D plot (top) and mass (GeV) contour plot (bottom) for the second lightest $\tilde{\chi}^0$ state as a function of $|\epsilon|$ and M_2, for $v_1/v_2=4$ and $\epsilon>0$.

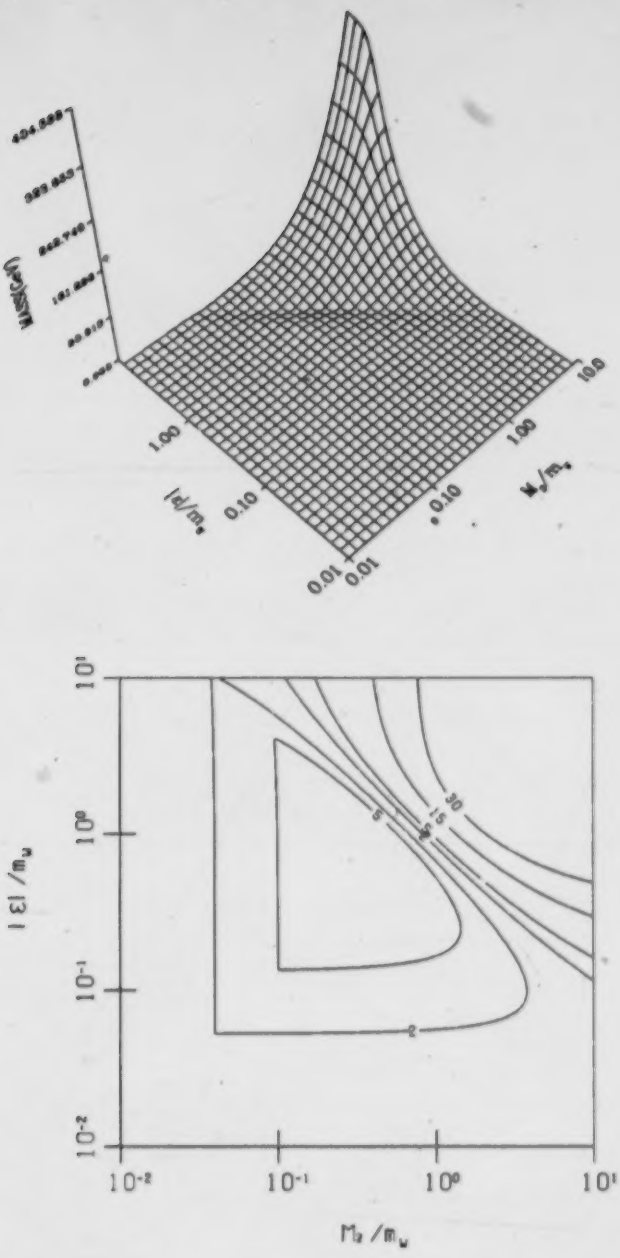

Fig. 2.7: Neutralino mass plots. 3D plot (top) and mass (GeV) contour plot (bottom) for the lightest $\tilde{\chi}^0$ state as a function of $|\epsilon|$ and M_2, for $v_1/v_2=4$ and $\epsilon<0$.

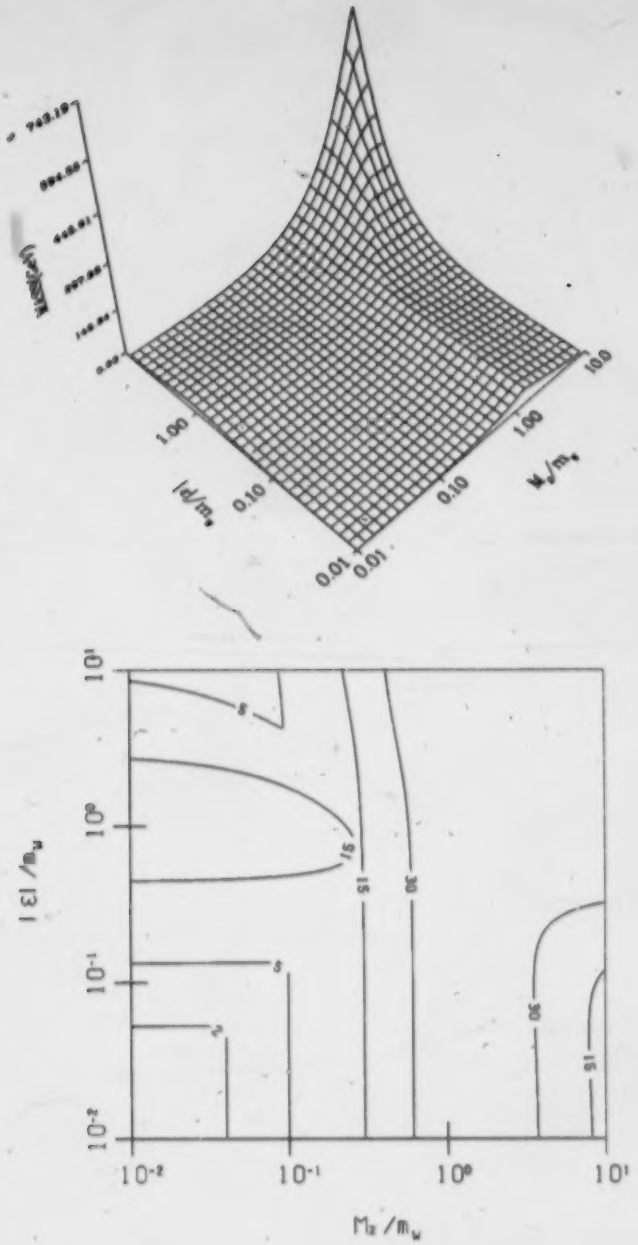

Fig. 2.8: Neutralino mass plots. 3D plot (top) and mass (GeV) contour plot (bottom) for the second lightest $\tilde{\chi}^0$ state as a function of $|\epsilon|$ and M_2, for $\nu_1/\nu_2=4$ and $\epsilon<0$.

From careful observation of these figures we see that typically there are two mass eigenstates ($\tilde{\chi}^0$ and $\tilde{\chi}^{0\prime}$) with mass < 30GeV when both M_2 and $\epsilon \lesssim O(m_w)$.

In the limit $\epsilon \longrightarrow 0$ mass matrix (25) gives us a light $\tilde{S}^0$ state

$$\tilde{S}^0 = \frac{v_2\tilde{H}_1^0 + v_1\tilde{H}_2^0}{v} \tag{2.26}$$

with mass equal to $2v_1v_2\epsilon/v^2$, where $v^2 = v_1^2 + v_2^2$. In the limit $M_2 \longrightarrow 0$ we obtain a light photino eigenstate

$$\tilde{\gamma} = \frac{g_1\tilde{W}^3 + g_2\tilde{B}^0}{\sqrt{g_1^2 + g_2^2}} \tag{2.27}$$

with mass

$$m_{\tilde{\gamma}} = \frac{8}{3}\frac{g_1^{\,2}}{g_1^{\,2} + g_2^{\,2}}M_2. \tag{2.28}$$

Finally, if we take both M_2 and ϵ to be small we obtain two mass eigenstates,

$$\tilde{Z}_{\pm}^0 = \frac{g_1\tilde{B}^0 - g_2\tilde{W}^3 \pm \sqrt{g_1^2 + g_2^2}\,\tilde{A}^0}{\sqrt{2(g_1^2 + g_2^2)}} \tag{2.29}$$

with mass $O(M_z)$, and

$$\tilde{A}^0 = \frac{v_1\tilde{H}_1^0 - v_2\tilde{H}_2^0}{v}. \qquad (2.30)$$

D. An Extra U(1)

So far we have only considered the minimal $SU_C(3)\otimes SU_L(2)\otimes U_Y(1)$ standard model, but there also exist models with an extra U(1). In particular, models which give further support for supersymmetry, are superstrings. This is due to fact that many of the superstring theories predict the existence of supersymmetry at accelerator energies.

In short, some approaches to superstrings predict as a minimal possible gauge group $SU_C(3)\otimes SU_L(2)\otimes U_Y(1)\otimes U_E(1)$ (CAM.86). Here, the new particles of interest are the $\tilde{N}$ Higgsino and $\tilde{B}_E$ gaugino which are a direct consequence of superstrings tagging on an extra $U_E(1)$. The inclusion of these new particles extends our previous neutral sector to a $(\tilde{W}_3,\tilde{B}^0,\tilde{H}_1^0,\tilde{H}_2^0,\tilde{B}_E,\tilde{N})$ basis. The mass mixing matrix (2.25) now becomes

$$(\tilde{W}^3,\tilde{B}^0,\tilde{H}_1^0,\tilde{H}_2^0,\tilde{B}_E,\tilde{N})\begin{bmatrix} M_2 & 0 & -\frac{g_2v_1}{\sqrt{2}} & \frac{g_2v_2}{\sqrt{2}} & 0 & 0 \\ 0 & \frac{5a_1}{3a_2}M_2 & \frac{g_1v_1}{\sqrt{2}} & -\frac{g_1v_2}{\sqrt{2}} & 0 & 0 \\ -\frac{g_2v_1}{\sqrt{2}} & \frac{g_1v_1}{\sqrt{2}} & 0 & \lambda x & -\frac{4}{3}\frac{g_1v_1}{\sqrt{2}} & \lambda v_2 \\ \frac{g_2v_2}{\sqrt{2}} & -\frac{g_1v_2}{\sqrt{2}} & \lambda x & 0 & -\frac{1}{3}\frac{g_1v_2}{\sqrt{2}} & \lambda v_1 \\ 0 & 0 & -\frac{4}{3}\frac{g_1v_1}{\sqrt{2}} & -\frac{1}{3}\frac{g_1v_2}{\sqrt{2}} & \frac{5a_1}{3a_2}M_2 & \frac{5}{3}\frac{g_1x}{\sqrt{2}} \\ 0 & 0 & \lambda v_2 & \lambda v_1 & \frac{5}{3}\frac{g_1x}{\sqrt{2}} & 0 \end{bmatrix}\begin{bmatrix} \tilde{W}^3 \\ \tilde{B}^0 \\ \tilde{H}_1^0 \\ \tilde{H}_2^0 \\ \tilde{B}_E \\ \tilde{N} \end{bmatrix}. \qquad (2.31)$$

In this model the values of the parameters ν_1, ν_2 and λ (the $H\bar{H}N$ superpotential coupling) are believed to lie in the ranges

$$1.7 \leq \frac{\nu_1}{\nu_2} \leq 5 \qquad (2.32)$$

and

$$0.10 \leq \lambda \leq 0.25. \qquad (2.33)$$

Figures (2.9) through (2.14) show graphs for the two lightest $\tilde{\chi}^0$ states, of mass matrix (2.31), for M_2 and λx (where $x \equiv \langle 0|N|0\rangle$) of $O(m_w)$, λ=0.1,0.18,0.25, and ν_1/ν_2=3.4.

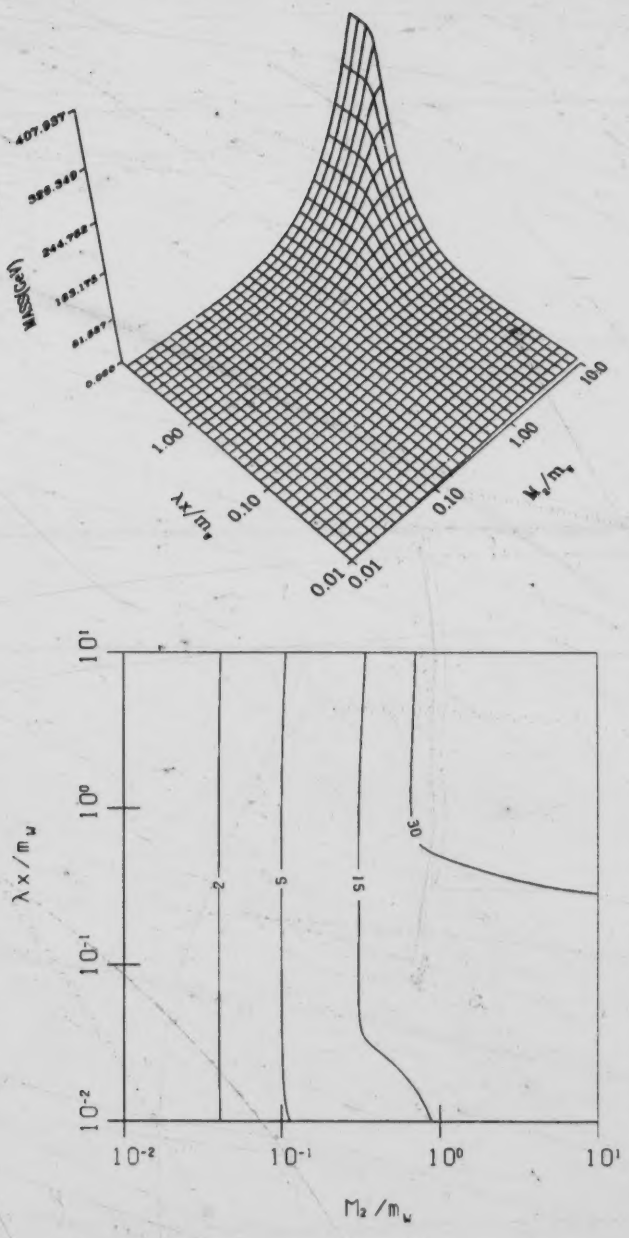

Fig. 2.9: Neutralino mass plots with an extra U(1). 3D plot (top) and mass (GeV) contour plot (bottom) for the lightest $\tilde{\chi}^0$ state as a function of x and M_2, for v_1/v_2=3.4 and λ=0.10.

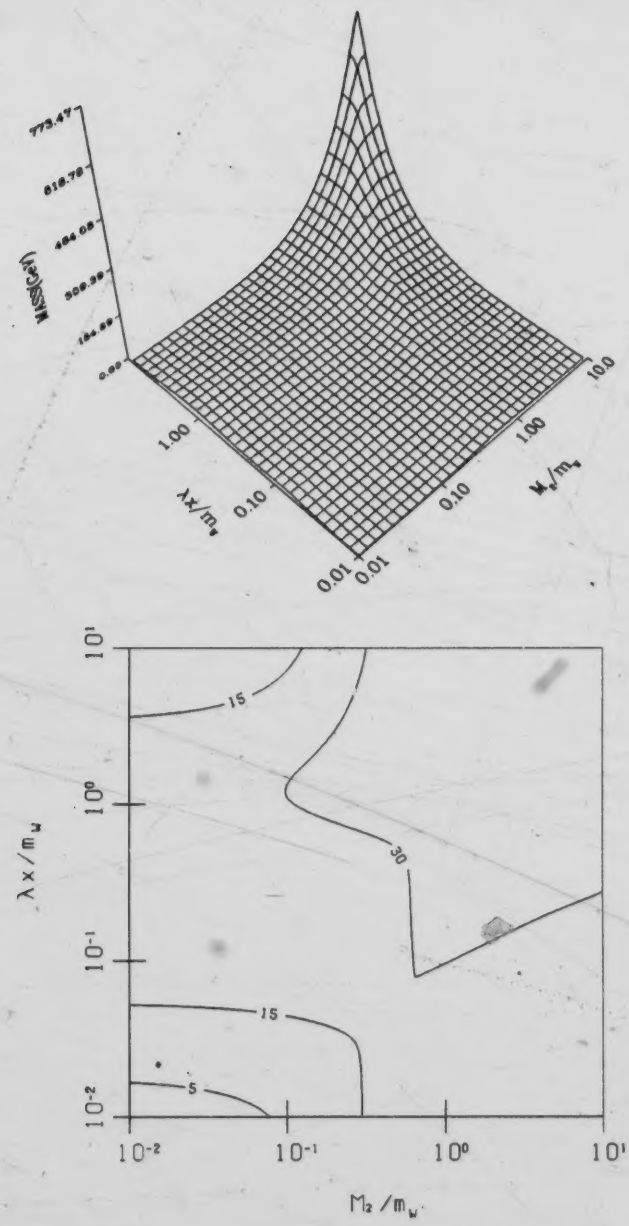

Fig. 2.10: Neutralino mass plots with an extra U(1). 3D plot (top) and mass (GeV) contour plot (bottom) for the second lightest $\tilde{\chi}^0$ state as a function of x and M_2, for v_1/v_2=3.4 and λ=0.10.

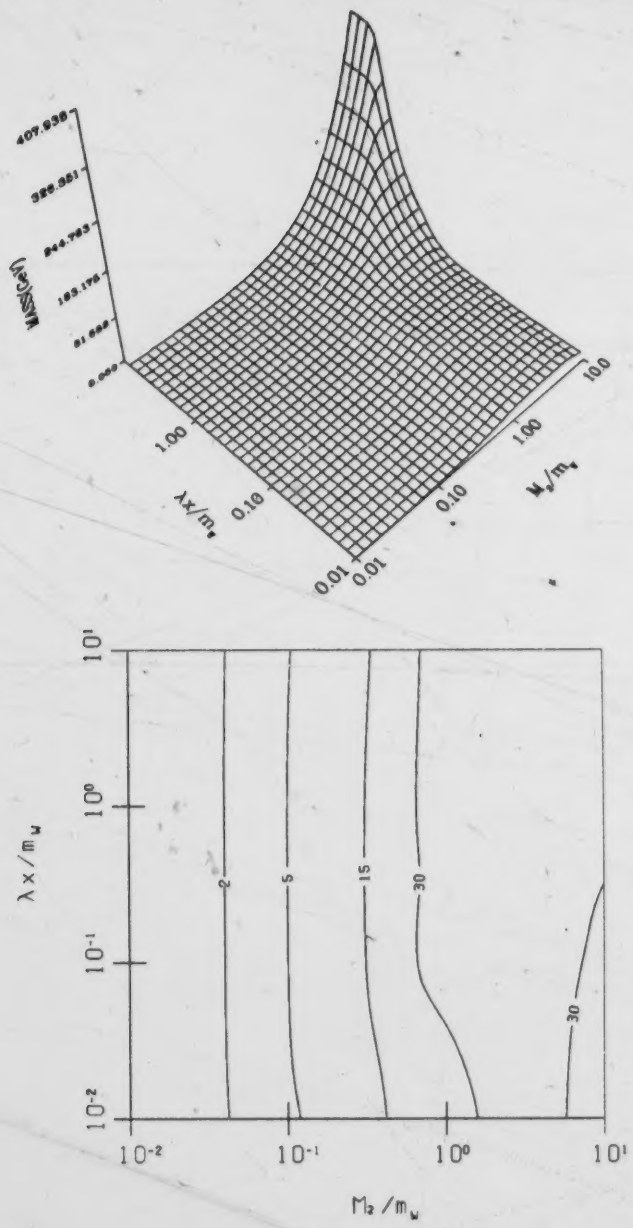

Fig. 2.11: Neutralino mass plots with an extra U(1). 3D plot (top) and mass (GeV) contour plot (bottom) for the lightest $\tilde{\chi}^0$ state as a function of x and M_2, for v_1/v_2=3.4 and λ=0.18.

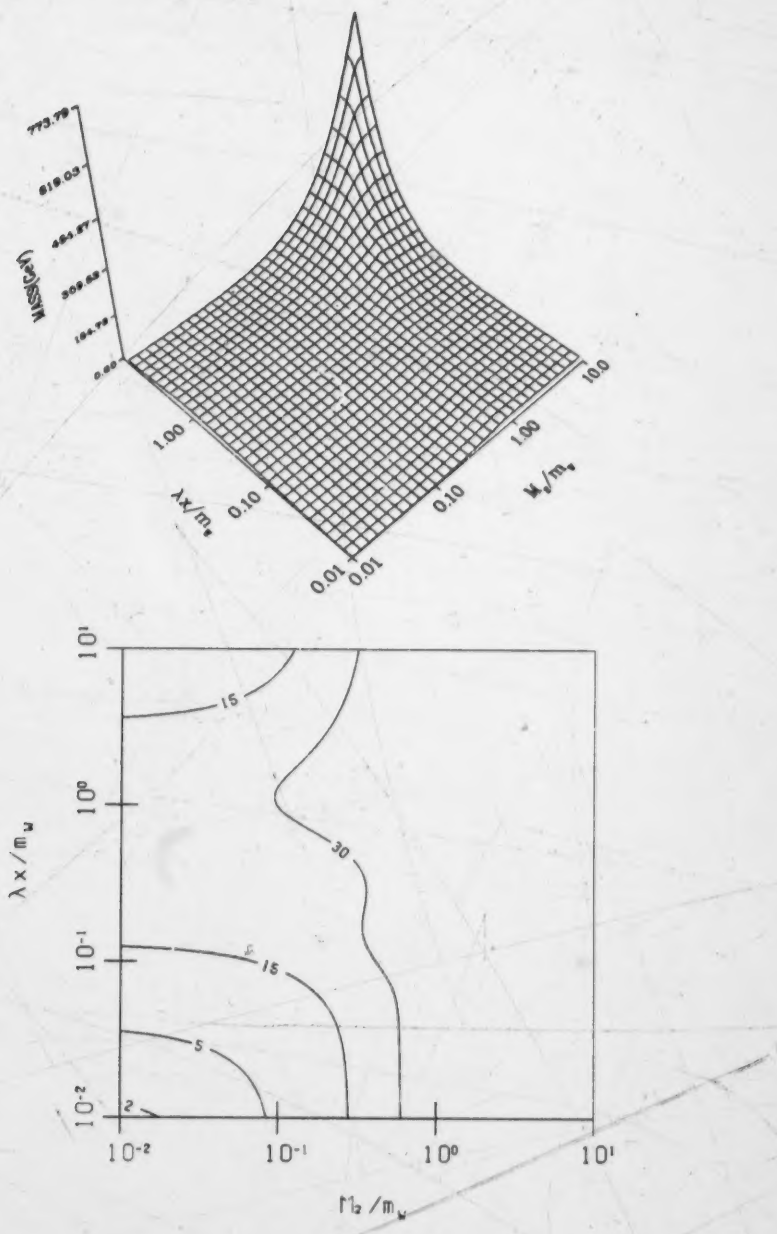

Fig. 2.12: Neutralino mass plots with an extra U(1). 3D plot (top) and mass (GeV) contour plot (bottom) for the second lightest $\tilde{\chi}^0$ state as a function of x and M_2, for v_1/v_2=3.4 and λ=0.18.

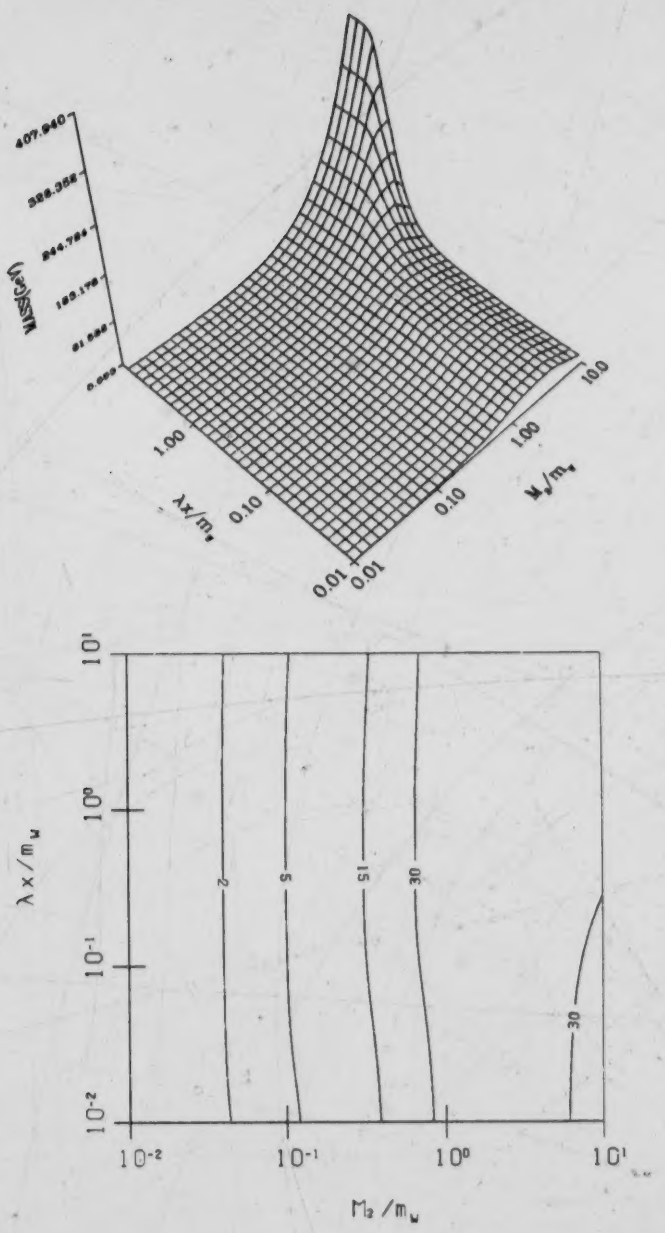

Fig. 2.13: Neutralino mass plots with an extra U(1). 3D plot (top) and mass (GeV) contour plot (bottom) for the lightest $\tilde{\chi}^0$ state as a function of x and M_2, for v_1/v_2=3.4 and λ=0.25.

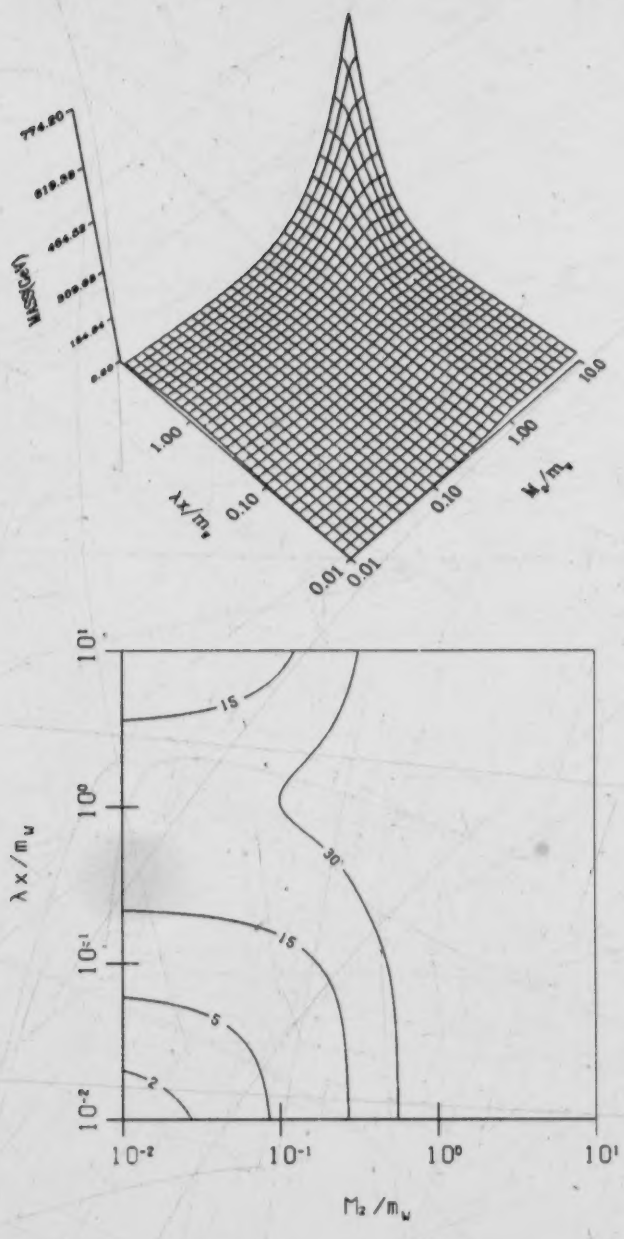

Fig. 2.14: Neutralino mass plots with an extra U(1). 3D plot (top) and mass (GeV) contour plot (bottom) for the second lightest $\tilde{\chi}^0$ state as a function of x and M_2, for v_1/v_2=3.4 and λ=0.25.

Similar observations, that where made for figures (2.1) through (2.8), can also be made for figures (2.9) through (2.14). In addition to these observations, if one were to overlay figures (2.1), (2.2), (2.5) and (2.6) on top of figures (2.9) through (2.14), one would observe striking similarities between plots with the same mass states. This of course is not too suprising, since one would expect only a slight enhancement to mass matrix (2.25), upon extension of the neutral sector.

E. Remarks

In section (B) we mentioned that L-R mixing (2.15) should be negligible with the exception of the heavy quark. Although the t quark has not yet been found, various experimental and theoretical findings seem to suggest that it should lie somewhere between 44Gev and 200GeV[1]. With such a large top mass one can now see how it contributes to large L-R mixing.

The decay mode of toponium, in which we are interested, is to two light $\tilde{\chi}^0$ states, hence the introduction of the various mass plots in section (C) and (D), which shall be used for later comparison with decay plots of chapter 3.

With this at hand, we are now ready to turn to toponium decay.

---

[1]See ALT.87, CUD.87A,B , HE.87, ...

III. Toponium Decay

A. Introduction

It is thought that quarkonia might be a possible hunting ground for SUSY. Why? Consider, for example the standard model decay of figure 3.1.

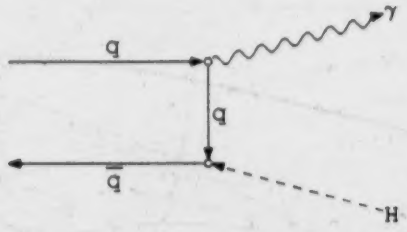

FIG. 3.1. Quarkonia to photon, Higgs.

Here, the Hqq vertex goes as the quark mass m_q (cf 2.5). It follows, from such simple arguments, that the Higgs should couple quite well to heavy quarkonia and so under exact SUSY, such reactions should also hold equally well for the corresponding spartner diagrams in figure 3.2.

FIG. 3.2. Quarkonia to photino, Higgsino.

However, as previously suggested, SUSY must be broken. In general, this means that the $\tilde{\gamma}$ and $\tilde{H}$ states will mix as shown in figure 3.3.

FIG. 3.3. Quarkonia to neutralino, neutralino'.

The amount of mixing is determined by the various free parameters of mass matrix (2.25) or (2.31), depending on your preference. So as one can see, broken SUSY washes away the dominant $\tilde{H}\tilde{q}q$ coupling. This at first may seem a bit disappointing. However, the amount of erosion occurring to the $\tilde{H}\tilde{q}q$ coupling depends on where it lies in the ϵ (or λx), M_2 parameter space. So, as suggested by (2.26) and (2.27), there should exist regions in this parameter space in which one can recover $\tilde{\gamma}$ and $\tilde{H}$-like interactions. In fact, there may even exist regions which enhance the $\tilde{H}\tilde{q}q$ coupling.

At present we have not found any scalar Higgs phenomenology associated with quarkonia, although many believe it should occur upon discovery of toponium. Taking this on faith leads one to believe the aforementioned SUSY phenomenology should also occur.

Here, we wish to examine neutralino production (fig 3.3). Since this is effectively a local interaction, one expects the radial excitations (P-states) to be suppressed (SCO.85). This leaves us to consider the $^1S_0$ and $^3S_1$ states. Computation of $^1S_0$ can be dispensed with, since quarkonia

production processes occur dominantly via S-channel intermediate vector bosons.

For $^3S_1$ processes one also picks up, in addition to figure 3.3, a Z-pole contribution from the diagram of figure 3.4.

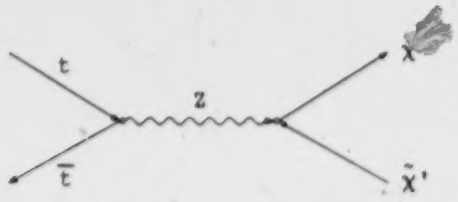

FIG. 3.4. Toponium via Z to neutralino pairs.

The Z^0 couples only to the Higgsino content of the neutralinos. Therefore the strength of the coupling depends on where the $\tilde{\chi}^0$ lies in the ϵ(or λx)-M_2, v_1/v_2 parameter space. For instance if $v_1/v_2=1$, then for identical neutralinos the $Z\tilde{\chi}\tilde{\chi}$ coupling (i.e. proportional to equation 3.55, such that γ_i and δ_i are defined by equation 3.5) goes to zero.

B. Toponium Decay Calculation

In order to calculate $t\bar{t}\rightarrow\tilde{\chi}_i\tilde{\chi}_j$ via the SUSY $SU_L(2)\otimes U_Y(1)$ Model, we consider the following SUSY Lagrangian mass term,

$$L_M \sim \tilde{\xi}^T M \tilde{\xi}, \qquad (3.1)$$

where

$$\tilde{\xi}^T \equiv (\tilde{W}^3, \tilde{B}^0, \tilde{H}_1^0, \tilde{H}_2^0) \tag{3.2}$$

and M is our $\tilde{\xi}$ mass mixing matrix (2.25).

Since M is a real symmetric matrix, one can diagonalize it by using an orthogonal similarity transformation. Under such a transformation the Lagrangian becomes

$$L_{M^D} \sim (U\tilde{\xi})^T (UMU^T)(U\tilde{\xi}) \equiv \tilde{\chi}^T M^D \tilde{\chi} \tag{3.3}$$

where the matrix U is defined by

$$U_{i1} = \alpha_i, \quad U_{i2} = \beta_i, \quad U_{i3} = \gamma_i, \quad U_{i4} = \delta_i \tag{3.4}$$

which implies

$$\tilde{\chi}_i \equiv \alpha_i \tilde{W}^3 + \beta_i \tilde{B}^0 + \gamma_i \tilde{H}_1^0 + \delta_i \tilde{H}_2^0. \tag{3.5}$$

Therefore, given

$$\tilde{\chi}_i = U_{ij} \tilde{\xi}_j, \tag{3.6}$$

we find our fields are shifted by

$$\tilde{\xi}_i = (U^T)_{ij} \tilde{\chi}_j. \tag{3.7}$$

Or more explicitly

$$\tilde{W}^3=\alpha_i\tilde{\chi}_i \qquad (3.8.a)$$

$$\tilde{B}^0=\beta_i\tilde{\chi}_i \qquad (3.8.b)$$

$$\tilde{H}_1^0=\gamma_i\tilde{\chi}_i \qquad (3.8.c)$$

$$\tilde{H}_2^0=\delta_i\tilde{\chi}_i . \qquad (3.8.d)$$

Stop squark exchange amplitude

Using equations (3.8) along with our SUSY Lagrangian (1.45), we find for gaugino interactions

$$L_{int}^{\tilde{G}}\sim-\sqrt{2}[g\bar{\tilde{W}}^3\phi_{\tilde{t}_L}^{\dagger}T_L^3L\psi_t+g'\bar{\tilde{B}}^0\phi_{\tilde{t}_L}^{\dagger}(Q_t-T_L^3)L\psi_t]$$

$$-\sqrt{2}[g\bar{\tilde{W}}^3\phi_{\tilde{t}_R}^{\dagger}T_R^3R\psi_t-g'\bar{\tilde{B}}^0\phi_{\tilde{t}_R}^{\dagger}(Q_t-T_R^3)R\psi_t]$$

$$+H.C. \qquad (3.9)$$

$$=-\sqrt{2}\bar{\tilde{\chi}}_i[\frac{1}{2}(\alpha_i g+\frac{1}{3}\beta_i g')L\tilde{t}_L^{\dagger}-\frac{2}{3}\beta_i g'R\tilde{t}_R^{\dagger}]t+H.C. \qquad (3.10)$$

where

$$Q_t=\frac{2}{3},\quad T_R^3=0,\quad T_L^3=\frac{1}{2}\begin{bmatrix}1 & 0\\ 0 & -1\end{bmatrix},\quad \psi_t=\tilde{\phi}_{\tilde{t}}\equiv\begin{bmatrix}t\\ 0\end{bmatrix}. \qquad (3.11)$$

The Higgsino interaction terms are obtained through the use of the superpotential term

$$W \sim g_{H_i^0 \tilde{t} t} \Phi_{t_L} \Phi_{t_L^c} \Phi_{H_{iL}^0} \tag{3.12}$$

where

$$\Phi_{t_L} = (t, \tilde{t})_L, \quad \Phi_{t_L^c} = (t^c, \tilde{t}^c)_L, \quad \Phi_{H_{iL}^0} = (\tilde{H}_1^0, H_1^0)_L \tag{3.13}$$

and

$$g_{H_i^0 \tilde{t} t} = \frac{1}{\sqrt{2}} g \frac{m_t}{m_W} \left[1 + \frac{1}{(v_1/v_2)^2} \right]^{1/2} . \tag{3.14}$$

Inserting this into equation (1.45.c) yields [1]

$$L_{int}^{\tilde{H}} \sim g_{H_i^0 \tilde{t} t} (\tilde{t}_L^c t_L^T C^{-1} \tilde{H}_{1L}^0 + \tilde{t}_L^{c*} \tilde{H}_{1L}^{0\dagger} C t_L^* + \tilde{t}_L \tilde{H}_{1L}^{0T} C^{-1} t_L^c + \tilde{t}_L^* t_L^{c\dagger} C \tilde{H}_{1L}^{0*}) \tag{3.15}$$

$$= -g_{H_i^0 \tilde{t} t} (\tilde{t}_L^c \bar{t}^c \tilde{H}_{1L}^0 + \tilde{t}_L^{c*} \bar{\tilde{H}}_1^0 t_R^c + \tilde{t}_L \bar{\tilde{H}}_1^{0c} t_L^c + \tilde{t}_L^* \bar{t}^c \tilde{H}_{1R}^{0c}) \tag{3.16}$$

Given $\tilde{H}_1^{0c} = \tilde{H}_1^0$, $\tilde{t}_{L,R}^* \equiv \tilde{t}_{R,L}^c$ and $\bar{\psi}_1^c P_{R,L} \psi_2^c = \bar{\psi}_2 P_{R,L} \psi_1$, we get [2]

$$L_{int}^{\tilde{H}} \sim -g_{H_i^0 \tilde{t} t} \tilde{t}_{R,L} \bar{t} P_{R,L} \tilde{H}_1^0 + H.C. \tag{3.17}$$

Using equation (3.8) gives

$$L_{int}^{\tilde{H}} \sim -g_{H_i^0 \tilde{t} t} \bar{t} \gamma_i P_{L,R} \tilde{t}_{R,L} \tilde{\chi}_i + H.C. \tag{3.18}$$

---

[1] Where $\bar{\psi}^c = \psi^{c\dagger} \gamma_0$.

[2] Using the label sum convention; $A_{a,b,\ldots} B_{i,j,\ldots} = A_a B_i + A_b B_j + \ldots$

Thus, using equations (3.10) and (3.18), we obtain the stop squark contribution to the interaction Lagrangian

$$L_{int} \sim -\sqrt{2}\tilde{t}_L \bar{t}[a_i R + b_i L]\tilde{x}_i - \sqrt{2}\tilde{t}_L^{\dagger}\bar{\tilde{x}}_i[a_i L + b_i R]t$$

$$-\sqrt{2}\tilde{t}_R \bar{t}[c_i L + b_i R]\tilde{x}_i - \sqrt{2}\tilde{t}_R^{\dagger}\bar{\tilde{x}}_i[c_i R + b_i L]t \qquad (3.19)$$

where

$$a_i = \frac{1}{2}(\alpha_i g + \frac{1}{3}\beta_i g') \qquad (3.20.a)$$

$$b_i = g_{H_i^0 \tilde{t} t}\gamma_i/\sqrt{2} \qquad (3.20.b)$$

$$c_i = -\frac{2}{3}g'\beta_i . \qquad (3.20.c)$$

The Feynman rules, which we now list in table (3.1) below, can be readily obtained from equation (3.19).

TABLE 3.1. Stop Squark exchange Feynman Rules.

t-Channel	u-Channel
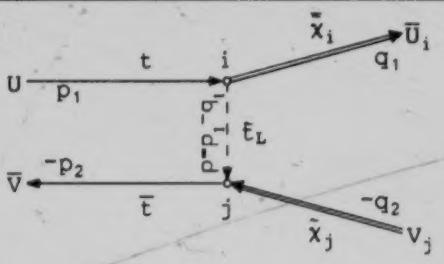	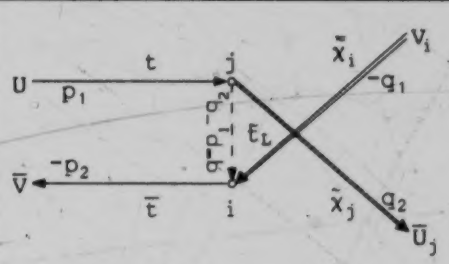
i-Vertex: $-i\sqrt{2}\,\bar{\tilde{x}}_i[a_iL+b_iR]t$	i-Vertex: $-i\sqrt{2}\,\bar{t}[a_iR+b_iL]\tilde{x}_i$
j-Vertex: $-i\sqrt{2}\,\bar{t}[a_jR+b_jL]\tilde{x}_j$	j-Vertex: $-i\sqrt{2}\,\bar{\tilde{x}}_j[a_jL+b_jR]t$
Prop: $i\Delta^p_L = \dfrac{i}{p^2-m_L^2}$	Prop: $i\Delta^q_L = \dfrac{i}{q^2-m_L^2}$
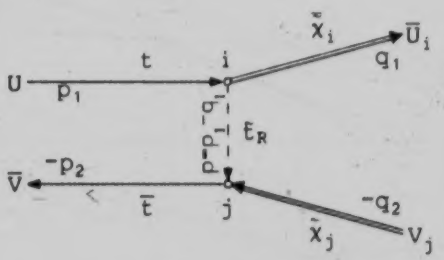	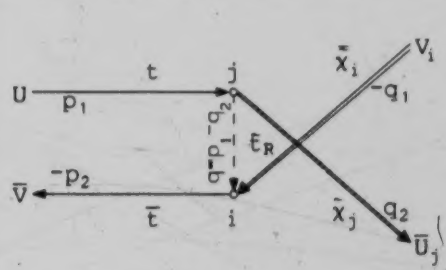
i-Vertex: $-i\sqrt{2}\,\bar{\tilde{x}}_i[c_iR+b_iL]t$	i-Vertex: $-i\sqrt{2}\,\bar{t}[c_iL+b_iR]\tilde{x}_i$
j-Vertex: $-i\sqrt{2}\,\bar{t}[c_jL+b_jR]\tilde{x}_j$	j-Vertex: $-i\sqrt{2}\,\bar{\tilde{x}}_j[c_jR+b_jL]t$
Prop: $i\Delta^p_R = \dfrac{i}{p^2-m_R^2}$	Prop: $i\Delta^q_R = \dfrac{i}{q^2-m_R^2}$

Using the Feynman rules given in table (3.1), we get the following amplitude[3]

$$M^{\tilde{t}}_{ij} \equiv M(t\bar{t} \to \tilde{x}_i \tilde{x}_j : \text{via } \tilde{t})$$

$$= -2i\{\bar{U}_i(q_1)[a_i L + b_i R]U(p_1)\Delta_L^p \bar{V}(p_2)[a_j R + b_j L]V_j(q_2)$$

$$-\bar{U}_j(q_2)[a_j L + b_j R]U(p_1)\Delta_L^q \bar{V}(p_2)[a_i R + b_i L]V_i(q_1)$$

$$+\bar{U}_i(q_1)[c_i R + b_i L]U(p_1)\Delta_R^p \bar{V}(p_2)[c_j L + b_j R]V_j(q_2)$$

$$-\bar{U}_j(q_2)[c_j R + b_j L]U(p_1)\Delta_R^q \bar{V}(p_2)[c_i L + b_i R]V_i(q_1)\} \qquad (3.21)$$

$$= -2i\{[a_i a_j \Delta_L^p + b_i b_j \Delta_R^p]\bar{U}_i(q_1)LU(p_1)\bar{V}(p_2)RV_j(q_2)$$

$$+[a_i b_j \Delta_L^p + b_i c_j \Delta_R^p]\bar{U}_i(q_1)LU(p_1)\bar{V}(p_2)LV_j(q_2)$$

$$+[b_i a_j \Delta_L^p + c_i b_j \Delta_R^p]\bar{U}_i(q_1)RU(p_1)\bar{V}(p_2)RV_j(q_2)$$

$$+[b_i b_j \Delta_L^p + c_i c_j \Delta_R^p]\bar{U}_i(q_1)RU(p_1)\bar{V}(p_2)LV_j(q_2)$$

$$-[a_i a_j \Delta_L^q + b_i b_j \Delta_R^q]\bar{U}_j(q_2)LU(p_1)\bar{V}(p_2)RV_i(q_1)$$

$$-[b_i a_j \Delta_L^q + c_i b_j \Delta_R^q]\bar{U}_j(q_2)LU(p_1)\bar{V}(p_2)LV_i(q_1)$$

---

[3] The relative minus signs in equation (3.21) can be obtained by a simple Wick expansion.

$$-[a_i b_j \Delta_L^q + b_i c_j \Delta_R^q]\bar{U}_j(q_2)RU(p_1)\bar{V}(p_2)RV_i(q_1)$$

$$-[b_i b_j \Delta_L^q + c_i c_j \Delta_R^q]\bar{U}_j(q_2)RU(p_1)\bar{V}(p_2)LV_i(q_1)\}. \qquad (3.22)$$

Applying Fierz transformations (C.14) through (C.17), we get

$$M_{ij}^{\tilde{t}} = -i\{[a_i a_j \Delta_L^p + b_i b_j \Delta_R^p]\bar{U}_i(q_1)\gamma_\mu RV_j(q_2)\bar{V}(p_2)\gamma^\mu LU(p_1)$$

$$+[a_i b_j \Delta_L^p + b_i c_j \Delta_R^p][\bar{U}_i(q_1)LV_j(q_2)\bar{V}(p_2)LU(p_1)$$

$$+\tfrac{1}{4}\bar{U}_i(q_1)L\sigma_{\mu\nu}V_j(q_2)\bar{V}(p_2)\sigma^{\mu\nu}U(p_1)]$$

$$+[b_i a_j \Delta_L^p + c_i b_j \Delta_R^p][\bar{U}_i(q_1)RV_j(q_2)\bar{V}(p_2)RU(p_1)$$

$$+\tfrac{1}{4}\bar{U}_i(q_1)R\sigma_{\mu\nu}V_j(q_2)\bar{V}(p_2)\sigma^{\mu\nu}U(p_1)]$$

$$+[b_i b_j \Delta_L^p + c_i c_j \Delta_R^p]\bar{U}_i(q_1)\gamma_\mu LV_j(q_2)\bar{V}(p_2)\gamma^\mu RU(p_1)$$

$$-[a_i a_j \Delta_L^q + b_i b_j \Delta_R^q]\bar{U}_j(q_2)\gamma_\mu RV_i(q_1)\bar{V}(p_2)\gamma^\mu LU(p_1)$$

$$-[b_i a_j \Delta_L^q + c_i b_j \Delta_R^q][\bar{U}_j(q_2)LV_i(q_1)\bar{V}(p_2)LU(p_1)$$

$$+\tfrac{1}{4}\bar{U}_j(q_2)L\sigma_{\mu\nu}V_i(q_1)\bar{V}(p_2)\sigma^{\mu\nu}U(p_1)]$$

$$-[a_i b_j \Delta_L^q + b_i c_j \Delta_R^q][\bar{U}_j(q_2)RV_i(q_1)\bar{V}(p_2)RU(p_1)$$

$$+\tfrac{1}{4}\bar{U}_j(q_2)R\sigma_{\mu\nu}V_i(q_1)\bar{V}(p_2)\sigma^{\mu\nu}U(p_1)]$$

$$-[b_ib_j\Delta_L^q+c_ic_j\Delta_R^q]\bar{U}_j(q_2)\gamma_\mu LV_i(q_1)\bar{V}(p_2)\gamma^\mu RU(p_1)\}. \qquad (3.23)$$

Using equation (B.7) and properties (A.17) through (A.20) we note that for an arbitrary 4×4 matrix O_k

$$\begin{aligned}\bar{U}_i(q_1)O_kV_j(q_2)&=\overline{C\bar{V}_i(q_1)^TO_kC\bar{U}_j(q_2)^T}\\&=-V_i(q_1)^TC^{-1}O_kC\bar{U}_j(q_2)^T\\&=-(\bar{U}_j(q_2)(C^{-1}O_kC)^TV_i(q_1))^T\\&=-\bar{U}_j(q_2)CO_k^TC^{-1}V_i(q_1) \qquad (3.24)\end{aligned}$$

where our $CO_k^TC^{-1}$ terms are given by

$$C(P_{R,L})^TC^{-1}=P_{R,L} \qquad (3.25)$$

$$C(\gamma_\mu P_{R,L})^TC^{-1}=-P_{R,L}\gamma_\mu \qquad (3.26)$$

$$C(P_{R\,L}\sigma_{\mu\nu})^TC^{-1}=-P_{R,L}\sigma_{\mu\nu}. \qquad (3.27)$$

Therefore our amplitude now becomes

$$M_{ij}^{\tilde{t}}=-i\{[a_ia_j\Delta_L^p+b_ib_j\Delta_R^p]\bar{U}_j(q_2)\gamma_\mu LV_i(q_1)\bar{V}(p_2)\gamma^\mu LU(p_1)$$

$$-[a_i a_j \Delta_L^q + b_i b_j \Delta_R^q]\bar{U}_j(q_2)\gamma_\mu R V_i(q_1)\bar{V}(q_2)\gamma^\mu L U(p_1)$$

$$-[(a_i b_j \Delta_L^p + b_i c_j \Delta_R^p) + (b_i a_j \Delta_L^q + c_i b_j \Delta_R^q)]\bar{U}_j(q_2) L V_i(q_1)\bar{V}(p_2) L U(p_1)$$

$$+\frac{1}{4}[(a_i b_j \Delta_L^p + b_i c_j \Delta_R^p) - (b_i a_j \Delta_L^q + c_i b_j \Delta_R^q)]$$

$$\circ \bar{U}_j(q_2) L \sigma_{\mu\nu} V_i(q_1)\bar{V}(p_2)\sigma^{\mu\nu} U(p_1)$$

$$-[(b_i a_j \Delta_L^p + c_i b_j \Delta_R^p) + (a_i b_j \Delta_L^q + b_i c_j \Delta_R^q)]\bar{U}_j(q_2) R V_i(q_1)\bar{V}(p_2) R U(p_1)$$

$$+\frac{1}{4}[(b_i a_j \Delta_L^p + c_i b_j \Delta_R^p) - (a_i b_j \Delta_L^q + b_i c_j \Delta_R^q)]$$

$$\circ \bar{U}_j(q_2) R \sigma_{\mu\nu} V_i(q_1)\bar{V}(p_2)\sigma^{\mu\nu} U(p_1)$$

$$+[b_i b_j \Delta_L^p + c_i c_j \Delta_R^p]\bar{U}_j(q_2)\gamma_\mu R V_i(q_1)\bar{V}(p_2)\gamma^\mu R U(p_1)$$

$$-[b_i b_j \Delta_L^q + c_i c_j \Delta_R^q]\bar{U}_j(q_2)\gamma_\mu L V_i(q_1)\bar{V}(p_2)\gamma^\mu R U(p_1)\}. \qquad (3.28)$$

Since the top quark is very massive, we find for low energy toponium

$$\Delta_{R,L}^p \sim \Delta_{R,L}^q \sim -m_{R,L}^{-2}. \qquad (3.29)$$

Therefore, using N.R. approximations (B.17) through (B.21), we have

$$M^{\tilde{t}}_{ij} \sim \frac{i}{2m_{RL}^2}\{A_{ij}\bar{U}_j(q_2)\gamma_\mu RV_i(q_1)(\phi^\dagger\sigma^i\chi\delta^\mu_i+\phi^\dagger\chi\delta^\mu_0)$$

$$-B_{ij}\bar{U}_j(q_2)\gamma_\mu RV_i(q_1)(\phi^\dagger\sigma^i\chi\delta^\mu_i-\phi^\dagger\chi\delta^\mu_0)$$

$$-(C_{ij}+D_{ij})\bar{U}_j(q_2)LV_i(q_1)\phi^\dagger\chi$$

$$-i(C_{ij}-D_{ij})\bar{U}_j(q_2)L\sigma^{0i}V_i(q_1)\phi^\dagger\sigma_i\chi$$

$$+(D_{ij}+C_{ij})\bar{U}_j(q_2)RV_i(q_1)\phi^\dagger\chi$$

$$-i(D_{ij}-C_{ij})\bar{U}_j(q_2)R\sigma^{0i}V_i(q_1)\phi^\dagger\sigma_i\chi$$

$$+B_{ij}\bar{U}_j(q_2)\gamma_\mu LV_i(q_1)(\phi^\dagger\sigma^i\chi\delta^\mu_i-\phi^\dagger\chi\delta^\mu_0)$$

$$-A_{ij}\bar{U}_j(q_2)\gamma_\mu LV_i(q_1)(\phi^\dagger\sigma^i\chi\delta^\mu_i+\phi^\dagger\chi\delta^\mu_0)\}, \qquad (3.30)$$

where

$$A_{ij}=b_ib_jm_R^2+c_ic_jm_L^2 \qquad (3.31.a)$$

$$B_{ij}=a_ia_jm_R^2+b_ib_jm_L^2 \qquad (3.31.b)$$

$$C_{ij}=a_ib_jm_R^2+b_ic_jm_L^2 \qquad (3.31.c)$$

$$D_{ij}=b_ia_jm_R^2+c_ib_jm_L^2 \qquad (3.31.d)$$

and

$$m_{RL} \equiv m_R m_L . \tag{3.32}$$

Using table (B.1) we find for a $^3S_1$ toponium (or orthotoponium, θ) state

$$^{3}s_{1}M^{\tilde{t}}_{ij} \sim \frac{-i}{2m_{RL}^{2}} \bar{U}_j(q_2)[(A_{ij}-B_{ij})(\gamma_1+i\gamma_2)R+i(C_{ij}-D_{ij})L(\sigma^{01}+i\sigma^{02})$$

$$+i(D_{ij}-C_{ij})R(\sigma^{01}+i\sigma^{02})+(B_{ij}-A_{ij})(\gamma_1+i\gamma_2)L]V_i(q_1) \tag{3.33}$$

$$=\frac{-i}{2m_{RL}^{2}} \bar{U}_j(q_2)[X_{ij}(\gamma_1+i\gamma_2)-iY_{ij}(\sigma^{01}+i\sigma^{02})]\gamma_5 V_i(q_1) \tag{3.34}$$

where

$$X_{ij} \equiv A_{ij}-B_{ij} \tag{3.35.a}$$

$$Y_{ij} \equiv C_{ij}-D_{ij} . \tag{3.35.b}$$

Using the definition of σ^{0i}, (A.12), and the algebra (A.8), we find

$$\sigma^{0i} \equiv i\gamma^0\gamma^i \tag{3.36}$$

which reduces (3.34) to

$$^{3}s_{1}M^{\tilde{t}}_{ij} \sim \frac{i}{2m_{RL}^{2}} \bar{U}_j(q_2)(X_{ij}-\gamma^0 Y_{ij})(\gamma^1+i\gamma^2)\gamma_5 V_i(q_1) . \tag{3.37}$$

Z-exchange amplitude

Consider the following diagram.

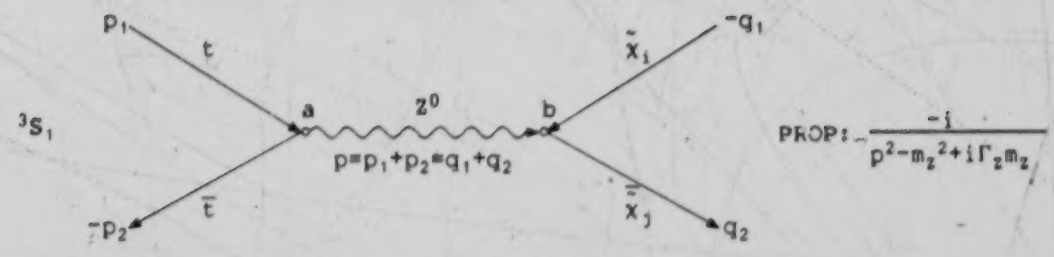

FIG. 3.5. Z exchange Feynman diagram.

To find the appropriate vertex couplings for this contribution to the amplitude we consider the following SUSY Lagrangian (see equation 1.45) term

$$L_M \supseteq i\bar{\psi}_{i_L} \not{\partial}^i_j \psi^j_L. \tag{3.38}$$

For an SU(2)⊗U(1) model, our covariant derivative is given by

$$D_\mu \psi = (\partial_\mu - \frac{i}{2} g' B_\mu Y - ig\vec{T}\cdot\vec{W}_\mu)\psi \tag{3.39}$$

where

$$\vec{T} = \frac{1}{2}\vec{\tau}. \tag{3.40}$$

Therefore the interaction Lagrangian that will give us the Z couplings, is

$$L_{Z\bar{t}t} \sim \frac{1}{2}\bar{\psi}_{i_L}(g' \not{B}^0 Y + g \not{W}^3_\mu \tau^3)^i_j \psi^j_L. \tag{3.41}$$

For the $Z\bar{t}t$ couplings we have

$$L_{Z\bar{t}t} \sim \frac{1}{2}\bar{\psi}_t \left(g' B^0 Y_L + g W_\mu^3 \tau_L^3\right) L\psi_t + \frac{1}{2} g' \bar{\psi}_t^c B^0 Y_L^c L \psi_t^c \qquad (3.42)$$

where $Y_L^c \equiv -Y_R$ ($Y=2(Q-T^3)$). The other terms are defined in equations (3.11) and (3.40). Noting that

$$\bar{\psi}_1^c \gamma^\mu P_{R,L} \psi_2^c = -\bar{\psi}_2 \gamma^\mu P_{L,R} \psi_1, \qquad (3.43)$$

we obtain

$$L_{Z\bar{t}t} \sim \frac{1}{2}\bar{t}\left[\left(\frac{1}{3}g' B^0 + g W^3\right) L + \frac{4}{3} g' B^0 R\right] t. \qquad (3.44)$$

Using the change of basis

$$B^0 = \hat{g} A - \hat{g}' Z \qquad (3.45.a)$$

$$W^3 = \hat{g}' A + \hat{g} Z \qquad (3.45.b)$$

where

$$\hat{g} \equiv \frac{g}{\sqrt{g^2+g'^2}} = \cos\theta_W \qquad (3.46.a)$$

$$\hat{g}' \equiv \frac{g'}{\sqrt{g^2+g'^2}} = \sin\theta_W \qquad (3.46.b)$$

and discarding the photon couplings, we get

$$L_{Z\tilde{t}t} \sim \frac{1}{2}\bar{t}Z[(g\hat{g}-\frac{1}{3}g'\hat{g}')L-\frac{4}{3}g'\hat{g}'R]t \tag{3.47}$$

$$=\frac{g}{6\cos\theta_W}Z_\mu \bar{t}\gamma^\mu[3L-4x_W]t. \tag{3.48}$$

Therefore vertex 'a' is given by

$$\frac{ig}{6\cos\theta_W}\bar{t}\gamma^\mu[3L-4x_W]t. \tag{3.49}$$

For the $Z\tilde{X}\tilde{X}'$ coupling we have

$$L_{Z\tilde{X}\tilde{X}'} \sim \frac{1}{2}\sum_{i=1,2}\bar{\psi}_{\tilde{H}_i^0}(g'\not{B}^0 Y_L + g\tau_L^3 \not{W}^3)L\psi_{\tilde{H}_i^0} \tag{3.50}$$

where

$$Y_L=-\tau_L^3,\quad \psi_{\tilde{H}_1^0}=\begin{bmatrix}0\\ \tilde{H}_1^0\end{bmatrix},\quad \psi_{\tilde{H}_2^0}=\begin{bmatrix}\tilde{H}_2^0\\ 0\end{bmatrix}. \tag{3.51}$$

Plugging this in, we find

$$L_{Z\tilde{X}\tilde{X}'} \sim -\frac{1}{2}\bar{\tilde{H}}_1^0(g'\not{B}^0-g\not{W}^3)L\tilde{H}_1^0-\frac{1}{2}\bar{\tilde{H}}_2^0(g'\not{B}^0-g\not{W}^3)L\tilde{H}_2^0. \tag{3.52}$$

Performing the change of bases (3.46) and (3.8), we find

$$L_{Z\tilde{X}\tilde{X}'} \sim -\frac{1}{2}\bar{\tilde{X}}_i Z_{ij}[g'(\hat{g}\not{X}-\hat{g}'\not{Z})-g(\hat{g}'\not{X}+\hat{g}\not{Z})]L\tilde{X}_j \tag{3.53}$$

$$=-\frac{1}{2}(g/\cos\theta_W)Z_{ij}\bar{\tilde{X}}_i \not{Z} L\tilde{X}_j \tag{3.54}$$

where

$$Z_{ij}=\gamma_i\gamma_j-\delta_i\delta_j. \tag{3.55}$$

Using equation (3.43) along with the property $\tilde{x}^c=\tilde{x}$, we find

$$L_{Z\tilde{x}\tilde{x}}\sim-\frac{1}{4}(g/\cos\theta_W)Z_{ij}\bar{\tilde{x}}_i\not{Z}(L-R)\tilde{x}_j \tag{3.56}$$

$$=\frac{1}{4}(g/\cos\theta_W)Z_{ij}Z_\mu\bar{\tilde{x}}_i\gamma^\mu\gamma_5\tilde{x}_j. \tag{3.57}$$

Therefore vertex 'b' is given by

$$\frac{ig}{4\cos\theta_W}Z_{ij}\bar{\tilde{x}}_i\gamma^\mu\gamma_5\tilde{x}_j. \tag{3.58}$$

Using Feynman rules (3.49) and (3.58) along with the propagator given in figure (3.5), we find our Z-exchange amplitude is given by

$$M^Z_{ij}\sim\frac{ig^2}{12\cos^2\theta_W(S-m_Z{}^2+i\Gamma_Z m_Z)}\bar{V}(p_2)\gamma^\mu(3L-4x_W)U(p_1)$$

$$\cdot\bar{U}_j(q_2)\gamma_\mu\gamma_5V_i(q_1). \tag{3.59}$$

Using N.R. approximations (B.18) and (B.19) we find that

$$\bar{V}(p_2)\gamma^\mu(3L-4x_W)U(p_1)\sim-\frac{3}{2}\phi^\dagger\chi\delta^\mu_0+\frac{3}{2}\phi^\dagger\sigma^i\chi\delta^\mu_i-4\phi^\dagger\sigma^i\chi\delta^\mu_i x_W. \tag{3.60}$$

For a $^3S_1$ state we find, via table (B.1), that (3.60) simplifies to

$$-\frac{1}{2}(3-8x_W).(\delta_1^\mu+i\delta_2^\mu) \tag{3.61}$$

and so

$$^{3S_1}M_{ij}^Z \sim \frac{ig^2(3-8x_W)Z_{ij}}{24\cos^2\theta_W(S-m_Z{}^2+i\Gamma_Z m_Z)}\bar{U}_j(q_2)(\gamma^1+i\gamma^2)\gamma_5 V_i(q_1). \tag{3.62}$$

Total amplitude

Adding (3.37) and (3.62) together we obtain our total amplitude

$$^{3S_1}M_{ij} \sim i\bar{U}_j(q_2)(R_+-\gamma^0 C)(\gamma^1+i\gamma^2)\gamma_5 V_i(q_1) \tag{3.63}$$

where

$$R_\pm \equiv A+\frac{B}{\delta \pm i\epsilon} \tag{3.64.a}$$

$$\delta = S-m_Z^2 \tag{3.64.b}$$

$$\epsilon = \Gamma_Z m_Z \tag{3.64.c}$$

$$A=\frac{X_{ij}}{2m_{RL}{}^2} \tag{3.64.d}$$

$$B=\frac{g^2(3-8x_W)Z_{ij}}{24.(1-x_W)} \tag{3.64.e}$$

$$C=\frac{Y_{ij}}{2m_{RL}{}^2}. \tag{3.64.f}$$

Noting that

$$\sum_f|\bar{U}_l(q_2)O_iV_k(q_1)|^2=\frac{1}{4m_{kl}}\mathrm{Tr}O_i(\not{q}_1-m_k)\bar{O}_i(\not{q}_2+m_l) \tag{3.65}$$

where

$$m_{kl}\equiv m_km_l \tag{3.66}$$

we find, via (A.22) and (A.25),

$$|{}^{3s_1}M_{ij}|^2\sim\frac{(1-\frac{1}{2}\delta_{ij})}{4m_{ij}}\mathrm{Tr}(R_+-\gamma^0C)(\gamma^1+i\gamma^2)(\not{q}_1+m_i)$$
$$\circ(R_-+\gamma^0C)(\gamma^1-i\gamma^2)(\not{q}_2+m_j) \tag{3.67}$$

where the $(1-\frac{1}{2}\delta_{ij})$ is to take care of identical particles. Using algebra (A.8) our trace term in (3.67) can be arranged as

$$\mathrm{Tr}(R_+-\gamma^0C)(\gamma^1+i\gamma^2)[(\not{q}_1+m_i)(\gamma^1-i\gamma^2)](R_-\gamma^0C)(\not{q}_2+m_j). \tag{3.68}$$

Observing that

$$\not{a}\gamma^{\mu}=2a^{\mu}-\gamma^{\mu}\not{a} \tag{3.69}$$

allows us to reduce the term in the square brackets, '[]', of (3.68), to

$$2(q_1^1-iq_1^2)-(\gamma^1-i\gamma^2)(\not{q}_1-m_i). \tag{3.70}$$

Putting (3.70) back into (3.68), we find that the first term of (3.70), gives

$$2(q_1^1-iq_1^2)\mathrm{Tr}[R_{+-}+\gamma^0C(R_+-R_-)\rightarrow C^2](\gamma^1+i\gamma^2)(\not{q}_2+m_j) \tag{3.71}$$

where

$$R_{+-}\equiv R_+R_-=A^2+\frac{(B+2\delta A)B}{\delta^2+\epsilon^2}. \tag{3.72}$$

Using trace theorem (A.32), (3.71) becomes

$$2(q_1^1-iq_1^2)\mathrm{Tr}(\gamma^1+i\gamma^2)[\Lambda_-\not{q}_2-\gamma^0C(R_+-R_-)m_j] \tag{3.73}$$

where

$$\Lambda_{\pm}\equiv R_{+-}\pm C^2. \tag{3.74}$$

The final result for (3.73) is obtained by an application of trace theorem (A.30):

$$8(q_1^1-iq_1^2)(q_2^1+iq_2^2)\Lambda_-. \qquad (3.75)$$

The second term in (3.70) gives rise, in equation (3.68), to the term

$$2Tr(1+i\gamma^1\gamma^2)[(R_+-\gamma^0C)(\not q_1-m_i)(R_--\gamma^0C)(\not q_2+m_j)]. \qquad (3.76)$$

Using theorem (A.32), the term in the square brackets, '[]', of (3.76) becomes

$$R_{+-}\not q_1\not q_2-m_jC(\not q_1\gamma^0R_++\gamma^0\not q_1R_-)-m_{ij}\Lambda_+$$

$$+m_iC\gamma^0\not q_2(R_++R_-)+C^2\gamma^0\not q_1\gamma^0\not q_2. \qquad (3.77)$$

Since this is part of (3.76) we are permitted to make the following transformation

$$-m_jC(\not q_1\gamma^0R_++\gamma^0\not q_1R_-) \longrightarrow -m_j\gamma^0\not q_1\Sigma_{+-} \qquad (3.78)$$

where

$$\Sigma_{+-}\equiv C(R_++R_-)=2C\left[A+\frac{\delta B}{\delta^2+\epsilon^2}\right]. \qquad (3.79)$$

Using this transformation, along with (3.69), (3.77) simplifies to

$$\Lambda_{-}\not{q}_1\not{q}_2+\Sigma_{+-}\gamma^0(m_i\not{q}_2-m_j\not{q}_1)-m_{ij}\Lambda_{+}+2E_1C^2\gamma^0\not{q}_2 \qquad (3.80)$$

where $q_1^0\equiv E_1$ and $q_2^0\equiv E_2$. Throwing (3.80) back into (3.79) we obtain

$$8[q_1\cdot q_2\Lambda_{-}+(m_iE_2-m_jE_1)\Sigma_{+-}-m_{ij}\Lambda_{+}+2E_1E_2C^2]$$

$$+2Tr\{i\gamma^1\gamma^2\not{q}_1\not{q}_2\Lambda_{-}-\gamma_5\gamma^3[(m_i\not{q}_2-m_j\not{q}_1)\Sigma_{+-}+2E_1C^2\not{q}_2]\} \qquad (3.81)$$

where we used theorems (A.29) and (A.30). Using theorems (A.31) and (A.35), the trace term of (3.80) becomes

$$8i[q_2^1q_1^2-q_1^1q_2^2]\Lambda_{-}. \qquad (3.82)$$

Finally, placing (3.82) back into (3.81), and then adding (3.81) and (3.75), gives us the final form of (3.67):

$$|^{3s_1}M_{ij}|^2\sim\frac{2(1-\frac{1}{2}\delta_{ij})}{m_{ij}}[(E_1E_2-m_{ij})\Lambda_{+}+(m_iE_2-m_jE_1)\Sigma_{+-}-q_1^3q_2^3\Lambda_{-}] \qquad (3.83)$$

Consider the following centre of mass diagram:

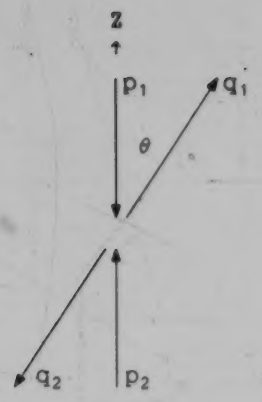

where

$p_1^2=p_2^2=m_t^2$

$q_1^2=m_i^2$

$q_2^2=m_j^2$

$\bar{p}_1=-\bar{p}_2$ & $m_t=m_{\bar{t}} \Rightarrow E_t=E_{\bar{t}}$

$\bar{q}_1=-\bar{q}_2$

Fig. 3.6. Toponium decay in C of M system.

Using C of M coordinates our decay amplitude (3.83) now becomes,

$$|^{3s_1}M_{ij}|^2 \sim \frac{2(1-\frac{1}{2}\delta_{ij})}{m_{ij}}[(E_1E_2-m_{ij})\Lambda_+$$

$$+(m_iE_2-m_jE_1)\Sigma_{+-}+|\bar{q}_1|^2\Lambda_-\cos^2\theta], \qquad (3.84)$$

where we used the fact that

$$q_1^3=|\bar{q}_1|\cos\theta \qquad (3.85)$$

$$q_2^3=-q_1^3. \qquad (3.86)$$

Here, we also note that

$$E_{cm}=\sqrt{s}=E_1+E_2=E_t+E_{\bar{t}}\sim 2m_t \qquad (3.87)$$

where

$$E_1=(m_i^2+\bar{q}_1^2)^{1/2} \tag{3.88}$$

$$E_2=(m_j^2+\bar{q}_2^2)^{1/2}=(m_j^2+\bar{q}_1^2)^{1/2} \tag{3.89}$$

which implies

$$|\bar{q}_1|^2=\frac{[S-(m_i+m_j)^2][S-(m_i-m_j)^2]}{4S}. \tag{3.90}$$

Decay width

Using the Van-Royen-Weisskopf formula (ROY.67) the partial decay width, for $^3S_1$ state, is

$$^{3S_1}\Gamma_{ij}\sim(2\pi)^3|A|^2|\psi(0)|^2 \tag{3.91}$$

where

$$|A|^2\equiv\Gamma(p)=\frac{\nu}{(2\pi)^3}\sigma_{fi}. \tag{3.92}$$

ν is the relative velocity between the quarks and $\psi(0)$ a non-relativistic wave function of the $q\bar{q}$ system at the origin. Using standard techniques, found in practically any

particle physics text book (BJO.64, QUI.83, WIL.71,···), we obtain

$$^{3}s_{1}\Gamma_{ij}\sim\frac{2m_{ij}m_t^{\,2}}{\pi S^{3/2}}|\bar{q}_1||\psi(0)|^2\int_{-1}^{1}|^{3}s_{1}M_{ij}|^2 d(\cos\theta) \qquad (3.93)$$

So

$$^{3}s_{1}\Gamma_{ij}\sim\frac{3(1-\frac{1}{2}\delta_{ij})}{\pi m_t}|\bar{q}_1||\psi(0)|^2[(E_1E_2-m_{ij})\Lambda_+$$

$$+(m_iE_2-m_jE_1)\Sigma_{+-}+|\bar{q}_1|^2\Lambda_-/3] \qquad (3.94)$$

where we have also multiplied by a factor of 3 to take into account colour,

i.e. $$|\bar{t}t\rangle_{colour}=\frac{1}{\sqrt{3}}(|\bar{R}R\rangle+|\bar{G}G\rangle+|\bar{B}B\rangle) \qquad (3.95)$$

is a colour singlet.

C. Results

The next problem is to decide for what parameters this decay has a chance of showing up as a bump in some experiment.

To avoid getting lost in any SUSY background our stop mass must be greater than the top mass. If $m_{\tilde{t}}<m_t$, then dominant decay modes such as $\theta\longrightarrow\bar{\tilde{t}}\tilde{t}$

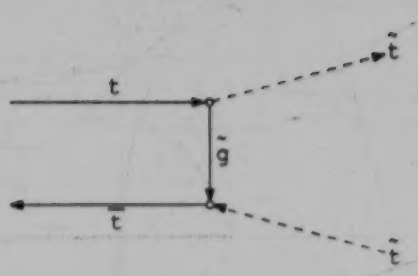

FIG. 3.7. Toponium to stop pairs.

and open top decays into $\tilde{t}+(\tilde{\gamma}$ or $\tilde{g})$, could drown out any chance of seeing neutralino production.

Aside from this, we have to worry about standard model decays. Here, the most dominant decay modes being $\theta \rightarrow \bar{f}f$

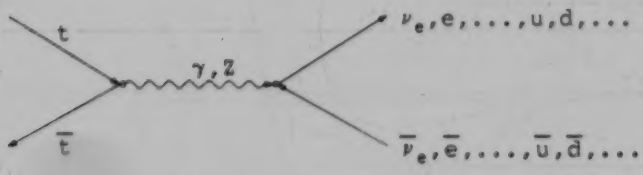

FIG. 3.8. Toponium to fermion-antifermion pairs.

and toponium β-decay.

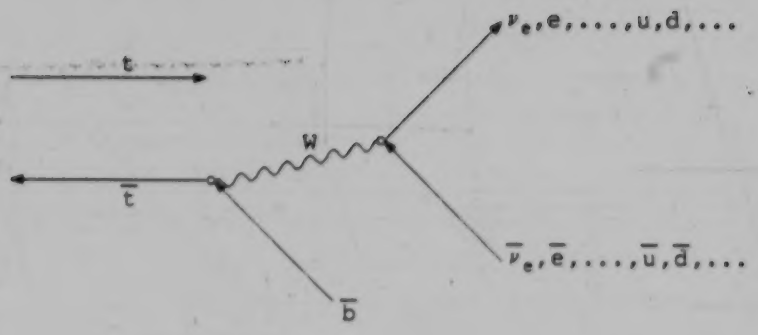

FIG. 3.9. Toponium beta decay.

For a toponium mass, m_θ, around the Z, $\theta \rightarrow \bar{f}f$ dominates ($\Gamma \sim O(55)$GeV) the β-decay modes. Around 110GeV these two decays become of the same order ($\Gamma \sim O(10^{-1}\text{GeV})$). In short, a peak occurs around the Z-mass (fig. 3.10 below) leaving us a useful range of toponium masses at least 10Gev above or below the Z.

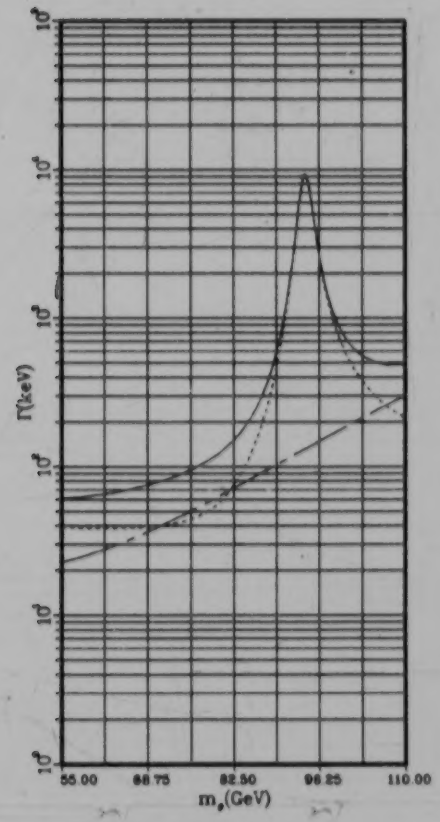

Fig. 3.10. Toponium width. Total θ width (——) and partial widths, for $\theta \rightarrow \bar{f}f$ (---) and θ β-decay (—-), as a function of m_θ.

Applying experimental constraints leads us to pick a toponium mass ~10GeV above the Z. Here, we consider our toponium mass to be 105GeV giving us a top mass of 52.5GeV. Picking $L^2\sim1$, $R^2\sim.5$ and $\tilde{m}$=80GeV in equation (2.14), gives us respective left and right stop masses (m_R, m_L) of 55GeV and 110GeV.

In figures (3.11) through (3.22) we have plotted $BR(^3S_1|\bar{t}t \rightarrow \tilde{x}_i\tilde{x}_j)$'s over the same parameter space as our neutralino mass plots of section 2.C. Our BR's being obtained by dividing (3.94) by the width for leading order $\theta \rightarrow \bar{f}f$ and $\theta \rightarrow t+\bar{b}+\bar{f}f$ decays (LEP.85)

$$\Gamma_{\bar{f}f}=\frac{c_f}{e_t^2}\left\{e_t^2e_f^2+2\frac{e_te_fv_tv_f}{y^2}Rex_Z+\frac{v_t^2(v_f^2+1)}{y^4}|x_Z|^2 +\delta_{f,b}\left[\frac{v_t(1-v_f)}{3xy^2}x_WRex_Z-\frac{e_te_f}{3x}x_W+\frac{1}{18x^2}x_W^2\right]\right\}\Gamma_0. \qquad (3.96)$$

Here[4]

$$x=4\sin^2\theta_W,\ y=4\sin\theta_W\cos\theta_W \qquad (3.97.a)$$

$$x_Z=\frac{m_\theta^2}{m_\theta^2-m_Z^2+i\Gamma_Zm_Z},\ x_W=\frac{m_\theta^2}{m_Z^2}\frac{m_W^2+(m_\theta^2/8)}{m_W^2+(m_\theta^2/4)} \qquad (3.97.b)$$

$$c_f=\begin{cases}3\ , & \text{quarks}\\ 1\ , & \text{leptons}\end{cases},\ \delta_{f,b}=\begin{cases}1\ , & f=b\\ 0\ , & f\neq b\end{cases} \qquad (3.97.c)$$

---

[4] Γ_Z~2.5GeV

$$e_u=e_c=e_t=\frac{2}{3},\ e_d=e_s=e_b=-\frac{1}{3} \tag{3.97.d}$$

$$e_{\nu_e}=e_{\nu_\mu}=e_{\nu_\tau}=0,\ e_e=e_\mu=e_\tau=-1 \tag{3.97.e}$$

$$v_u=v_c=v_t=1-\frac{2}{3}x,\ v_d=v_s=v_b=-1+\frac{1}{3}x \tag{3.97.f}$$

$$v_{\nu_e}=v_{\nu_\mu}=v_{\nu_\tau}=1,\ v_e=v_\mu=v_\tau=-1+x \tag{3.97.g}$$

and

$$\Gamma_\beta\sim 8.4\left[\frac{m_t}{40\text{GeV}}\right]^5 f\left[\frac{m_t^2}{m_W^2},\frac{m_b^2}{m_t^2}\right]\Gamma_0. \tag{3.98}$$

The function f is

$$f(\rho,\mu)\sim\frac{2}{\rho^4}\{6[\rho+(1-\rho)\ln(1-\rho)]-3\rho^2-\rho^3\} \tag{3.99}$$

with

$$\Gamma_0(\theta)=\frac{64\pi\alpha_{em}^2}{9m_\theta^2}[1-\frac{16}{3\pi}\alpha_s(m_\theta)]|\psi(0)|^2 \tag{3.100}$$

where

$$\alpha_s(m_\theta)=\frac{12\pi}{23\ln[m_\theta/(0.1\text{Gev})]^2}. \tag{3.101}$$

It should be noted that for $\Gamma_{\bar{f}f}$, with the exception of the $b\bar{b}$ final state, we have neglected the charged-current contributions which are Cabibbo suppressed.

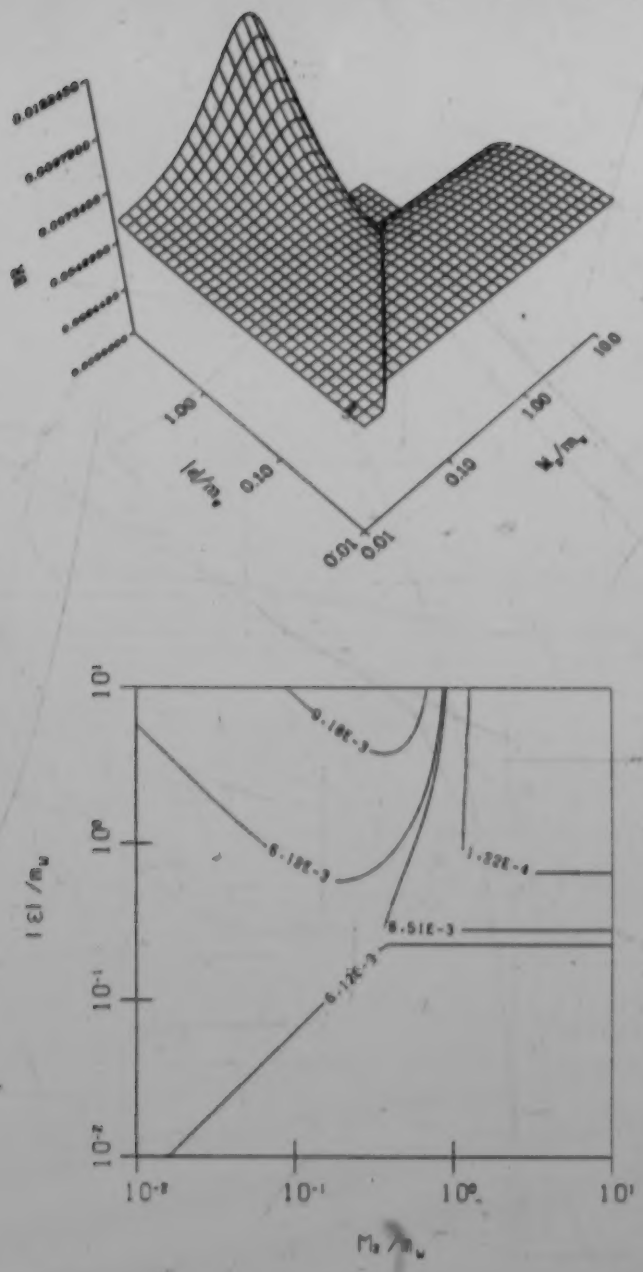

Fig. 3.11: Toponium BR plots. 3D plot (top) and contour plot (bottom) for $BR(^3S_1|t\bar{t} \rightarrow \tilde{\chi}^0\tilde{\chi}^0)$ as a function of $|\epsilon|$ and M_2, for $\nu_1/\nu_2=1$, $\epsilon>0$ and $m_t=52.5$.

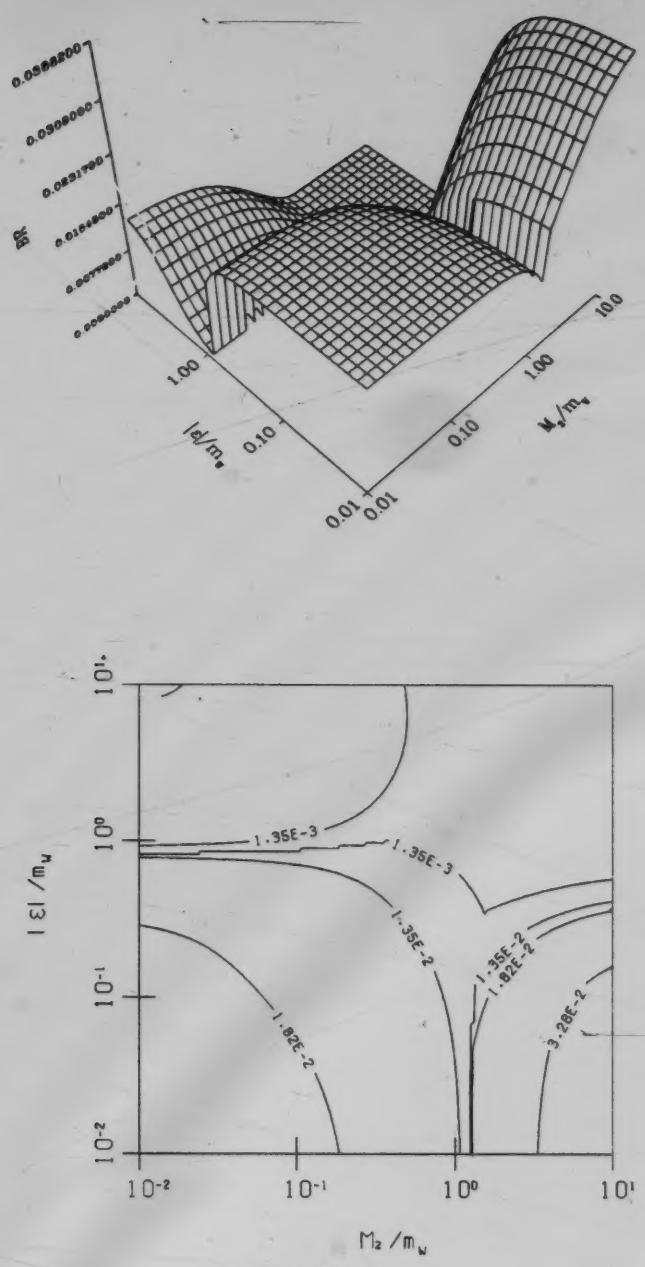

Fig. 3.12: Toponium BR plots. 3D plot (top) and contour plot (bottom) for $BR(^3S_1|t\bar{t} \rightarrow \tilde{\chi}^{0'}\tilde{\chi}^0)$ as a function of $|\epsilon|$ and M_2, for $\nu_1/\nu_2=1$, $\epsilon>0$ and $m_t=52.5$.

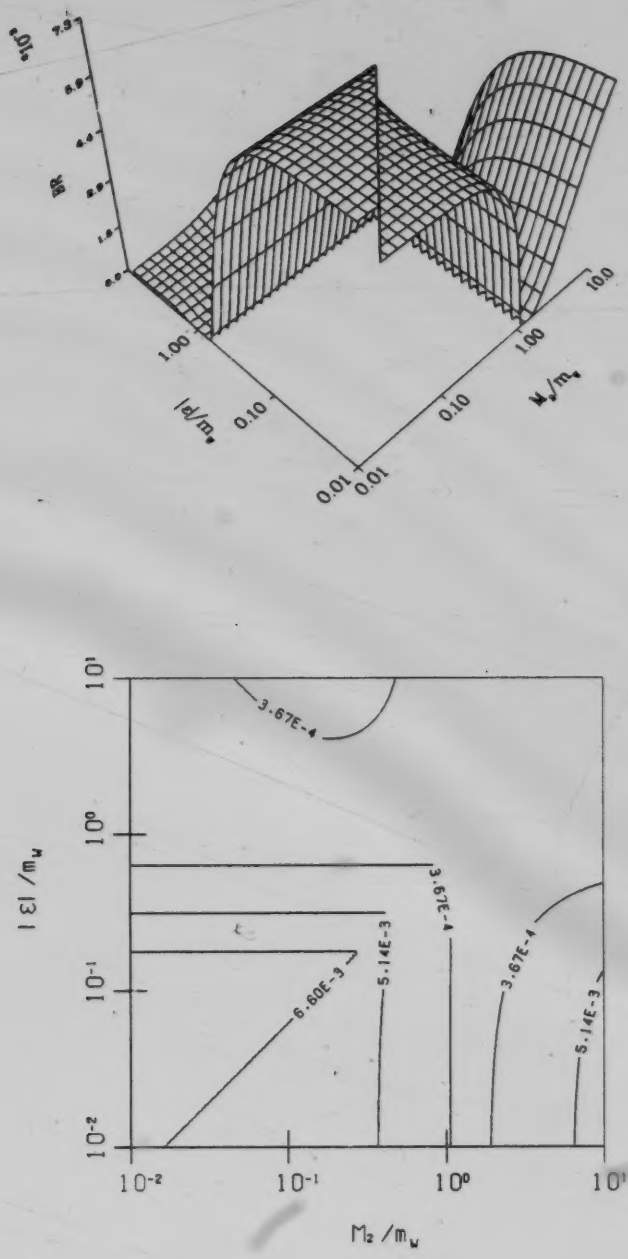

Fig. 3.13: Toponium BR plots. 3D plot (top) and contour plot (bottom) for $BR(^3S_1|t\bar{t} \rightarrow \tilde{\chi}^{0'}\tilde{\chi}^{0'})$ as a function of $|\epsilon|$ and M_2, for $\nu_1/\nu_2=1$, $\epsilon>0$ and $m_t=52.5$.

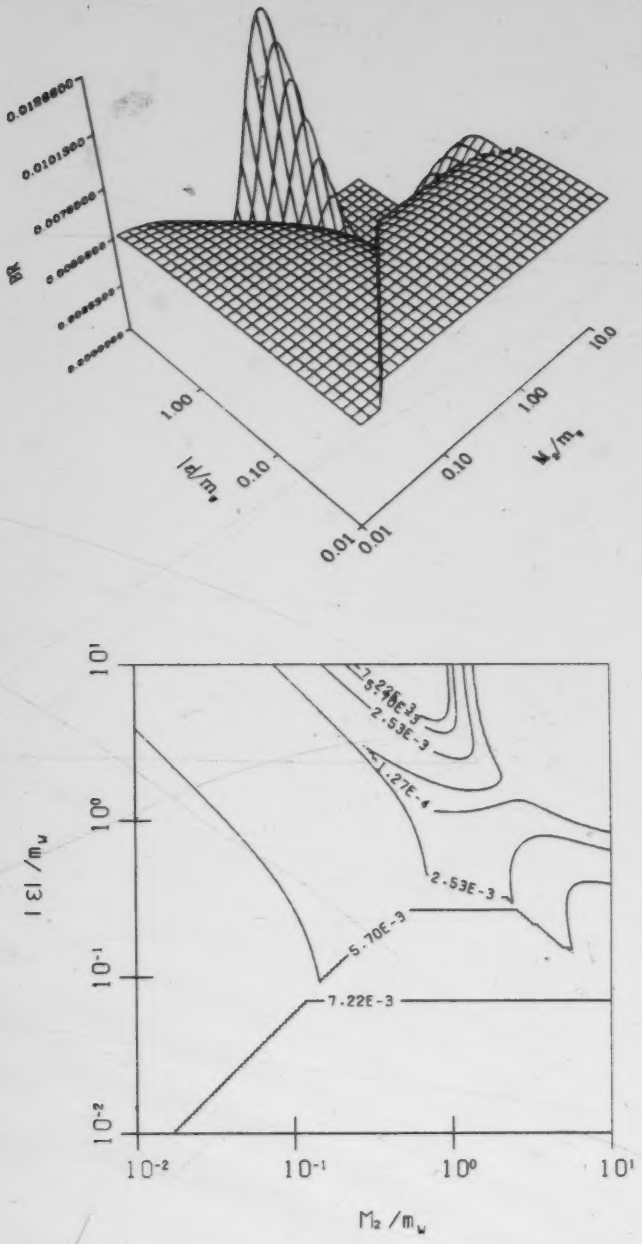

Fig. 3.14: Toponium BR plots. 3D plot (top) and contour plot (bottom) for $BR(^3S_1|t\bar{t} \rightarrow \tilde{\chi}^0\tilde{\chi}^0)$ as a function of $|\epsilon|$ and M_2, for $\nu_1/\nu_2=1$, $\epsilon<0$ and $m_t=52.5$.

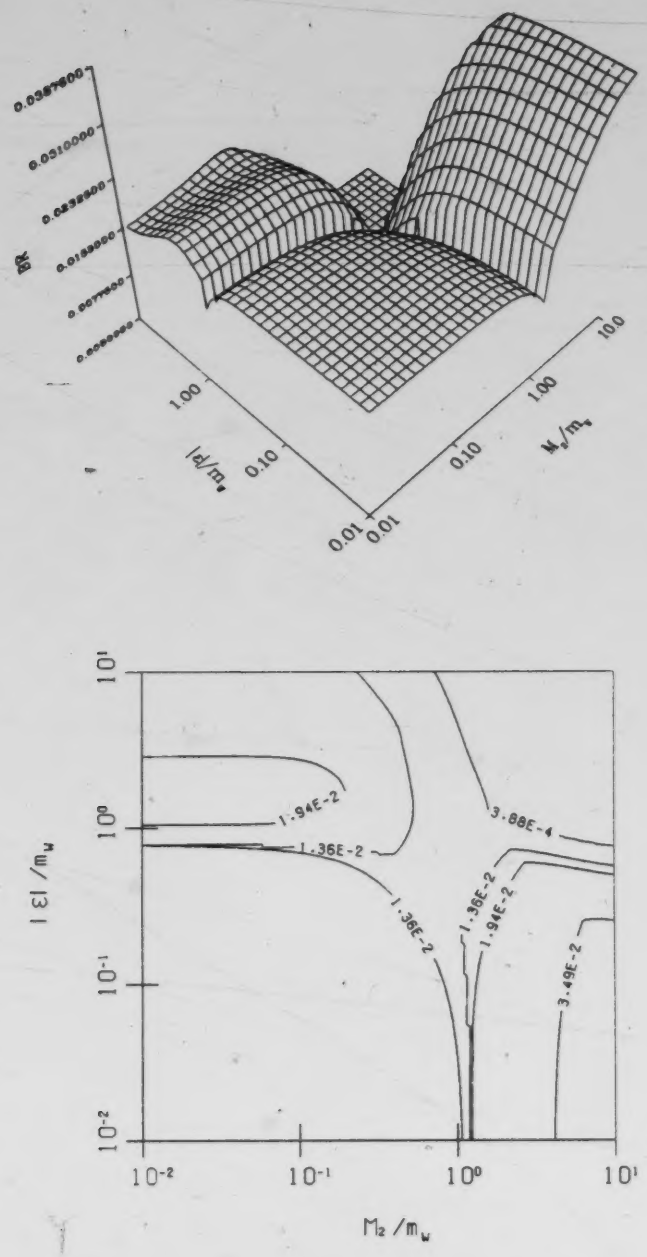

Fig. 3.15: Toponium BR plots. 3D plot (top) and contour plot (bottom) for $BR(^3S_1|t\bar{t} \rightarrow \tilde{\chi}^{0'}\tilde{\chi}^0)$ as a function of $|\epsilon|$ and M_2, for $\nu_1/\nu_2=1$, $\epsilon<0$ and $m_t=52.5$.

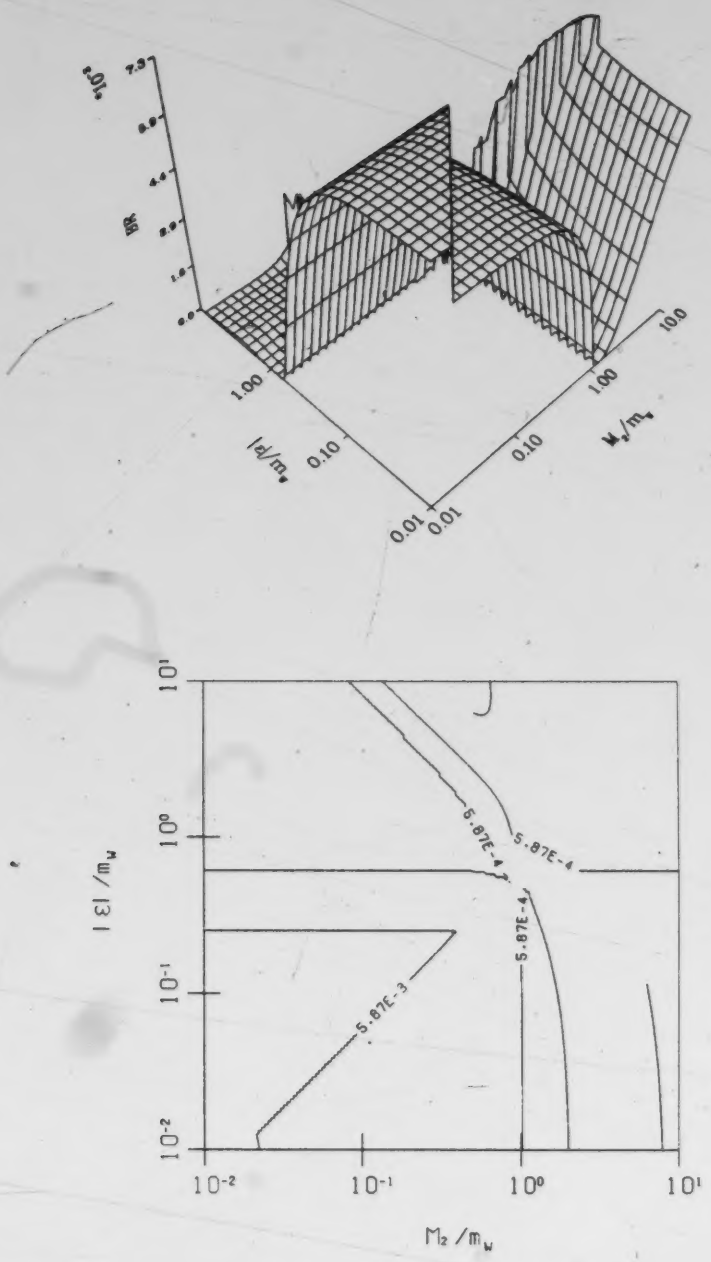

Fig. 3.16: Toponium BR plots. 3D plot (top) and contour plot (bottom) for $BR(^3S_1|t\bar{t} \rightarrow \tilde{\chi}^{0'}\tilde{\chi}^{0'})$ as a function of $|\epsilon|$ and M_2, for $\nu_1/\nu_2=1$, $\epsilon<0$ and $m_t=52.5$.

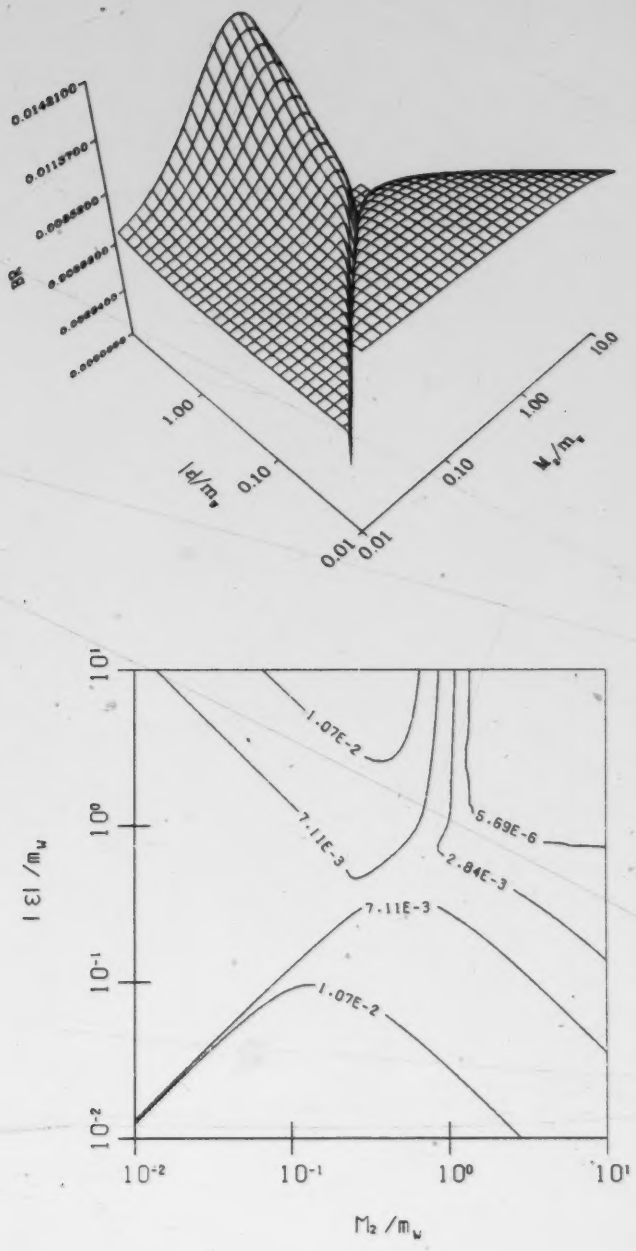

Fig. 3.17: Toponium BR plots. 3D plot (top) and contour plot (bottom) for $BR(^3S_1|t\bar{t} \rightarrow \tilde{\chi}^0\tilde{\chi}^0)$ as a function of $|\epsilon|$ and M_2, for $\nu_1/\nu_2=4$, $\epsilon>0$ and $m_t=52.5$.

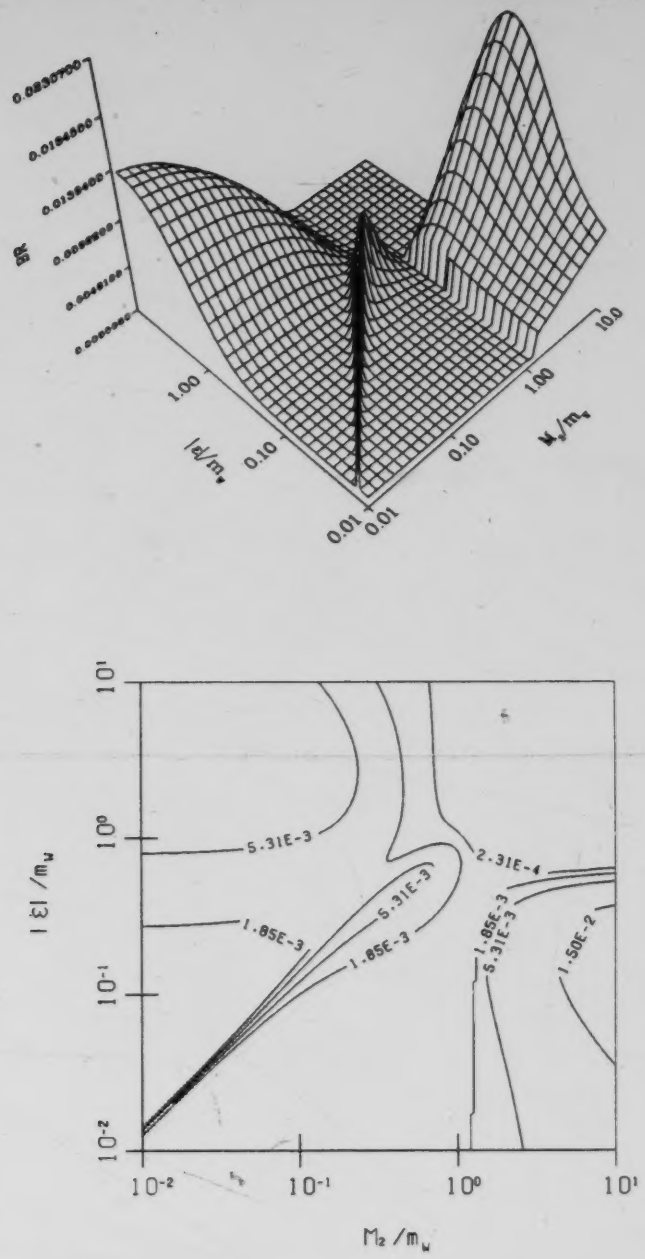

Fig. 3.18: Toponium BR plots. 3D plot (top) and contour plot (bottom) for $BR(^3S_1|t\bar{t} \rightarrow \tilde{\chi}^{0\prime}\tilde{\chi}^0)$ as a function of $|\epsilon|$ and M_2, for $\nu_1/\nu_2=4$, $\epsilon>0$ and $m_t=52.5$.

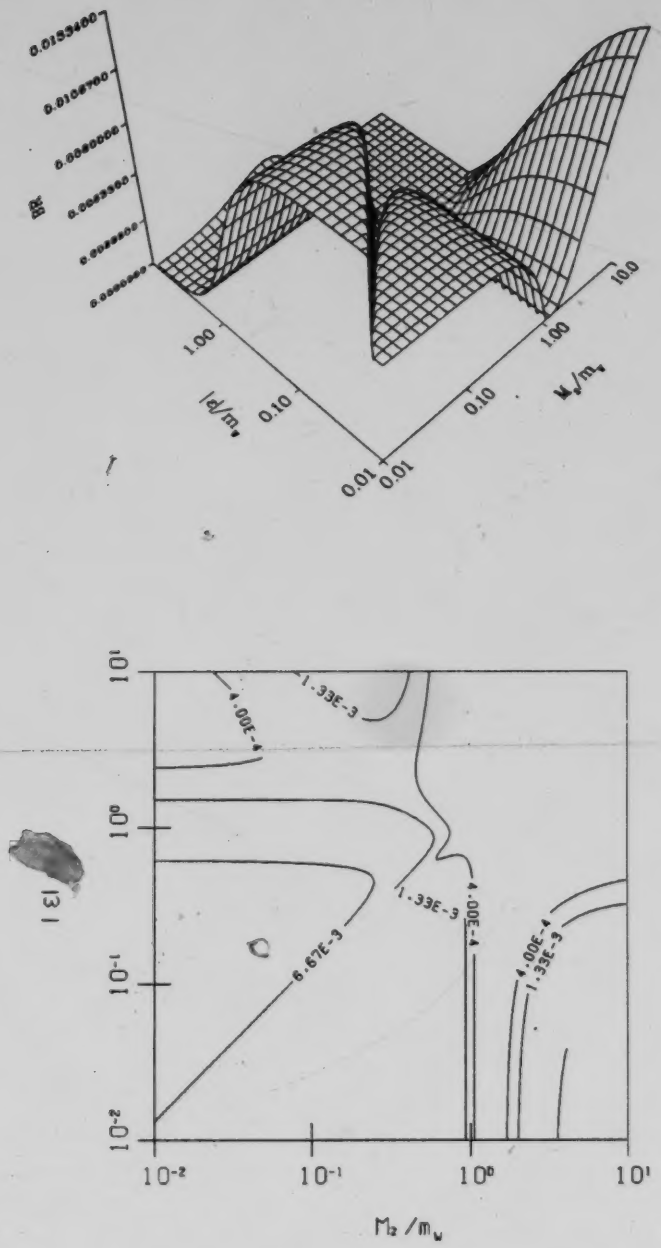

Fig. 3.19: Toponium BR plots. 3D plot (top) and contour plot (bottom) for $BR(^3S_1|t\bar{t} \rightarrow \tilde{\chi}^{0'}\tilde{\chi}^{0'})$ as a function of $|\epsilon|$ and M_2, for $\nu_1/\nu_2=4$, $\epsilon>0$ and $m_t=52.5$.

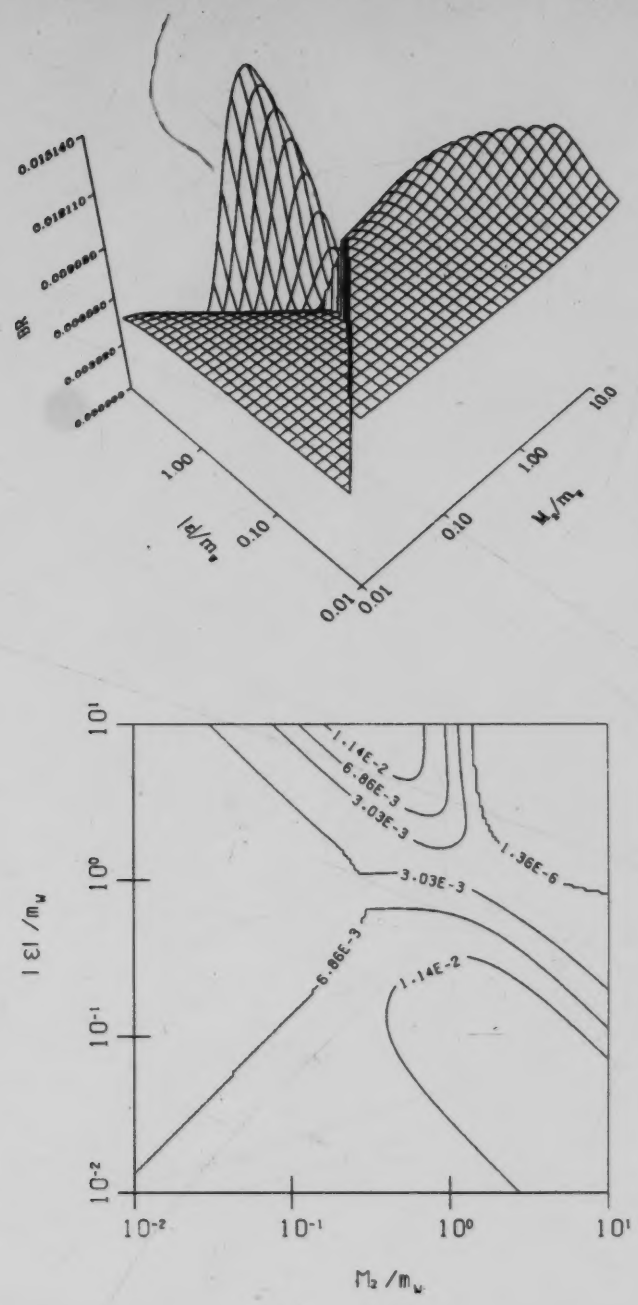

Fig. 3.20: Toponium BR plots. 3D plot (top) and contour plot (bottom) for $BR(^3S_1|t\bar{t} \rightarrow \tilde{\chi}^0\tilde{\chi}^0)$ as a function of $|\epsilon|$ and M_2, for $\nu_1/\nu_2=4$, $\epsilon<0$ and $m_t=52.5$.

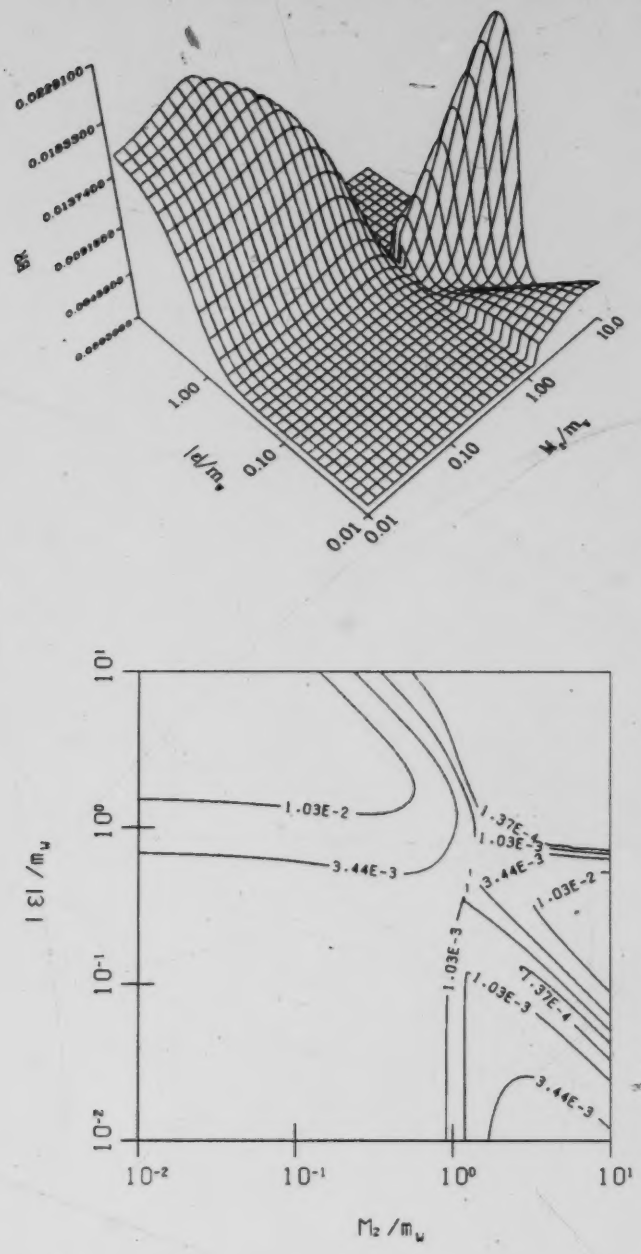

Fig. 3.21: Toponium BR plots. 3D plot (top) and contour plot (bottom) for $BR(^3S_1|t\bar{t} \rightarrow \tilde{\chi}^{0'}\tilde{\chi}^0)$ as a function of $|\epsilon|$ and M_2, for $\nu_1/\nu_2=4$, $\epsilon<0$ and $m_t=52.5$.

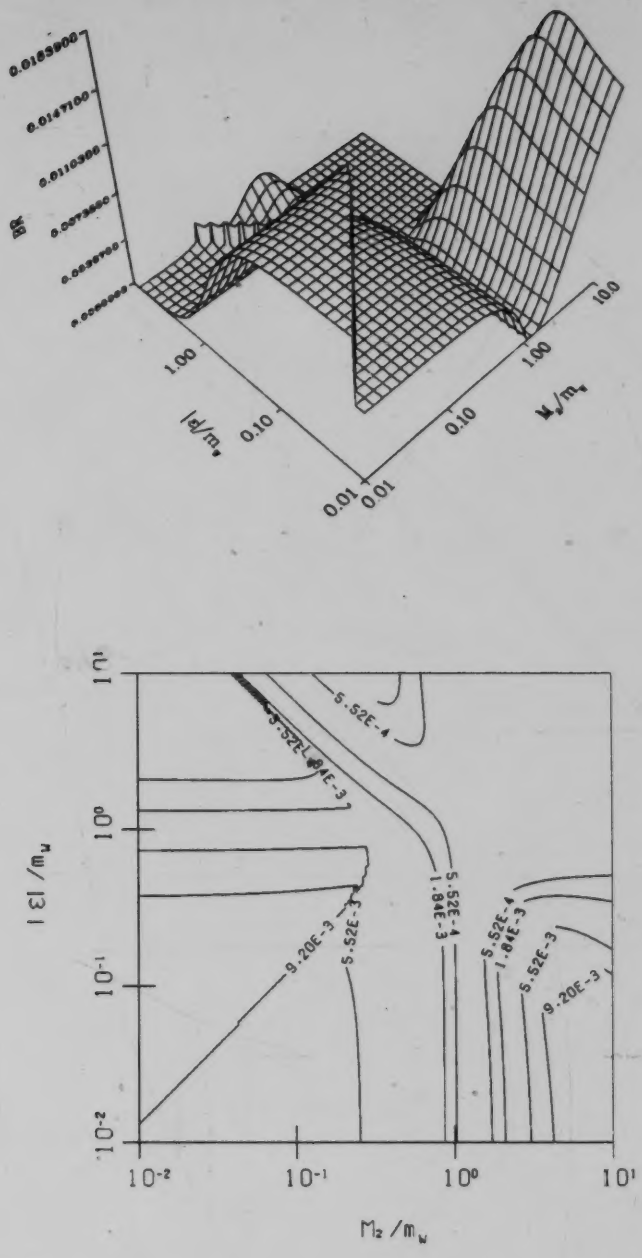

Fig. 3.22: Toponium BR plots. 3D plot (top) and contour plot (bottom) for $BR(^3S_1|t\bar{t} \rightarrow \tilde{\chi}^{0'}\tilde{\chi}^{0'})$ as a function of $|\epsilon|$ and M_2, for $\nu_1/\nu_2=4$, $\epsilon<0$ and $m_t=52.5$.

Incomplete contour lines (such as in figure 3.16; top middle of contour plot) correspond to insufficient data or not enough room to put in a contour label.

D. Toponium Decay Revisited

In this section, we consider toponium decay in the $SU_L(2)\otimes U_Y(1)\otimes U_E(1)$ scenario. Here the $\tilde{\xi}$ of equation (3.1) are simply extended to

$$\tilde{\xi}^T\equiv(\tilde{W}^3,\tilde{B}^0,\tilde{H}_1^0,\tilde{H}_2^0,\tilde{B}_E,\tilde{N}) \qquad (3.102)$$

and the M matrix replaced by (2.31). This new M matrix is also real and symmetric, and so can be diagonalized under the same scheme as in equation (3.3). Therefore replacing the U matrix of (3.3), with the corresponding one for (3.102), we obtain definition (3.4) along with the additional elements

$$U_{i5}=\kappa_i,\ U_{i6}=\lambda_i \qquad (3.103)$$

where i now runs from 1 to 6.

So, our new eigenstates are simply of the form

$$\tilde{\chi}_i\equiv\alpha_i\tilde{W}^3+\beta_i\tilde{B}^0+\gamma_i\tilde{H}_1^0+\delta_i\tilde{H}_2^0+\kappa_i\tilde{B}_E+\lambda_i\tilde{N}. \qquad (3.104)$$

From this and equation (3.7) we find that our shifted fields

are now those of (3.8) along with the additional terms

$$\tilde{B}_E=\kappa_i\tilde{\chi}_i \qquad (3.8.e)$$

$$\tilde{N}=\lambda_i\tilde{\chi}_i \qquad (3.8.f)$$

Stop squark exchange amplitude

In the gaugino sector the interaction Lagrangian is that of (3.10) plus the term

$$L_{int}^{\tilde{B}_E}\sim-\sqrt{2}\, g_E\bar{\tilde{B}}_E\phi^\dagger\tilde{t}_L\frac{Y_E}{2}L\psi_t-\sqrt{2}\, g_E\bar{\tilde{B}}_E\phi^\dagger\tilde{t}_R\frac{Y_E}{2}R\psi_t+H.C. \qquad (3.105)$$

$$=-\sqrt{2}\, g'\kappa_i\bar{\tilde{\chi}}_i[L\tilde{t}_L^\dagger+R\tilde{t}_R^\dagger]t/3+H.C. \qquad (3.106)$$

where (CAM.86)

$$g_E=g',\ Y_E=\frac{2}{3}. \qquad (3.107)$$

In the Higgsino sector the N field has zero hypercharge (CAM.86) and so does not contribute to the quark-squark vertices. The only Higgsino contribution is that of equation (3.18).

Using equation (3.10), (3.18) and (3.106), we simply get equation (3.19), where the terms (3.20) are replaced by

$$a_i=\frac{1}{2}(\alpha_i g+\frac{1}{3}\beta_i g')+\frac{1}{3}g'\kappa_i \qquad (3.108.a)$$

$$b_i=g_{H_i^0\bar{t}t}\gamma_i/\sqrt{2} \qquad (3.108.b)$$

$$c_i=-\frac{2}{3}g'\beta_i+\frac{1}{3}g'\kappa_i . \qquad (3.108.c)$$

Therefore, our squark contribution to the amplitude is that of (3.37), with definitions (3.20) replaced by (3.108).

Z-exchange amplitude

Since the Higgsino has zero hypercharge, it does not contribute to the $Z\bar{t}t$ coupling. However, in this model, there exists an extra Z; the Z_E, which is pure B_E in content. So, in addition to the Z, we have a Z_E contribution (i.e. figure 3.5, with Z replaced by Z_E.) Fortunately, due to phenomenological contraints (CAM.86)

$$m_{Z_E}>>m_Z \qquad (3.109)$$

and so to first order we can neglect the Z_E contribution.

Total amplitude

It follows that our result for Γ is that of (3.94), with definitions (3.20) replaced by (3.108).

E. Results

In figures (3.23) through (3.31) we have plotted $BR(^3S_1|\bar{t}t \rightarrow \tilde{\chi}_i\tilde{\chi}_j)$ over the same parameter space as our neutralino mass plots of section 2.D. Our BR's being obtained in the same manner as in section C.

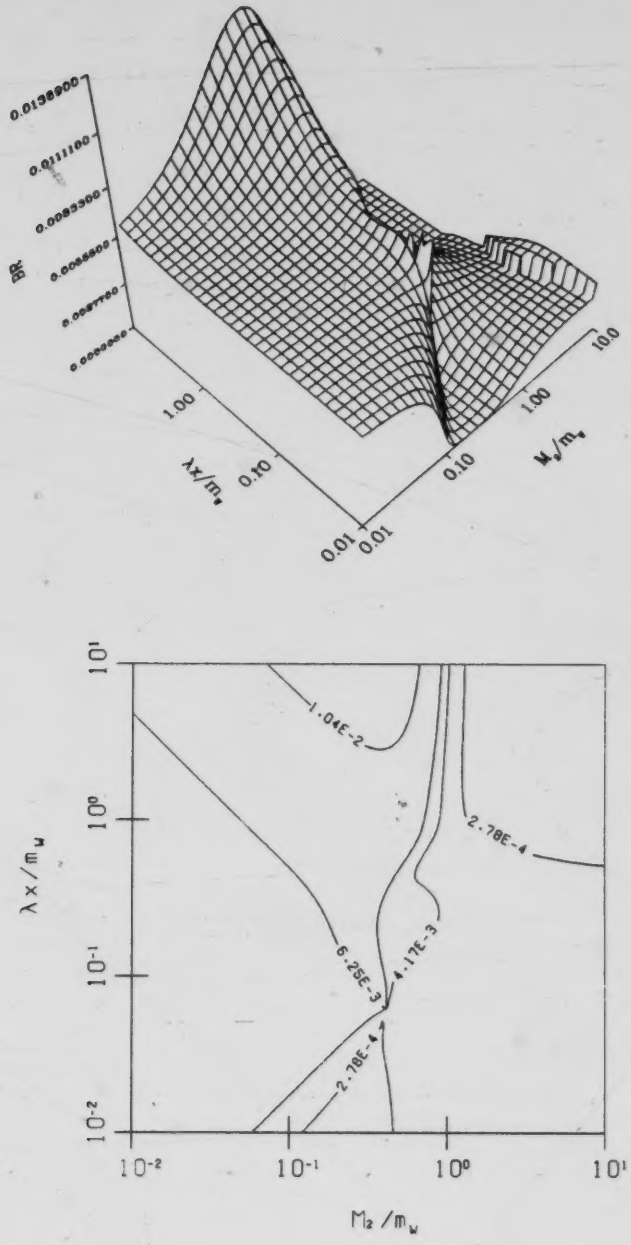

Fig. 3.23: Toponium BR plots with an extra U(1). 3D plot (top) and contour plot (bottom) for $BR(^3S_1|t\bar{t} \rightarrow \tilde{\chi}^0\tilde{\chi}^0)$ as a function of x and M_2, for $v_1/v_2=3.4$, $\lambda=0.10$ and $m_t=52.5$.

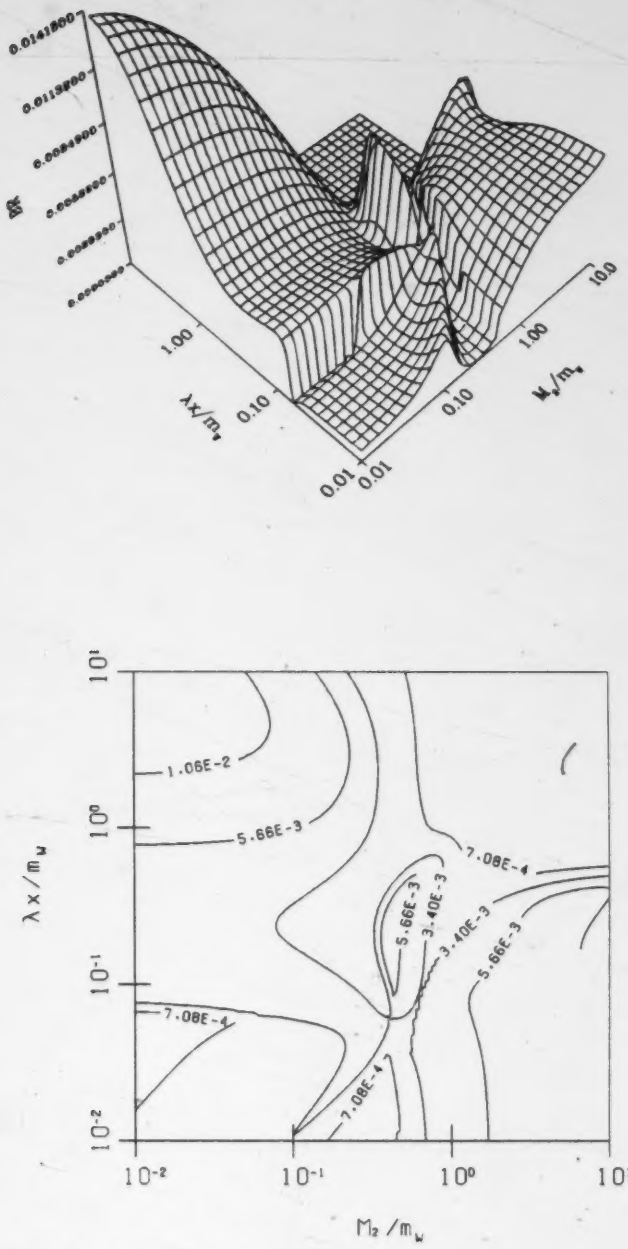

Fig. 3.24: Toponium BR plots with an extra U(1). 3D plot (top) and contour plot (bottom) for $BR(^3S_1|t\bar{t} \rightarrow \tilde{\chi}^{0'}\tilde{\chi}^0)$ as a function of x and M_2, for v_1/v_2=3.4, λ=0.10 and m_t=52.5.

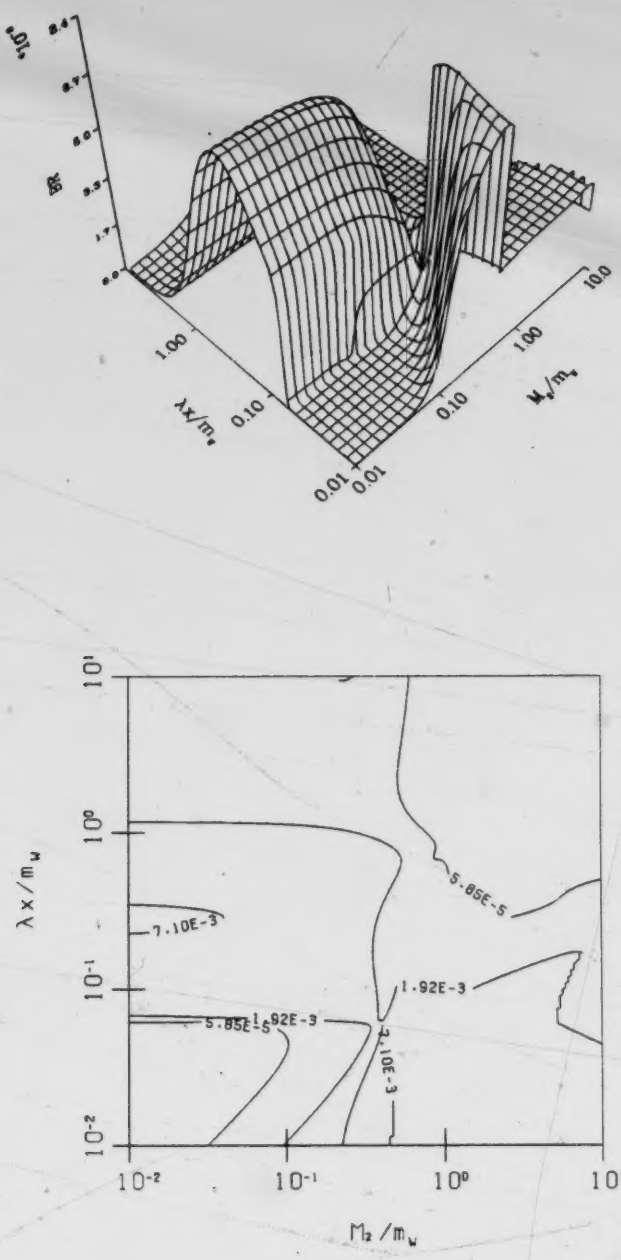

Fig. 3.25: Toponium BR plots with an extra U(1). 3D plot (top) and contour plot (bottom) for $BR(^3S_1|t\bar{t} \rightarrow \tilde{\chi}^{0'}\tilde{\chi}^{0'})$ as a function of x and M_2, for $v_1/v_2=3.4$, $\lambda=0.10$ and $m_t=52.5$.

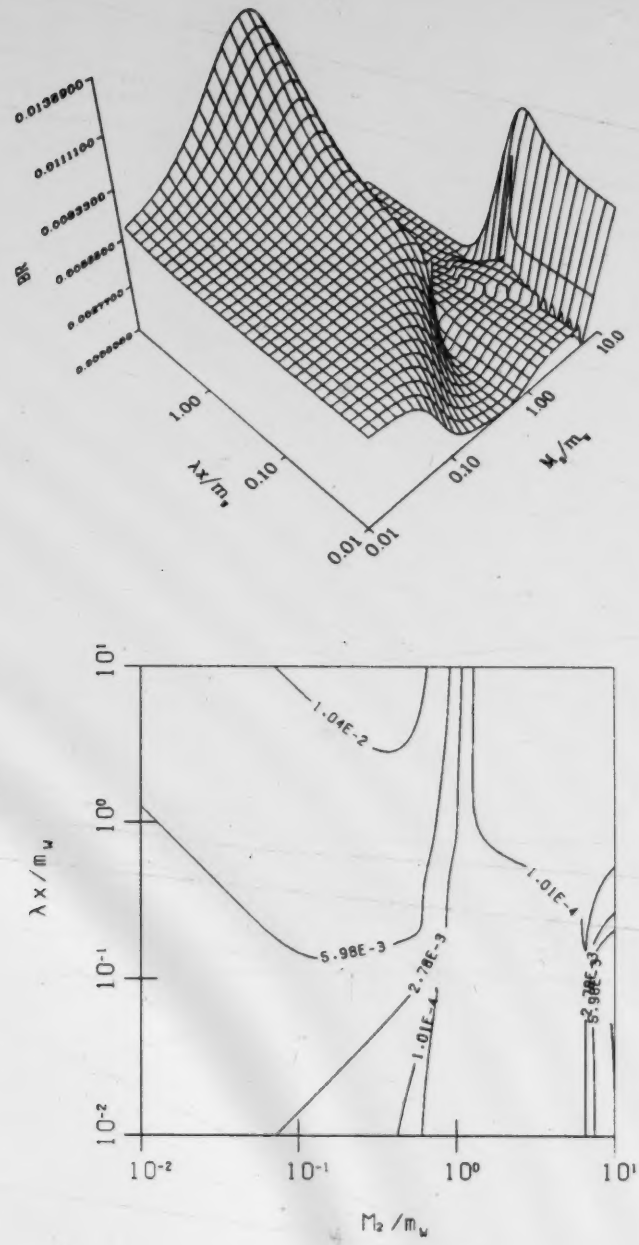

Fig. 3.26: Toponium BR plots with an extra U(1). 3D plot (top) and contour plot (bottom) for $BR(^3S_1|t\bar{t} \rightarrow \tilde{\chi}^0\tilde{\chi}^0)$ as a function of x and M_2, for $v_1/v_2=3.4$, $\lambda=0.18$ and $m_t=52.5$.

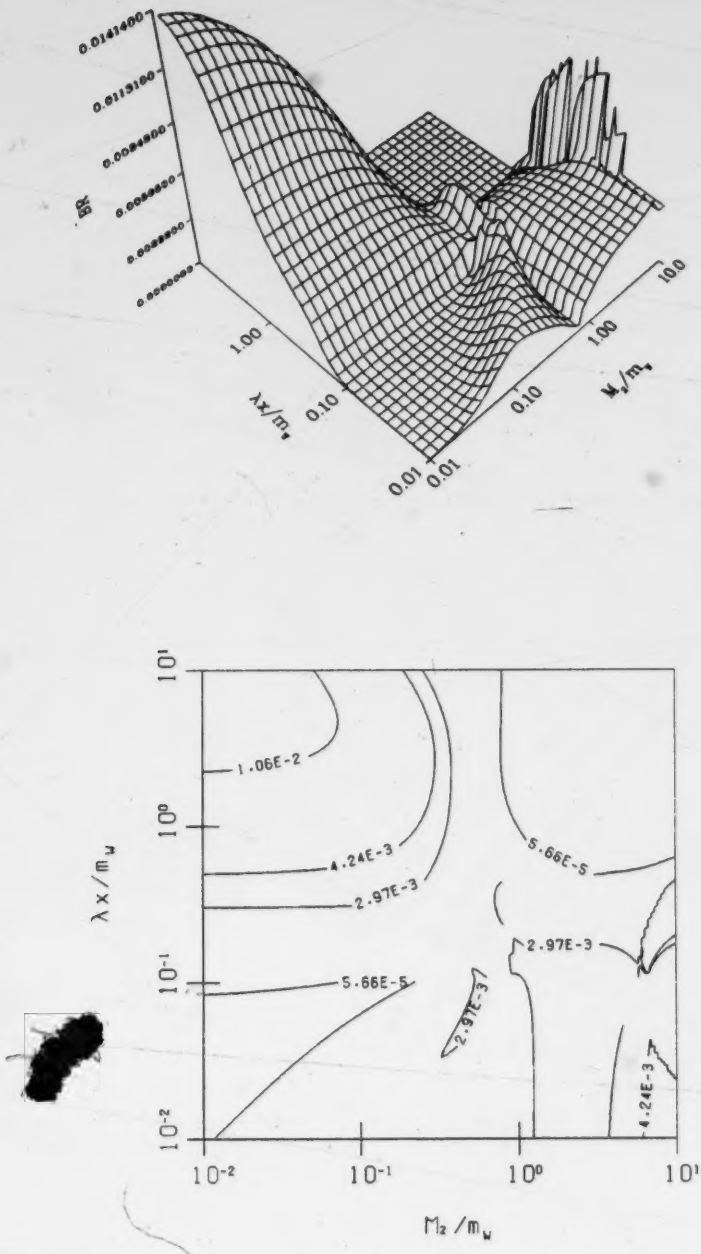

Fig. 3.27: Toponium BR plots with an extra U(1). 3D plot (top) and contour plot (bottom) for $BR(^3S_1|t\bar{t} \rightarrow \tilde{\chi}^{0'}\tilde{\chi}^0)$ as a function of x and M_2, for $v_1/v_2=3.4$, $\lambda=0.18$ and $m_t=52.5$.

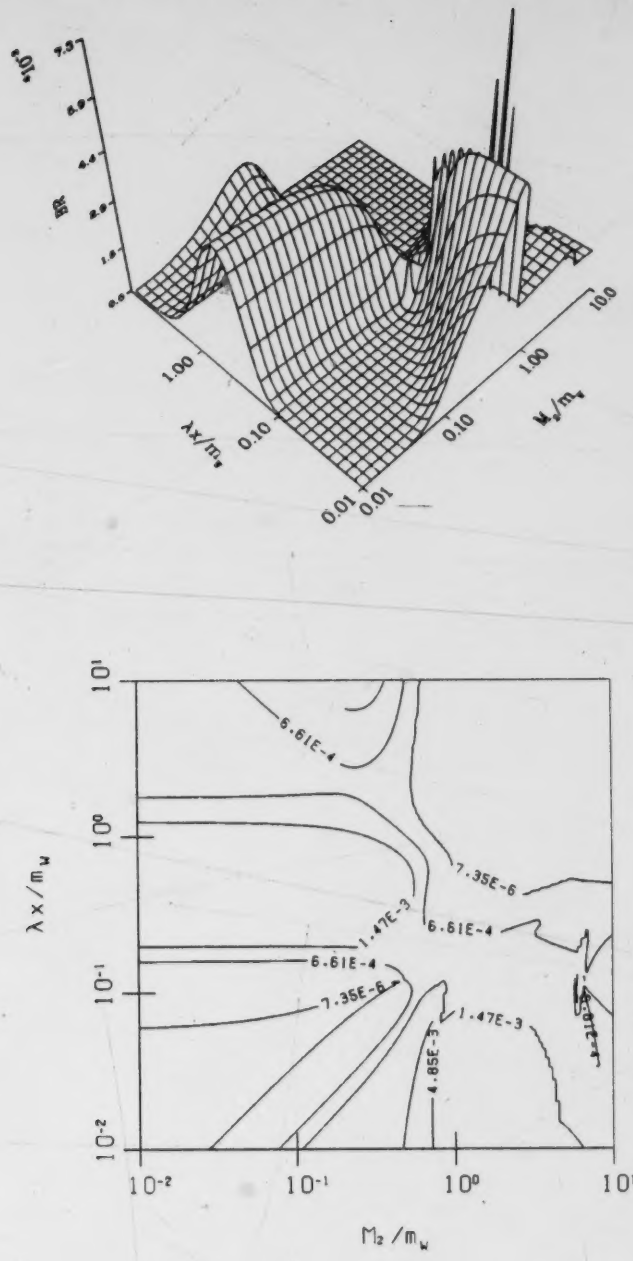

Fig. 3.28: Toponium BR plots with an extra U(1). 3D plot (top) and contour plot (bottom) for $BR(^3S_1|t\bar{t} \rightarrow \tilde{\chi}^{0'}\tilde{\chi}^{0'})$ as a function of x and M_2, for $v_1/v_2=3.4$, $\lambda=0.18$ and $m_t=52.5$.

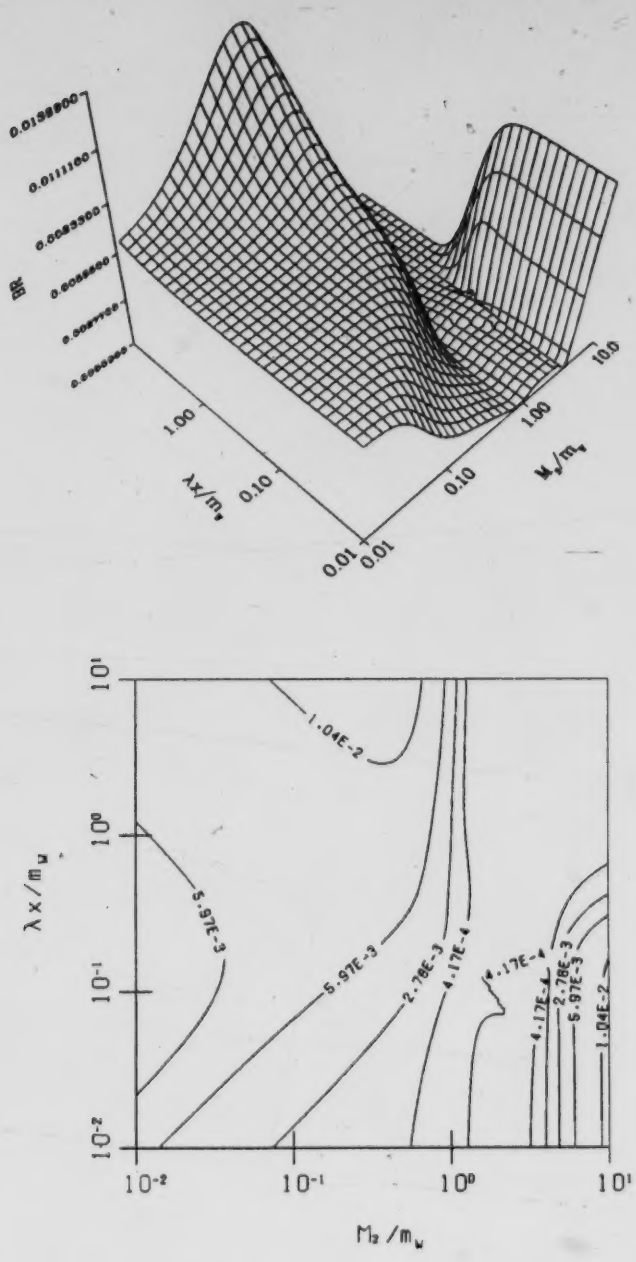

Fig. 3.29: Toponium BR plots with an extra U(1). 3D plot (top) and contour plot (bottom) for $BR(^3S_1|t\bar{t} \rightarrow \tilde{\chi}^0\tilde{\chi}^0)$ as a function of x and M_2, for $v_1/v_2=3.4$, $\lambda=0.25$ and $m_t=52.5$.

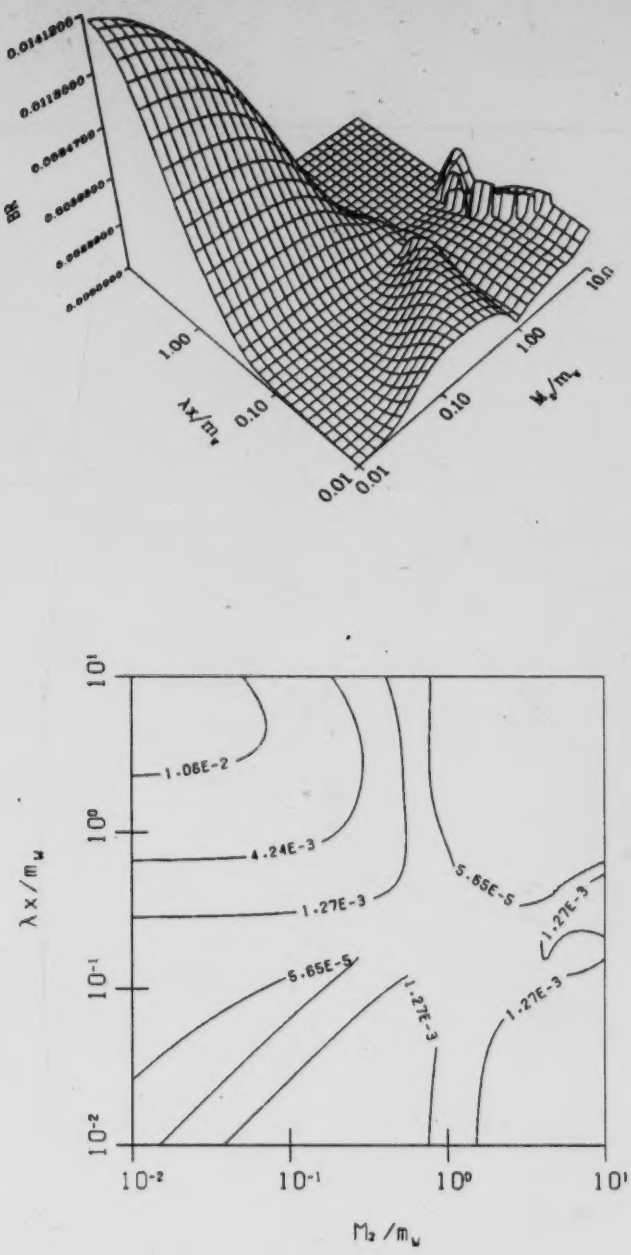

Fig. 3.30: Toponium BR plots with an extra U(1). 3D plot (top) and contour plot (bottom) for $BR(^3S_1|t\bar{t} \rightarrow \tilde{\chi}^{0\prime}\tilde{\chi}^0)$ as a function of x and M_2, for $\nu_1/\nu_2=3.4$, $\lambda=0.25$ and $m_t=52.5$.

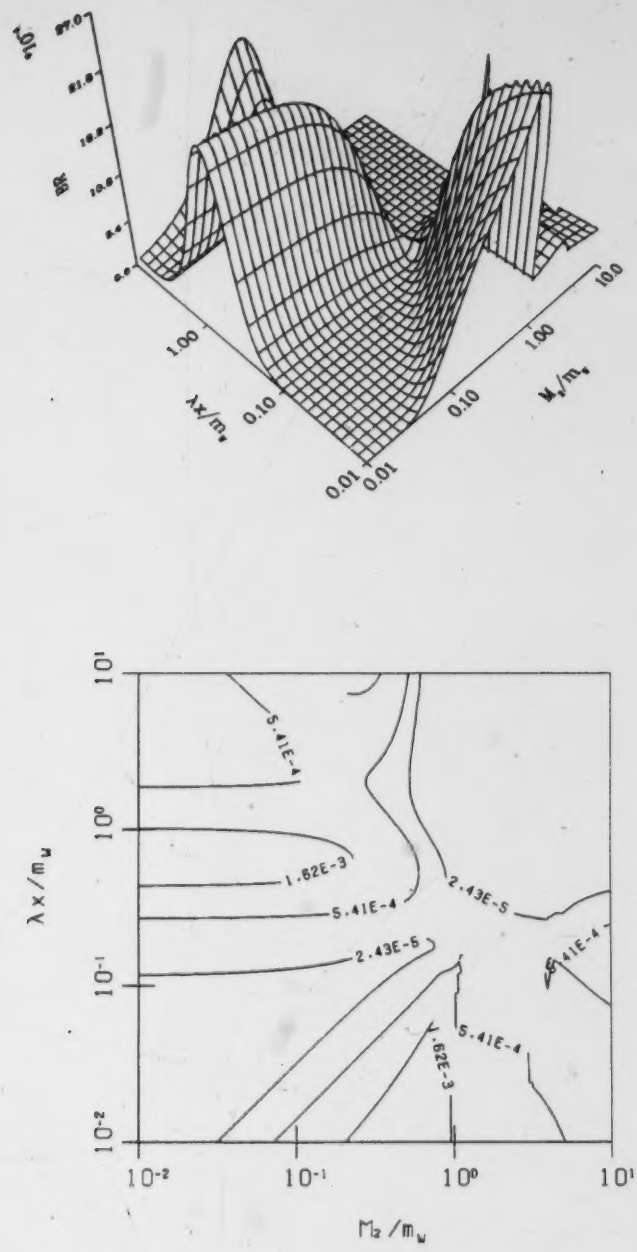

Fig. 3.31: Toponium BR plots with an extra U(1). 3D plot (top) and contour plot (bottom) for $BR(^3S_1|t\bar{t} \rightarrow \tilde{\chi}^{0'}\tilde{\chi}^{0'})$ as a function of x and M_2, for v_1/v_2=3.4, λ=0.25 and m_t=52.5.

F. Observations

From the complexity of the surface topologies of our decay plots, one can see that the combination of 3-D and contour plots are invaluable interpretative tools.

One thing that becomes immediately noticeable is that some plots seem to have a discontinuity; for instance, in plot 3.11. After some careful examination of mass contour plots 2.1 and 2.2, one can see that there is a mass flip between plots 2.1 and 2.2 along a line corresponding to the discontinuity observed in plot 3.11. So, since we are considering θ decaying to two light $\tilde{\chi}^0$'s (fig. 3.11), we see a discontinuity corresponding to a change of eigenstates. Since there is a flip between heavy and light states along this line, we also expect a corresponding discontinuity for θ to two heavy $\tilde{\chi}^0$ states. This corresponds to figure 3.13. For a mixing of states (i.e. $\theta \rightarrow \tilde{\chi}^{0'}\tilde{\chi}^0$) we expect to see no discontinuities, since the amplitude should be invariant under an interchange of eigenstates, $\tilde{\chi}^{0'}$ and $\tilde{\chi}^0$. As expected, we see no discontinuties in the corresponding figure, figure 3.12.

Another interesting, but not so obvious point, is that all decays are zero in the upper right hand corner (i.e. ϵ(or λx) and M_2 large) of our ϵ (or λx) M_2 parameter space. These correspond to kinematically inaccessible regions (i.e. $\sqrt{S} < m_{\chi}+m_{\chi'}$). Upon observation of mass plots 2.1 through 2.14, one can see why: In the regions of large ϵ (or λx) and M_2,

the neutralino masses rapidly exceed $\sqrt{S}$. So, as the neutralino mass gets large the decay approaches zero.

This, also explains the apparent discontinuity in figure 3.12, which I conveniently forgot to mention while dicussing mass flips. Here, the decay approaches zero (valley region of 3-D plot 3.12, where ϵ and $M_2 \rightarrow O(m_W)$) as the neutralino mass goes up (ridge region of 3-D plot 2.2, where ϵ and $M_2 \rightarrow O(m_W)$). However, in this region, the neutralino mass doesn't quite get high enough, and so the decay never quite goes to zero.

This line of reasoning, explains many of the bizarre surface topologies encountered throughtout figures 3.11 to 3.31.

I should also mention, that spikey figures such as 3.16, require no further reasoning, since these spikes are due to insufficent plotting data.

As a final note, one can see that decay plots, with an extra U(1) content, seem to give generally smoother surface topologies, than the plots without. Careful observation, shows that there are many similarities between these plots, even though the surface topologies may at first glance look drastically different.

G. Varying the Top Mass

In figures 3.11 through 3.31, we have only considered a toponium mass of 52.5 GeV. The grounds for choosing this mass was based on recent UA1 results. However, these results are held under close scutiny by some theorists who would rather trust the more solid TRISTAN results. If we use TRISTAN's results, then we could consider top masses as low as O(28)GeV.

In figures 3.32 through 3.38 we have plotted neutralino BR's as a function of m_{θ}, for 55 GeV $\leq m_{\theta} \leq$ 110 GeV, and $(|\epsilon|, M_2, \lambda x)/m_W \sim O(1/3)$.

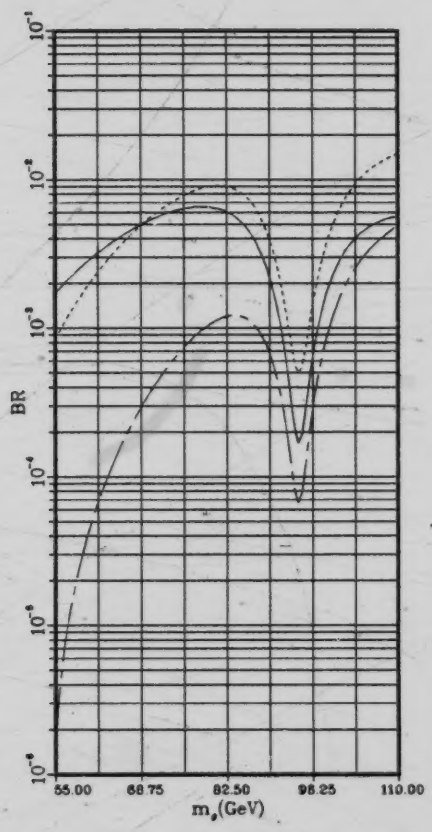

Fig. 3.32. Toponium BR plots. θ BR'S to two light (——), one light & one heavy (---), and two heavy (—-) neutralinos, as a function of m_θ, for $\epsilon=M_2=\frac{1}{3}m_W$ and $\nu_1/\nu_2=1$.

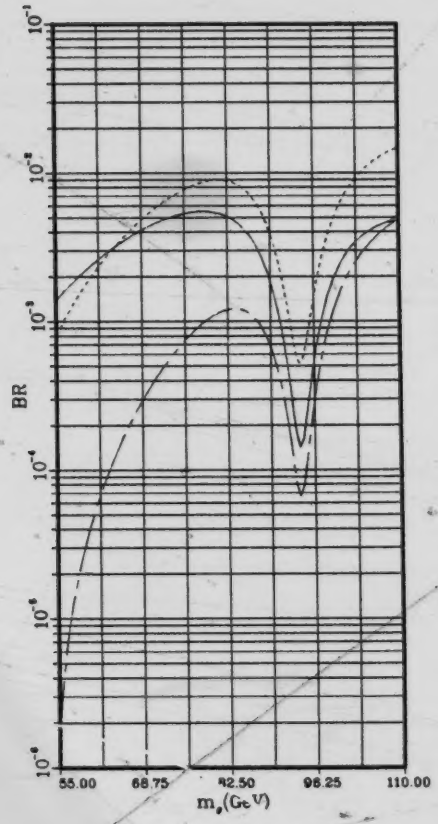

Fig. 3.33. Toponium BR plots. θ BR'S to two light (——), one light & one heavy (---), and two heavy (—-) neutralinos, as a function of m_θ, for $\epsilon = -M_2 = -\frac{1}{3}m_W$ and $v_1/v_2 = 1$.

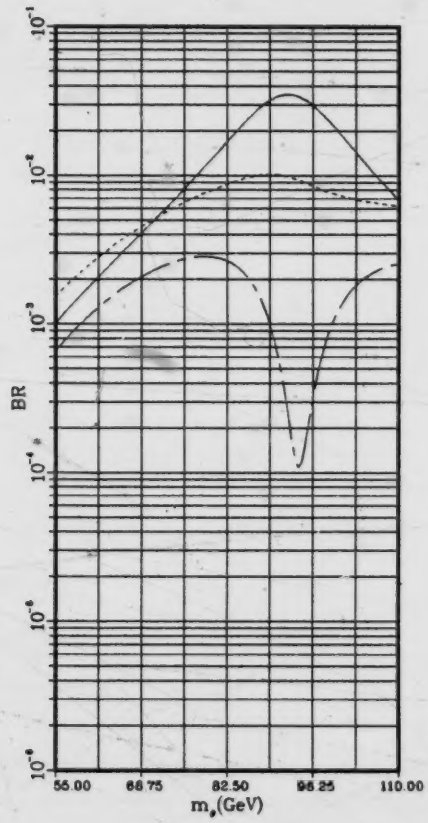

Fig. 3.34. Toponium BR plots. θ BR'S to two light (——), one light & one heavy (---), and two heavy (—-) neutralinos, as a function of m_θ, for $\epsilon = M_2 = \frac{1}{3}m_W$ and $v_1/v_2 = 4$.

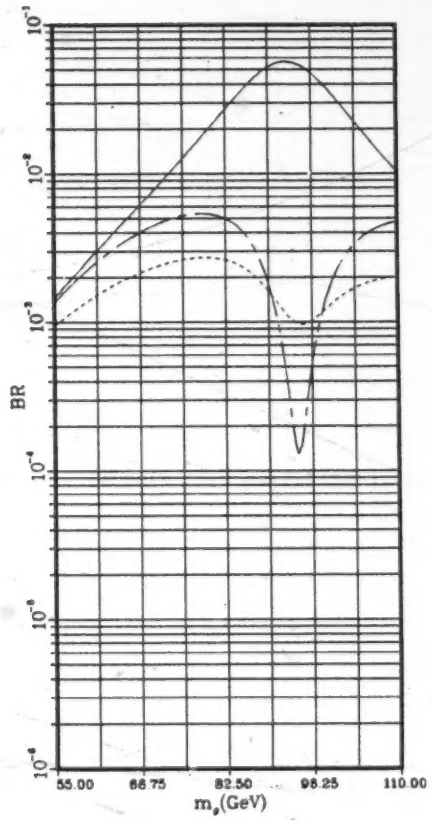

Fig. 3.35. Toponium BR plots. θ BR'S to two light (——), one light & one heavy (---), and two heavy (—·—) neutralinos, as a function of m_θ, for $\epsilon=-M_2=-\frac{1}{3}m_W$ and $v_1/v_2=4$.

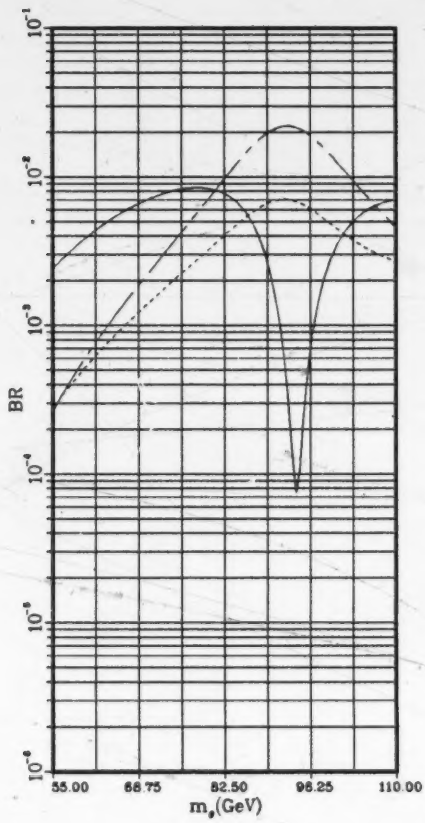

Fig. 3.36. Toponium BR plots with an extra U(1). θ BR'S to two light (——), one light & one heavy (---), and two heavy (—-) neutralinos, as a function of m_θ, for $\lambda x = M_2 = \frac{1}{3} m_W$, $\lambda = 0.10$ and $v_1/v_2 = 3.4$.

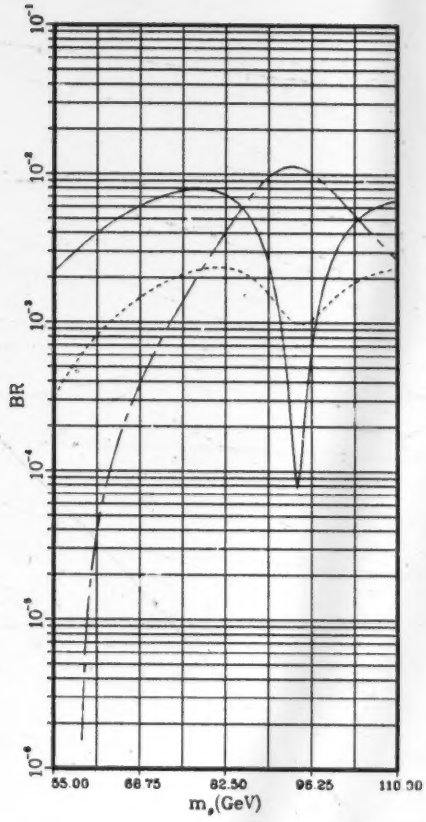

Fig. 3.37. Toponium BR plots with an extra U(1). θ BR'S to two light (——), one light & one heavy (---), and two heavy (—·—) neutralinos, as a function of m_θ, for $\lambda x = M_2 = \frac{1}{3} m_W$, $\lambda = 0.18$ and $v_1/v_2 = 3.4$.

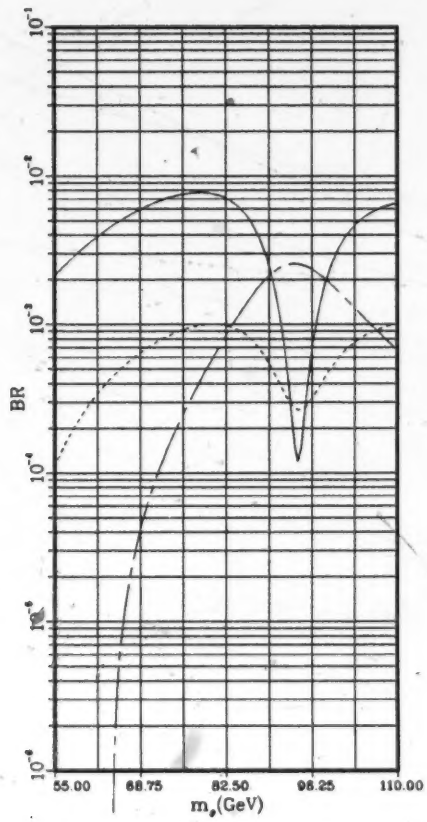

Fig. 3.38. Toponium BR plots with an extra U(1). θ BR'S to two light (——), one light & one heavy (---), and two heavy (—-) neutralinos, as a function of m_θ, for $\lambda x = M_2 = \frac{1}{3} m_W$, $\lambda = 0.25$ and $v_1/v_2 = 3.4$.

The O(1/3) value, for the parameters $(|\epsilon|, M_2, \lambda x)/m_W$, turns out to be a good rule of thumb when considering kinematically inaccessible (as per previous section) and cosmologically disallowed regions (ELL.83B, CAM.86), of the ϵ (or λx), M_2 plain, when varying over the parameters, ϵ, M_2, v_1/v_2, λx and m_ϕ.

The topological properties of figures 3.11 through 3.31 change very little as one varies m_ϕ [5]. So, these figures along with figures 3.32 through 3.38, give an overall picture of neutralino production.

H. Experimental Consequences

Now that we have looked at neutralino production for orthotoponium, the final question remains whether or not this phenomenon can be observed at any of the present day accelerators.

Here we concentrate on e^+e^- machines only; since the production of $q\bar{q}$ states entails just electroweak interactions. Hadronic machines, on the other hand, involve more complicated processes which lead to predictions of low production cross sections for heavy $q\bar{q}$ bound states (e.g. $p\bar{p} \rightarrow t\bar{t}+X$ (HAB.85)).

---

[5] It should be noted that, as one makes m_ϕ small, more regions, of the ϵ (or λx), M_2 plain, become kinematically inaccessible. There is also a bit of topological deformation near the Z-pole, however this region is of no value to us (see section H).

To try and narrow down which of the present day e^+e^- machines are capable of neutralino production, we give a brief summary, of the θ BR predictions, of figures 3.32 through 3.38, in table 3.2 below.

TABLE 3.2. A list of some typical θ BR's.

Masses (GeV)			$\sim\theta$ BR's		
m_θ	m_R	m_L	$\tilde{x}\tilde{x}$	$\tilde{x}\tilde{x}'$	$\tilde{x}'\tilde{x}'$
55	91	53	10^{-3}	10^{-4}-10^{-3}	$10^{-\infty}$-10^{-3}
70	96	54	10^{-2}	10^{-3}	10^{-4}-10^{-3}
105	109	55	10^{-2}	10^{-3}	10^{-4}-10^{-3}

In picking these values, we have ignored contributions near the region $m_z-2\Gamma_z<m_\theta<m_z+2\Gamma_z$; since, in this region, θ production is expected to be suppressed, due to Z-$\bar{t}t$ interferences (KÜH.85). Scanning the table, we find BR's range typically from $O(10^{-4})$ to $O(10^{-2})$.

For e^+e^- machines, predictions for $t\bar{t}$ production cross-sections range anywhere from $O(10^1)$ to $O(10^2)$ pb; depending on the production energy, W, and the machines design energy spread, δW. This means our neutralino production cross-sections would be of order $O(10^{-3})$-$O(10^0)$pb. So, one would require integrated luminosities, ℓ ($\equiv\int Ldt$),

of at least $O(10^2)pb^{-1}$, before standing a good chance of observing neutralino production.

Todays high energy accelerators have typical experimental runs of about $O(10^7)s$. Therefore, our candidate e^+e^- machines, should have luminosities, L, of at least $O(10^{31})cm^{-2}s^{-1}$ and work above a $\sqrt{S} \gtrsim O(55)GeV$ energy regime. These contraints quickly narrow us down to one machine: LEP ($\sqrt{S} \sim 100\text{-}170$ GeV, $L \sim 10^{31}\text{-}.5\times10^{32}$ $cm^{-2}s^{-1}$; CHE.88) with TRISTAN ($\sqrt{S} \sim 56\text{-}70$ GeV, $L \sim 3\times10^{29}\text{-}1\times10^{31}$(peak) $cm^{-2}s^{-1}$; VEN.88) and SLC ($\sqrt{S} \sim 100$GeV, $L \sim 10^{28}\text{-}10^{30}$ $cm^{-2}s^{-1}$; CHE.88) trailing slightly behind.

Table 3.3, below, compares the predicted number of neutralino events, associated with typical BR's given in table 3.2, to the number of predicted hadronic events, observed in a typical experimental year ($O(10^7)s \rightarrow \ell \sim 111pb$), at LEP.

TABLE 3.3. Some typical Neutralino Events at LEP.

W	δW	Number of events				
(GeV)	(MeV)	$\tilde{\chi}\tilde{\chi}$	$\tilde{\chi}\tilde{\chi}'$	$\tilde{\chi}'\tilde{\chi}'$	N^{θ}_{Had}	$N^{\gamma,Z}_{Had}$
55	14	319	32-319	0-319	319 000	160 000
70	23	177	18	2-18	17 700	17 700
105	67	79	8	1-8	7 890	87 690

N^{θ}_{Had} and $N^{\gamma,Z}_{Had}$ represent the number of hadronic events, produced from, $e^+e^- \rightarrow \theta \rightarrow$ had, and the continuum ($e^+e^- \rightarrow \gamma,Z \rightarrow$ had), respectively. The number of neutralino and θ related hadronic events can vary by a factor of about two due to theoretical uncertainties in $\psi(0)$ [6].

Essentially the results of table 3.3 speak for themselves. Empirically, they imply a good chance of seeing at least the lightest species of neutralinos over our $55 \leq \sqrt{s} \leq 105$GeV energy regime. Or do they?

If one carefully examines equation (1.45), for the appropriate particle-sparticle spectrum as described in chapters 1 and 2, one will notice a discrete symmetry which basically says: that for each standard model vertex one must replace partners by their spartners, in pairs. This symmetry is called R-parity, and is +1 for standard model particles and -1 for their spartners. The main consequence of this symmetry of interest here is that it predicts that there should exist at least one stable lightest supersymmetric particle (LSP)[7].

It is believed that the LSP candidate, is either a light $\tilde{\chi}^0$ (i.e. the $\tilde{\gamma}$) or $\tilde{\nu}$ state. Either way, it doesn't matter, since the net result of light $\tilde{\chi}^0$ production is $\theta \rightarrow$ nothing. This would, of course, be experimentally

---

[6] See LEP.85 for further details regarding table 3.3.

[7] Here, we have assumed R-parity is an exact symmetry. If this were not the case, then the LSP would decay, which would, typically, lead to lepton number violation (e.g. $\tilde{\gamma} \rightarrow \gamma + \nu$).

difficult to detect, since one would have to employ ν counting techniques (i.e. $e^+e^- \rightarrow \gamma\bar{\nu}\nu$).

The signature associated with mixed neutralino production ($\theta \rightarrow \tilde{\chi}\tilde{\chi}'$), however, leads to more striking one sided events; $\theta \rightarrow \bar{f}f+\tilde{\chi}^0$ (HAB.85), which are virtually uncontaminated by standard model backgrounds.

For heavy neutralino production, the signatures are also expected to be good; although not as striking as mixed neutralino events.

In closing, we conclude that it should be possible to observe neutralino production at LEP (and perhaps TRISTAN), or at least rule out some of the cosmologically allowed regions of the neutralino sector.

IV. Summary and Conclusions

In this thesis, we gave a brief introduction to SUSY (chap. 1). We followed this up by considering some softly broken N=1 SUSY models (chap. 2), namely, SU(2)⊗U(1) and SU(2)⊗U(1)⊗U(1). Particular attention was paid, when taking into account the $\tilde{\chi}^0_{1,2}$ mass spectrum. Finally, this information was implemented in chap 3, where we looked at the various θ BR's associated with $\tilde{\chi}^0_{1,2}$ production.

Here, we scanned the m_e mass over a 55 to 110 GeV energy regime, while fixing the soft breaking SUSY parameters ϵ, M_2 and λx at $\frac{1}{3}$ the W mass. We found that θ BR's typically ranged anywhere from $O(10^{-4})$ to $O(10^{-2})$.

Essentially, we found that such events, if observable at all, should appear at LEP (or perhaps TRISTAN).

REFERENCES

(ALT.87) G. Altarelli, CERN-TH.4855/87, oct(1987).

(BAG.82) J. Bagger and J. Wess, 'Supersymmetry and Supergravity', Princeton University Press 1983.

(BJO.64) Bjorken and Drell, Relativistic Quantum Mechanics, Vol. I, McGraw-Hill Inc., 1964.

(CAM.82) B.A. Campbell, ''The Hitch Hiker's Guide to Supersymmetry'', Lectures presented at Carleton University, Fall(1982), Unpublished.

(CAM.86) B.A.Campbell, J. Ellis, K. Enqvist, D.V. Nanopoulos, J.S. Hagelin, K.A. Olive, CERN-TH.4385/86, Feb 86, MIU-THP-86/004, UMN-TH-522/86.

(CHE.88) M. Chen, C. Dionisi, M. Martinez and X. Tata, Phys. Rep., **159**, Nos. 4-5(1988)201-301.

(COM.83) E.D. Commins and P.H. Bucksbaum, 'Weak Interactions of Leptons and Quarks', Cambridge University Press, 1983.

(CUD.87A) J.R. Cudell, F. Halzen, 'Is a low-mass top quark ruled out?', University of Wisconsin-Madison, MAD/PH/353, UH-511-622-87(June 1987).

(CUD.87B) J.R. Cudell, F. Halzen, X-G. HE and S. Pakvasa, 'B-$\bar{B}$ Mixing does not exclude M(top)<$M_Z/2$', University of Wisconsin-Madison MAD/PH/376, UH-511-636-87, Oct. 87.

(DEW.75) B. de Witt, D.Z. Freedman, Phys. Rev. D, 12, No. 6, 15 Oct.(1975)2286-2297.

(DOB.88) A. Dobado, Phys. Lett. B, 211, No. 4, 8 Sept. (1988)485-488.

(EIN.05) A. Einstein,'Zur Elektrodynamik bewegter Körper', Ann. Phys(Germany)17, (1905)891-921.

For translation see:

A. Einstein, H.A. Lorentz, H. Minkowski, and H. Weyl, 'The Principle of Relativity', Mathuen & Co. Ltd., (1923)36-66.

(ELL.83A) J. Ellis,'... AND FOR OUR NEXT SPECTROSCOPY?', Lectures presented at the SLAC Insititute on Particle Physics July 18-29(1983), CERN-TH.3747-CERN Oct. 1983.

(ELL.83B) J. Ellis, J.S. Hagelin, D.V. Nanopoulos and M. Srednicki, Phys. Lett. 127B, Nos. 3-4, July 28 (1983)453-476.

(ELL.83C) J. Ellis and S. Rudaz, Phys. Lett., 128B, 248(1983).

(ELL.84) J. Ellis, J.S. Hagelin, D.V. Nanopoulos, K. Olive and M. Srednicki, Nuc. Phys. B238(1984)453-476.

(ELL.85) J. Ellis, 'Supersymmetry, Supergravity and Superstring Phenomenology', Lectures presented at the 28th Scottish Universities Summer School in Physics, Edinburgh, Scotland July 28th to August 17th, CERN-TH.4255/85.

(HAB.85) H.E. Haber, G.L. Kane, Phys. Rep.(Rev. § of Phys. Lett.)117, Nos. 2-4(1985)75-263.

(HE.87) Xiao-Gang He and S. Pakvasa, Phys. Lett. B, 193 No. 1, 30 July(1987).

(HEI.32) W. Heisenberg, Zeitschrift Fur Physik, 77, 7 Jun. (1932)1-11.

(JOG.84) S.D. Joglekar, 'Introduction to Global Supersymmetry.', Lecture Notes in Physics 208 on 'Supersymmetry and Supergravity Nonperturbative QCD Proceedings, Mahabaleshwar, India 1984',

Springer-Verlag (1984)1-30.

(KÜH.85) J. H. Kühn and P. M. Zerwas, Phys. Lett., **154B**, No. 5, 6 May (1985)448-451.

(LEP.85) Toponium Physics at LEP, MPI-PAE/PTh 85/85, Dec. 1985.

(LOS.86) J. M. LoSecco, Proceedings of the First Lake Louise Winter Institute on New Frontiers in Particle Phycsics, (1986)376-392.

(MOH.86) R.N. Mohapatra, 'Unification and Supersymmetry', Springer-Verlag N.Y. Inc., 1986.

(NAN.84) D.V. Nanopoulos, Phys. Rep.(Rev. S of Phys. Lett.)**105**, Nos. 1-2(1984)71-89.

(PER.82) D.H. Perkins, 'Introduction to High Energy Physics', Addison Wesley, 1982.

(PET.87) K.A. Peterson, M.Sc. Thesis, 'Topics in Supersymmetry', University of Alberta, 1987.

(QUI.83) C. Quigg, 'Gauge Theories of the Strong, Weak, and Electromagnetic Interactions', Benjamin/Cummings, 1983.

(RAM.81) P. Ramond, 'Field Theory A Modern Primer', Benjamin/Cummings, 1981.

(ROS.85) G.G. Ross, 'Grand Unified Theories', Benjamin/Cummings, 1985.

(ROS.87) J.L. Rosner, Proceedings of the Second Lake Louise Winter Institute on New Frontiers in Particle Physics, (1987)91-170.

(ROY.67) J. Van Royen and V. Weiskopf, Nuovo Cimento **50A**, 617(1967).

(SCO.85) J.A.B. Scott, Ph.D. Thesis on 'Topics on Phenomenology in Supersymmetric gauge theories', Carleton University, Ottawa, Ontario 1985.

(SOH.85) M.F. Sohnius, Phys. Rep.(Rev. § of Phys. Lett.)128, Nos. 2-3(1985)39-204.

(UA1.83) UA1 Collaboration, CERN, Geneva, Switzerland, Phys. Lett. **126B**, No. 5, July 7 (1983)398-410.

(UA2.83) The UA2 Collaboration, Phys. Lett. **122B**,No. 5, 6(1983)476-485.

(WES.74) J. Wess & B. Zumino, Nucl. Phys, **B70**, 39(1974).

(VEN.88) VENUS collaboration, Proceedings of the Third Lake Louise Winter Institute, on, 'Quantum Chromodynamics: Theory and Experiment'; editors, B. A. Campbell, A. N. Kamal, F. C. Khanna and M. K. Sundaresan; World Scientific.

(WIL.71) W.S.C. Williams, 'An Introduction to Elementary Particles', Academic Press, 1971.

(ZUM.84) B. Zumino, Phys. Rep.(Rev. § of Phys. Lett.)104, Nos. 2-4(1984)113-128.

APPENDIX A--Notation

The notation that I am using is basically that of Bjorken and Drell. However, for completeness sake, I shall list the notation which is implemented in my thesis.

Minkowski Space

The usual Minkowski space-time coordinates $(t,\bar{x})$ (where we assume $c=1$ and $\hbar=1$) are denoted by a contravariant four-vector x^{μ}. Lower case Greek letters are assumed to sum from zero to three over the space-time coordinates and lower case Roman letters from one to three over the space coordinates. Covariant four-vectors x_{μ} are obtained by the use of the metric tensor $g_{\mu\nu}=\text{diag}(+,-,-,-)$.

i.e. $$x_{\mu}=g_{\mu\nu}x^{\nu} \qquad (A.1)$$

where we assume Einstein's Σ convention, unless otherwise specified($\not\Sigma$).

Momentum four-vectors may also be similarly defined.

$$p^{\mu}=(E,\bar{p}). \qquad (A.2)$$

The four-vector potential is given by

$$A^{\mu}=(\phi,\bar{A}) \qquad (A.3)$$

whose field strengths are defined by

$$F^{\mu\nu}=\partial^{[\mu}A^{\nu]}\equiv\partial^{\mu}A^{\nu}-\partial^{\nu}A^{\mu} \tag{A.4}$$

where

$$\partial^{\mu}\equiv\frac{\partial}{\partial x_{\mu}}=(\partial_{t},\vec{\nabla}),\ \partial_{t}\equiv\partial^{0} \tag{A.5}$$

and transforms as a contravariant four-vector:

$$\partial^{\mu}\partial_{\mu}\equiv\frac{\partial}{\partial x_{\mu}}\frac{\partial}{\partial x^{\mu}}=\partial_{t}^{2}-\vec{\nabla}^{2}\equiv\Box. \tag{A.6}$$

A four-vector product between any two four-vectors A and B is defined as

$$A\cdot B=A_{\mu}B^{\mu}=g_{\mu\nu}A^{\nu}B^{\mu}=A^{0}B^{0}-\vec{A}\cdot\vec{B} \tag{A.7}$$

where the three-vector product $\vec{A}\cdot\vec{B}$ is defined by $A^{k}B^{k}$.

Dirac Matrices

The Dirac gamma matrices satisfy the Clifford algebra

$$\gamma^{\{\mu}\gamma^{\nu\}}\equiv\gamma^{\mu}\gamma^{\nu}+\gamma^{\nu}\gamma^{\mu}=2g^{\mu\nu}. \tag{A.8}$$

Here

$$\gamma^0=\begin{bmatrix}1 & 0\\ 0 & -1\end{bmatrix},\quad \vec{\gamma}=\{\gamma^i\}=\begin{bmatrix}0 & \vec{\sigma}\\ -\vec{\sigma} & 0\end{bmatrix} \tag{A.9}$$

are the Dirac gamma matrices whose elements in the Bjorken and Drell representation, are the usual Pauli spin matrices

$$\sigma^0=\begin{bmatrix}1 & 0\\ 0 & 1\end{bmatrix},\quad \sigma^1=\begin{bmatrix}0 & 1\\ 1 & 0\end{bmatrix},\quad \sigma^2=\begin{bmatrix}0 & -i\\ i & 0\end{bmatrix},\quad \sigma^3=\begin{bmatrix}1 & 0\\ 0 & -1\end{bmatrix}. \tag{A.10}$$

The Pauli matrices obey the Lie algebra

$$[\sigma^i,\sigma^j]=2i\epsilon^{ijk}\sigma^k \tag{A.11}$$

and anti-commute (note $\sigma_i\equiv-\sigma^i$ & $\sigma_0\equiv\sigma^0$.)

Some useful combinations of gamma matrices are:

(i)
$$\sigma^{\mu\nu}=\frac{i}{2}[\gamma^\mu,\gamma^\nu]=(i\delta^{\mu\nu}_{k0}\gamma_5-\epsilon^{0\mu\nu}{}_k 1)\otimes\sigma^k$$

$$\equiv(i\delta^{\mu\nu}_{k0}\gamma_5-\epsilon^{0\mu\nu}{}_k)\sigma^k \tag{A.12}$$

where

$$\delta^{\mu\nu}_{k0}\equiv\delta^\mu_k\delta^\nu_0-\delta^\nu_k\delta^\mu_0 \tag{A.13}$$

and

$$\gamma_5\equiv\gamma^5=i\gamma^0\gamma^1\gamma^2\gamma^3=\begin{bmatrix}0 & 1\\ 1 & 0\end{bmatrix}. \tag{A.14}$$

(ii) The left and right chiral projection operators are respectively given by

$$P_L \equiv L \equiv \frac{1-\gamma_5}{2} = \frac{1}{2}\begin{bmatrix} 1 & -1 \\ -1 & 1 \end{bmatrix} \tag{A.15}$$

and

$$P_R \equiv R \equiv \frac{1+\gamma_5}{2} = \frac{1}{2}\begin{bmatrix} 1 & 1 \\ 1 & 1 \end{bmatrix}. \tag{A.16}$$

(iii) The charge conjugation operator is

$$C = i\gamma^2\gamma^0. \tag{A.17}$$

It has the properties

$$C = -C^{\dagger} = -C^{T} = -C^{-1} \tag{A.18}$$

and

$$C\gamma^{\mu T}C^{-1} = -\gamma^{\mu} \tag{A.19}$$

which imply

$$C\Gamma_A^T C^{-1} = (1, \gamma_5, -\gamma_\mu, i\gamma_\mu\gamma_5, \sigma_{\mu\nu}) \tag{A.20}$$

where Γ_A is the set of all the linearly independent

combinations of gamma matrices given by equation (C.1).

(iv) The conjugate $\bar{O}_i$ of an arbitrary 4×4 matrix O_i is defined by

$$\bar{O}_i=\gamma_0 O_i^\dagger \gamma^0. \tag{A.21}$$

eg: $$\bar{\Gamma}_A=\gamma_0\Gamma_A^\dagger\gamma^0=(1,-\gamma_5,\gamma_\mu,i\gamma_\mu\gamma_5,\sigma_{\mu\nu}). \tag{A.22}$$

(v) Commutator relations

$$[\gamma_\mu,\sigma_{\rho\sigma}]=2ig_{\mu[\rho}\gamma_{\sigma]} \tag{A.23}$$

$$[\gamma_5,\sigma_{\rho\sigma}]=0 \tag{A.24}$$

$$\{\gamma_5,\gamma^\mu\}=0 \tag{A.25}$$

$$[P_{R,L},\sigma_{\rho\sigma}]=0 \tag{A.26}$$

$$[\gamma_5,P_{L,R}]=0 \tag{A.27}$$

One can also take the Feynman dagger, or slash, of a four-vector by contracting it with the gamma matrices

$$\not{A}\equiv\gamma_\mu A^\mu=\gamma^0A^0-\bar{\gamma}\cdot\bar{A}. \tag{A.28}$$

Trace Theorems

Some useful trace theorems are:

$$\mathrm{Tr}1=4 \tag{A.29}$$

$$\mathrm{Tr}\not{a}\not{b}=4a\cdot b \tag{A.30}$$

$$\mathrm{Tr}\not{a}_1\not{a}_2\not{a}_3\not{a}_4=4[a_1\cdot a_2 a_3\cdot a_4+a_1\cdot a_4 a_2\cdot a_3-a_1\cdot a_3 a_2\cdot a_4] \tag{A.31}$$

$$\mathrm{Tr}\not{a}_1\not{a}_2\ldots\not{a}_{2n-1}=0 \tag{A.32}$$

$$\mathrm{Tr}\not{a}_1\not{a}_2\ldots\not{a}_{2n}=a_1\cdot a_2\mathrm{Tr}\not{a}_3\ldots\not{a}_{2n}-a_1\cdot a_3\mathrm{Tr}\not{a}_2\not{a}_4\ldots\not{a}_{2n}$$

$$+\ldots+a_1\cdot a_{2n}\mathrm{Tr}\not{a}_2\ldots\not{a}_{2n-1} \tag{A.33}$$

$$\mathrm{Tr}\gamma_5=0 \tag{A.34}$$

$$\mathrm{Tr}\gamma_5\not{a}\not{b}=0 \tag{A.35}$$

$$\mathrm{Tr}\gamma_5\not{a}\not{b}\not{c}\not{d}=4i\epsilon_{\alpha\beta\gamma\delta}a^\alpha b^\beta c^\gamma d^\delta. \tag{A.36}$$

Proof of these theorems can be found in Bjorken and Drell (BJO.64).

APPENDIX B--Spinorology

Dirac Spinors

For a free Dirac particle boosted from its rest frame one obtains, for positive-energy states, the free Dirac spinor

$$U(P)=N\begin{bmatrix}\chi\\ \frac{\vec{\sigma}\cdot\vec{P}}{E+m}\chi\end{bmatrix} \tag{B.1}$$

where N is a normalization factor and χ a two component spinor with spin up and spin down degrees of freedom, which we will respectively denote by

$$\chi_{\uparrow}=\begin{bmatrix}1\\0\end{bmatrix} \qquad \text{spin up particle} \tag{B.2}$$

$$\chi_{\downarrow}=\begin{bmatrix}0\\1\end{bmatrix} \qquad \text{spin down particle.} \tag{B.3}$$

The normalization factor N can be obtained by imposing the normalization

$$\bar{U}(p)U(p)=1 \tag{B.4}$$

where the 'bar' over the Dirac spinor is the Pauli adjoint

$$\bar{U}(p)=U(p)^{\dagger}\gamma^{0}. \tag{B.5}$$

Therefore, imposing condition (B.4) we have

$$N=\left(\frac{E+m}{2m}\right)^{1/2}. \tag{B.6}$$

Negative-energy states are just, to within a phase, the charge-conjugate of positive-energy states;

i.e. $$V(p)=-C\bar{U}^{T}(p) \tag{B.7}$$

which implies

$$V(P)=N\begin{bmatrix}\frac{\bar{\sigma}\cdot\bar{P}}{E+m}\phi\\ \phi\end{bmatrix} \tag{B.8}$$

where

$$\phi=i\sigma^{2}\chi \tag{B.9}$$

and has respectively the spin up and spin down degrees of freedom

$$\phi_{\uparrow}=\begin{bmatrix}1\\0\end{bmatrix} \qquad \text{spin down antiparticle} \tag{B.10}$$

$$\phi_{\downarrow}=\begin{bmatrix}0\\-1\end{bmatrix} \qquad \text{spin up antiparticle.} \tag{B.11}$$

Either by equation (B.7) or by (B.8) one can show that the negative-energy states satisfy the normalization condition

$$\bar{V}(p)V(p)=-1. \tag{B.12}$$

By taking tensor products of spinors with their Pauli adjoints and summing over their spin degrees of freedom we find the useful conditions

$$\sum_{\uparrow\downarrow} U(p)\bar{U}(p)=\frac{\not{p}+m}{2m} \tag{B.13}$$

and

$$\sum_{\uparrow\downarrow} V(p)\bar{V}(p)=\frac{\not{p}-m}{2m}. \tag{B.14}$$

N.R. Approx.

In the limit $v<<1$ we find

$$N=\left(\frac{E+m}{2m}\right)^{1/2}\sim\left(\frac{m+m}{2m}\right)^{1/2}=1 \tag{B.15}$$

which implies

$$U(P)\sim\begin{bmatrix}\chi\\ \frac{\bar{\sigma}\cdot\bar{P}}{2m}\chi\end{bmatrix} \;\&\; V(P)\sim\begin{bmatrix}\frac{\bar{\sigma}\cdot\bar{P}}{2m}\phi\\ \phi\end{bmatrix} \tag{B.16}$$

Using these approximations we find, with very little effort, the following useful approximations:

$$\bar{V}(p_2)P_{R,L}U(p_1)\sim\mp\frac{1}{2}\phi^{\dagger}\chi+O(\frac{\bar{p}}{m}) \tag{B.17}$$

$$\bar{V}(p_2)\gamma^{\mu}U(p_1)\sim\phi^{\dagger}\sigma^{i}\chi\delta^{\mu}_{i}+O(\frac{\bar{p}}{m}) \tag{B.18}$$

$$\bar{V}(p_2)\gamma^{\mu}P_{R,L}U(p_1)\sim\pm\frac{1}{2}\phi^{\dagger}\chi\delta^{\mu}_{0}+\frac{1}{2}\phi^{\dagger}\sigma^{i}\chi\delta^{\mu}_{i}+O(\frac{\bar{p}}{m}) \tag{B.19}$$

$$\bar{V}(p_2)\sigma_{0i}U(p_1)\sim-i\phi^{\dagger}\sigma_{i}\chi+O(\frac{\bar{p}}{m}) \tag{B.20}$$

$$\bar{V}(p_2)\sigma_{ij}U(p_1)\sim O(\frac{\bar{p}}{m}). \tag{B.21}$$

The terms in approximations (B.17) through (B.21) contain various spin degrees of freedom, which we now summarize in table (B.1) below:

TABLE B.1. N.R. Approx. Expectation Values.

Term	Spin degrees of freedom			
$\|\chi\phi\rangle$	$\|\uparrow\downarrow\rangle$	$\|\uparrow\uparrow\rangle$	$\|\downarrow\downarrow\rangle$	$\|\downarrow\uparrow\rangle$
$\phi^{\dagger}\chi$	1	0	0	-1
$\phi^{\dagger}\sigma^{1}\chi$	0	-1	1	0
$\phi^{\dagger}\sigma^{2}\chi$	0	-i	-i	0
$\phi^{\dagger}\sigma^{3}\chi$	1	0	0	1

NOTE: $|\chi_{\uparrow}\rangle=|\uparrow\rangle$, $|\chi_{\downarrow}\rangle=|\downarrow\rangle$, $|\phi_{\uparrow}\rangle=|\downarrow\rangle$, $|\phi_{\downarrow}\rangle=|\uparrow\rangle$

APPENDIX C--Fierz Identities

In order to obtain the Fierz transformations, used in our decay calculation, we consider the fact that any 4×4 matrix can be expressed by a linear combination of the 16 linearily independent matrices

$$\Gamma_A=(1,\gamma_5,\gamma_\mu,i\gamma_\mu\gamma_5,\sigma_{\mu\nu}) \tag{C.1}$$

with, in particular, the property that

$$Tr(\Gamma^A\Gamma_B)=4\delta^A{}_B. \tag{C.2}$$

Therefore, if we desire to express a direct product of two arbitrary 4×4 matrices in terms of direct products of the complete set of matrices given above, we consider

$$A_{\alpha\beta}B_{\rho\sigma}=\Sigma_A C^A_{\alpha\sigma}(\Gamma_A)_{\rho\beta}. \tag{C.3}$$

If we now contract the left hand side of this relation with

$$(\Gamma^B)_{\beta\rho} \tag{C.4}$$

we obtain, via relation (C.2),

$$(\Gamma^B)_{\beta\rho}A_{\alpha\beta}B_{\rho\sigma}=\Sigma_A C^A_{\alpha\sigma}Tr(\Gamma_A\Gamma^B)=4C^B_{\alpha\sigma} \tag{C.5}$$

which implies

$$C^A_{a\sigma}=\tfrac{1}{4}(A\Gamma^A B)_{a\sigma}. \qquad (C.6)$$

Thus we obtain the desired result

$$A_{a\beta}B_{\rho\sigma}=\tfrac{1}{4}\Sigma_A(A\Gamma_A B)_{a\sigma}(\Gamma^A)_{\rho\beta}. \qquad (C.7)$$

or, in shorthand notation, we have

$$A\otimes B=\tfrac{1}{4}(A\Gamma_A B)\otimes(\Gamma^A). \qquad (C.8)$$

More explicitly

$$A\otimes B=\tfrac{1}{4}\{AB\otimes 1+A\gamma_5 B\otimes\gamma^5+A\gamma_\mu B\otimes\gamma^\mu-A\gamma_\mu\gamma_5 B\otimes\gamma^\mu\gamma^5+\tfrac{1}{2}A\sigma_{\mu\nu}B\otimes\sigma^{\mu\nu}\} \qquad (C.9)$$

where the extra factor of a half in the last term is to take care of double counting.

Thus, using equation (C.9), we obtain the Fierz identities

$$R\otimes R=\tfrac{1}{2}[R\otimes R+\tfrac{1}{4}R\sigma_{\mu\nu}\otimes\sigma^{\mu\nu}] \qquad (C.10)$$

$$R\otimes L=\tfrac{1}{2}\gamma_\mu L\otimes\gamma^\mu R \qquad (C.11)$$

$$L\otimes L=\tfrac{1}{2}[L\otimes L+\tfrac{1}{4}L\sigma_{\mu\nu}\otimes\sigma^{\mu\nu}] \qquad (C.12)$$

$$L\otimes R=\tfrac{1}{2}\gamma_\mu R\otimes\gamma^\mu L \qquad (C.13)$$

which gives us the following Fierz transformations

$$\bar{U}_A R U_B \bar{V}_C R V_D = \tfrac{1}{2}[\bar{U}_A R V_D \bar{V}_C R \bar{V}_B + \tfrac{1}{4}\bar{U}_A R \sigma_{\mu\nu} V_D \bar{V}_C \sigma^{\mu\nu} U_B] \qquad (C.14)$$

$$\bar{U}_A R U_B \bar{V}_C L V_D = \tfrac{1}{2}\bar{U}_A \gamma_\mu L V_D \bar{V}_C \gamma^\mu R \bar{V}_B \qquad (C.15)$$

$$\bar{U}_A L U_B \bar{V}_C L V_D = \tfrac{1}{2}[\bar{U}_A L V_D \bar{V}_C L \bar{V}_B + \tfrac{1}{4}\bar{U}_A L \sigma_{\mu\nu} V_D \bar{V}_C \sigma^{\mu\nu} U_B] \qquad (C.16)$$

$$\bar{U}_A L U_B \bar{V}_C R V_D = \tfrac{1}{2}\bar{U}_A \gamma_\mu R V_D \bar{V}_C \gamma^\mu L \bar{V}_B . \qquad (C.17)$$